Theses and Dissertations   1. Thesis and Dissertation Collection, all items

1993-03

Laser Doppler velocimetry measurements across a normal shock in transonic flow

Perretta, David Arthur

Monterey, California. Naval Postgraduate School

https://hdl.handle.net/10945/26610

LASER DOPPLER VELOCIMETRY
MEASUREMENTS ACROSS A NORMAL
SHOCK IN TRANSONIC FLOW

by

David A. Perretta
Lieutenant, United States Navy
B.S., Marquette University, 1982

Submitted in partial fulfillment
of the requirements for the degree of

MASTER OF SCIENCE IN AERONAUTICAL ENGINEERING

from the

POSTGRADUATE SCHOOL

REPORT DOCUMENTATION PAGE

1a Report Security Classification: Unclassified		1b Restrictive Markings			
2a Security Classification Authority		3 Distribution/Availability of Report			
2b Declassification/Downgrading Schedule		Approved for public release; distribution is unlimited.			
4 Performing Organization Report Number(s)		5 Monitoring Organization Report Number(s)			
6a Name of Performing Organization Naval Postgraduate School	6b Office Symbol (if applicable) 31	7a Name of Monitoring Organization Naval Postgraduate School			
6c Address (city, state, and ZIP code) Monterey CA 93943-5000		7b Address (city, state, and ZIP code) Monterey CA 93943-5000			
8a Name of Funding/Sponsoring Organization	6b Office Symbol (if applicable)	9 Procurement Instrument Identification Number			
8c Address (city, state, and ZIP code)		10 Source of Funding Numbers			
		Program Element No	Project No	Task No	Work Unit Accession N

11 Title (include security classification) Laser Doppler Velocimetry Measurements Across a Normal Shock in Transonic Flow

12 Personal Author(s) Perretta, David A.

13a Type of Report Master's Thesis	13b Time Covered From To	14 Date of Report (year, month, day) 1993, March, 25	15 Page Count 118

16 Supplementary Notation The views expressed in this thesis are those of the author and do not reflect the official policy or position of the Department of Defense or the U.S. Government.

17 Cosati Codes			18 Subject Terms (continue on reverse if necessary and identify by block number)
Field	Group	Subgroup	Laser Doppler Velocimetry, Normal Shock, Transonic, Back Scatter Mode

19 Abstract (continue on reverse if necessary and identify by block number)

One-dimensional laser-Doppler velocimetry measurements were taken with standard optics in back scatter mode across a normal shock at a Mach number of 1.35. Back pressure on a blow-down supersonic tunnel was controlled to place a normal shock in a 4 by 4 inch test section and schlieren visualization techniques were used to verify and record shock position and behavior. Velocity surveys were taken across the shock, using various filtering techniques, in an attempt to quantify shock unsteadiness. Additional surveys were performed to further characterize the flow in the test section. The velocity surveys upstream and downstream of the shock compared favorably with pressure and temperature data and normal shock relations. Surveys across the shock indicated distinct and repeatable velocity patterns, and the measured location of the shock closely matched schlieren photographs.

20 Distribution/Availability of Abstract _ unclassified/unlimited __ same as report __ DTIC users	21 Abstract Security Classification Unclassified	
22a Name of Responsible Individual Garth V. Hobson	22b Telephone (include Area Code) 408 656-2888	22c Office Symbol AAHg

DD FORM 1473, 84 MAR   83 APR edition may be used until exhausted   security classification of this page

All other editions are obsolete   Unclassified

ABSTRACT

One-dimensional laser-Doppler velocimetry measurements were taken with standard optics in back scatter mode across a normal shock at a Mach number of 1.35. Back pressure on a blow-down supersonic tunnel was controlled to place a normal shock in a 4 by 4 inch test section and schlieren visualization techniques were used to verify and record shock position and behavior. Velocity surveys were taken across the shock, using various filtering techniques, in an attempt to quantify shock unsteadiness. Additional surveys were performed to further characterize the flow in the test section. The velocity surveys upstream and downstream of the shock compared favorably with pressure and temperature data and normal shock relations. Surveys across the shock indicated distinct and repeatable velocity patterns, and the measured location of the shock matched schlieren photographs.

TABLE OF CONTENTS

iv

v

I. INTRODUCTION

A. THEORETICAL BACKGROUND

In many experimental studies in fluid mechanics and aerodynamics, accurate velocity measurements within flowfields are of fundamental importance. Detailed research of complex, turbulent, or high speed flows is virtually impossible without the aid of sophisticated velocity measuring devices. Laser Doppler velocimetry (LDV) is a non-intrusive optical technique that uses the Doppler principle to measure the velocity of particles in a fluid. Over the past three decades, LDV has evolved into a highly adaptive and precise tool that is widely used in the measurement of flow fields.

The relative motion between a source of radiation and a moving body will cause the observed frequency of the source to be Doppler shifted. When a beam is directed onto a particle moving in the flow, the particle will scatter light. The scattered light is frequency shifted and the velocity can be measured from the shift in this scattered light.

Although there are several types of optical systems utilized by LDV, the most common type is the dual beam system which uses optics to divide the laser beam into two parallel beams of equal intensity. The two beams are then focused by a lens such that they intersect at a point in the flow. The

1

constructive interference from the coherent light waves of each beam form interference fringes and as a particle passes through the fringes it will alternately scatter or not scatter light as it crosses a light or dark fringe.

The rate at which the particle crosses the fringes is equal to the rate of oscillation of the signal from the scattered light which is collected by a lens and directed onto a photo detector. Fringe spacing can be calculated by the equation:

$$S = \frac{\lambda}{2 \sin\theta} \tag{1}$$

where λ is the wavelength of light used and θ is the half angle of the two beams after passing through the focusing lens [Ref. 1]. By obtaining the frequency of the oscillating signal, f_d, with a photo detector, the velocity of the particle can be determined by the following equation [Ref. 1].

$$V = S f_D = \frac{\lambda f_D}{2 \sin\theta} \tag{2}$$

If the particle is small enough such that it moves with the flow of the fluid then the velocity of the fluid is equal to the velocity of the particle.

Frequency shifting is commonly employed as a means of creating a fringe velocity. A Bragg cell is used to shift one of the dual beams thus creating a pattern of moving fringes.

The fringe movement, with the appropriate downshifting of the signal, allows measurement of reverse, low velocity, and highly turbulent flows.

The region of intersection of the two beams is referred to as the probe volume. Each beam must have a Gaussian intensity distribution and the volume created when the two beams intersect is an ellipsoid. As a particle crosses the probe volume two separate signals are produced. The Doppler signal, as discussed earlier, is produced by the relative motion of the particle with respect to the fringes. Also, a pedestal signal is created due to the Gaussian variation of the light intensity in the beams.

The Doppler signal is superimposed on the pedestal signal which can easily be filtered out since the pedestal frequency ranges from 0 to several kHz and the Doppler frequency is in the range of hundreds of kHz to Mhz. The total signal that is produced by a particle crossing the probe volume is termed a Doppler burst. The duration of the burst can be estimated by knowing the velocity of the particle and the dimensions of the probe volume. It is these bursts that are processed to obtain velocity information. [Ref. 1]

The signal to noise ratio (SNR) of a LDV signal is given by:

$$SNR = C \frac{\eta_q P_o}{\Delta f} [\frac{D_a D_e^{-2}}{r_a f}]^2 d_p^2 G V^2 \tag{3}$$

where η_q is the quantum efficiency of the photo detector, P_o is the laser power, Δf is the velocity bandwidth, d_p is the particle size, G is the scattering parameter, V is the visibility, D_a is the collection aperture, r_a is the focal length, D_{e-2} is the diameter of the intersecting region, and C is a constant of proportionality [Ref. 2]. It can be seen from the above equation that laser power or particle size can be increased to increase the SNR but power increases can be expensive and larger particles may not follow the flow accurately. Increasing the collection aperture by increasing the size of the collecting lens or increasing the diameter of the intersecting region by means of beam expansion are more popular methods of increasing the SNR.

The beam that is emitted from the laser source is vertically polarized and has a divergence angle of a few milliradians. It is essentially a parallel beam but also has a region of minimum diameter which is referred to as the waist. The light waves at the waist are plane waves therefore it is here that beam crossing is accomplished. If this is not the case, the fringes that are formed are curved instead of parallel which can cause errors in velocity measurement. To correct for this phenomenon, most systems install collimators before the beams are split to increase the parallelism of the beams.

The source of the LDV signal is totally dependent on the particles that are entrained in the flow. Although particles

4

that are naturally present in most flows are capable of producing LDV signals, artificial particle generation is generally used to produce particles of uniform size. It is highly desirable to have particles which have good reflective properties and the ability to closely follow the flow. Size becomes a critical factor in that the particles must be large enough to scatter light effectively yet small enough to avoid lagging through areas of high velocity gradients.

The introduction of particles to a flow is termed seeding and is accomplished by atomizers and fluidized bed generators. There are numerous types of seeding material which can be used depending on the application. Atomized water or oils can be used when uniform particle size is not critical. Solid particles in solution, such as polystyrene latex (PSL) particles in an alcohol solution, can be utilized to create particles of a more uniform size. This type of solution is introduced at a location such that the alcohol evaporates in the flow prior to the test section leaving only the solid particles.

Photo detectors convert the scattered light into a voltage. This voltage, which corresponds to the Doppler frequency, is used by the signal processor to obtain the velocity data. One of the more common types of signal processors used in LDV systems is the counter. A counter measures the frequency of the Doppler burst by measuring the time required for a number of cycles. For example, the time is

5

measured for 8 cycles in a signal. This time is then compared with the time for 5 cycles of the same signal. The ratio of the two times, in an ideal case, would be 5 to 8. An error limit is set on the ratio as a means of validation and if the time is within the preset limits, it is used to calculate the velocity. [Ref. 2]

The obvious advantage that LDV presents over conventional techniques such as pitot probes and hot wires is the ability to make measurements without disturbing the flow field. LDV is also ideally suited for precise measurement of single or multiple components of the velocity vector, needs no calibration, and can be used in a wide variety of fluids and flows. Despite many advantages, however, LDV does possess a unique set of problems such as the dependence on effective seeding, the cost of optical systems and signal processors, and the difficulty of correctly interpreting LDV data by statistical analysis.

B. HISTORICAL BACKGROUND

LDV was first used to measure the velocity of a flow field by Yeh and Cummins in 1964 [Ref. 3]. Since that time, a continuous effort has been made by the Aerodynamic community to develop and improve LDV as an invaluable means of accurate flow velocity measurement. As Stevenson [Ref. 4] points out in his historical review of LDV, advances have been focused on optical design, signal processing, and data analysis.

The first system used by Yeh and Cummins split the light emitted from a helium-neon laser into a measurement and a reference beam, as shown in Figure 1. This configuration was similar to a Mach-Zehnder interferometer but was difficult to use due to the inability to consistently align the various optical components. Around 1970, systems began to incorporate a differential Doppler arrangement which divided the beam into two parallel beams that could be focused at a point by a single lens as shown in Figure 2. Hanson [Ref. 5] theorized that a variation in the fringe spacing, which would effect the Doppler frequency, was a potential problem due to the Gaussian nature of the laser beam. Durst and Stevenson [Ref. 6] verified Hanson's theory experimentally and eliminated the unwanted variations by placing correction lenses between the laser and the beam divider.

Another optical advance has been the practice of decreasing the focused beam diameter by means of expanders inserted between the beam divider and the focusing lens as shown in Figure 3. Also, many advances have been made in the general construction of precise optical equipment which has led to refined LDV measurements.

Improvements in signal processing units have also played a large role in the development of LDV systems. Devices such as the frequency tracker, burst processor (counter), and the photo detector have been specifically designed to handle the
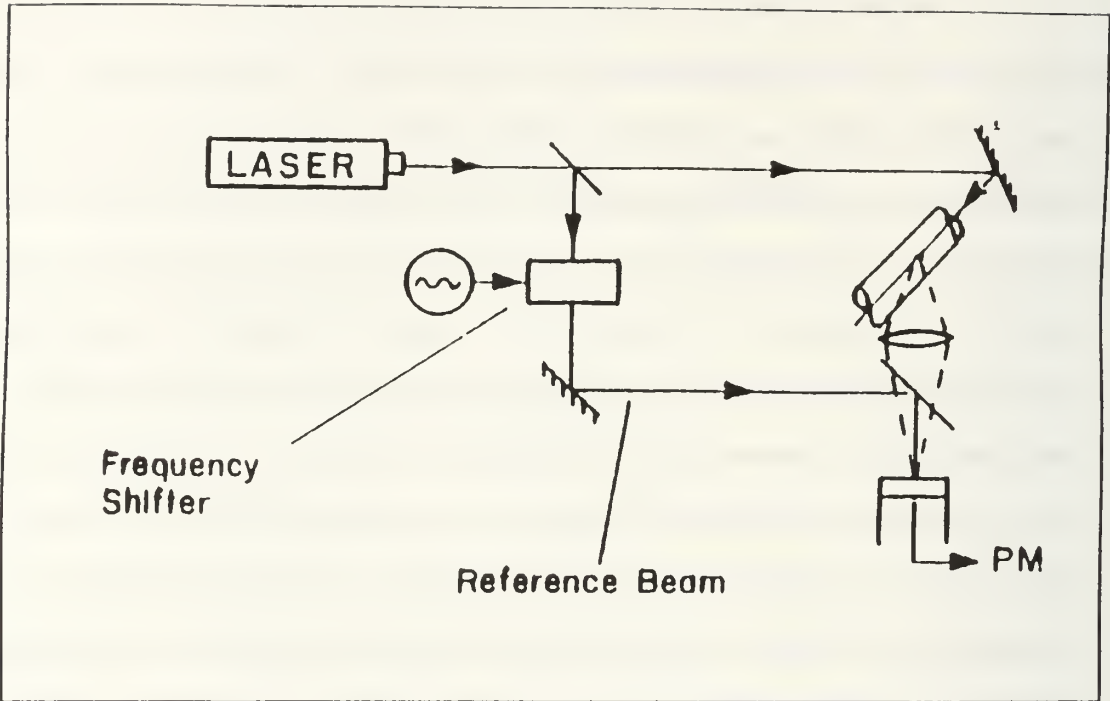
Figure 1. Yeh and Cummins System (1964), From Ref. 4
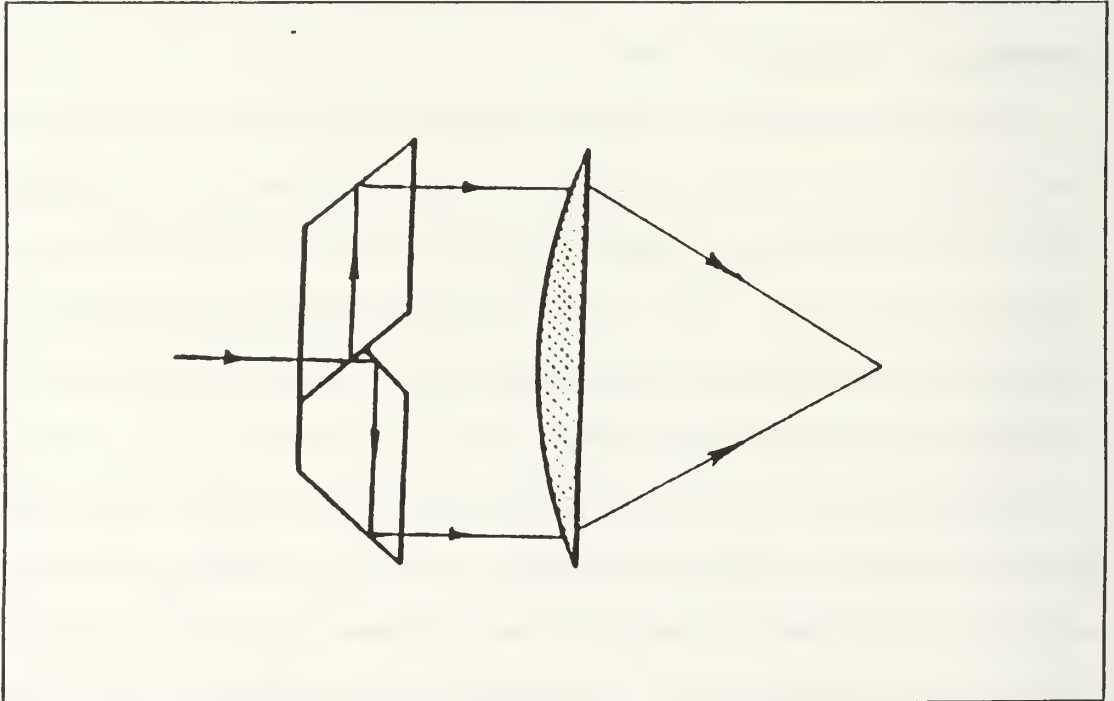
Figure 2. Single Prism Beam Divider, From Ref. 4

8
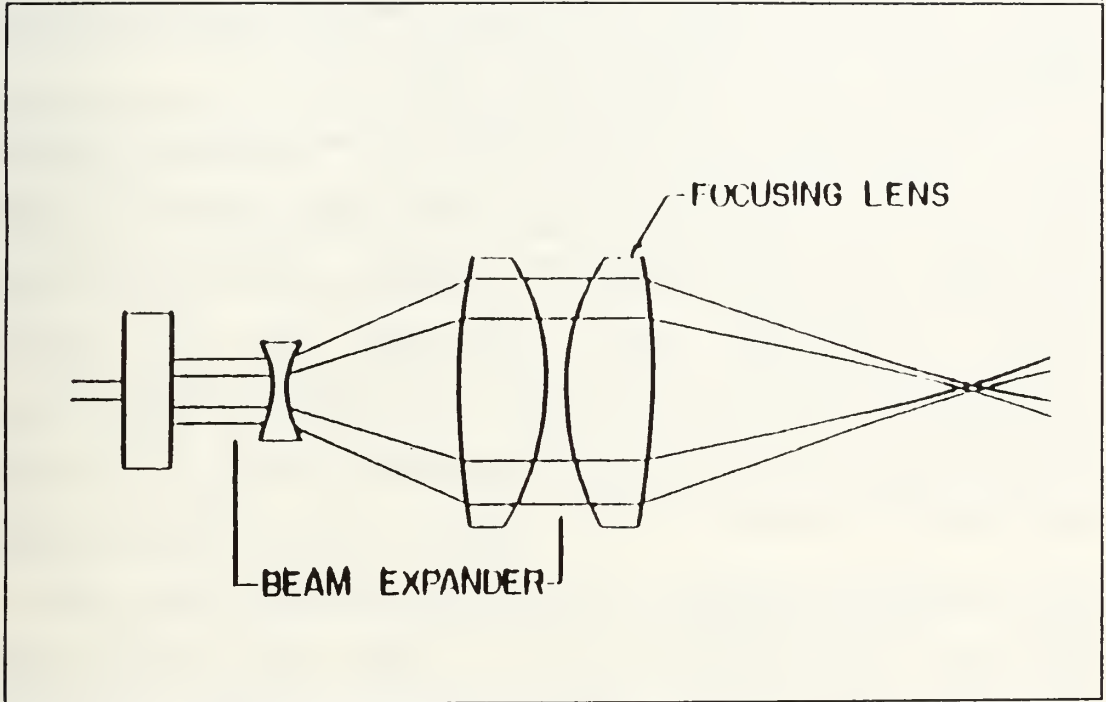
Figure 3. Beam Expander, From Ref. 4

signals encountered in LDV measurements. Early work with frequency trackers proved reliable up to about 50 MHz and with heavy seeding. Modern counters, however, allow the user to select the number of cycles to be counted and have a Doppler frequency limit of approximately 200 MHz. Photo detectors were first introduced as a means of obtaining measurements from low levels of scattered light around 1972. Improvements have continuously been made to the frequency capabilities and processing time of these units. [Ref. 7]

Data analysis can be divided into two general categories. First, corrections for velocity errors associated with seeding and probe volume size effects. Second, corrections for large errors associated with turbulence due to processor characteristics and the nature of the Doppler signal [Ref. 4]. Methods for correcting the velocity errors have included averaging to obtain a mean particle velocity and rejecting high amplitude signals to eliminate large particle lag time. McLaughlin and Tiederman [Ref. 8] used time averaging rather than particle averaging to eliminate velocity error. They theorized that more high velocity than low velocity particles would cross a probe volume over a given period of time which would lead to an incorrect mean velocity reading. Methods used to correct for errors in measured turbulence parameters have become well understood and are corrected by methods described by George [Ref. 9].

Refinements over the last twenty years have allowed LDV to become an integral part of a wide range of aerodynamic studies. LDV measurements, such as those performed by Goebel, Dutton, Krier, and Renie [Ref. 10], have documented the behavior of supersonic mixing layers. Supersonic separated flow in a compression corner has been investigated with the use of three-dimensional traversing LDV systems as in the work of Baroth [Ref 11]. Detailed studies of flows through turbomachinery have been performed such as the tests conducted by Ceman [Ref. 12] in which he used LDV to study air flows through a high-speed ducted fan. Precise airfoil evaluations and studies of trailing edge flows have also been presented as in the report of Absil and Passchier [Ref. 13]. Virtually every facet of aerodynamic flow, at velocities ranging from near stationary to well into the supersonic range, has been examined with the aid of LDV.

One area that has been studied intensely over the past five years is shock-boundary layer interaction. The current designs for turbofan engines, which are called upon to deliver high levels of thrust, require fan and leading compressor stage relative Mach numbers that are supersonic. The location and control of the shock systems in such stages is of great interest to the designers. A shock will likely form at the leading edge of each blade and will impinge on the suction side boundary layer of the adjacent blade as shown in Figure 4. This shock structure is termed a lambda-foot.
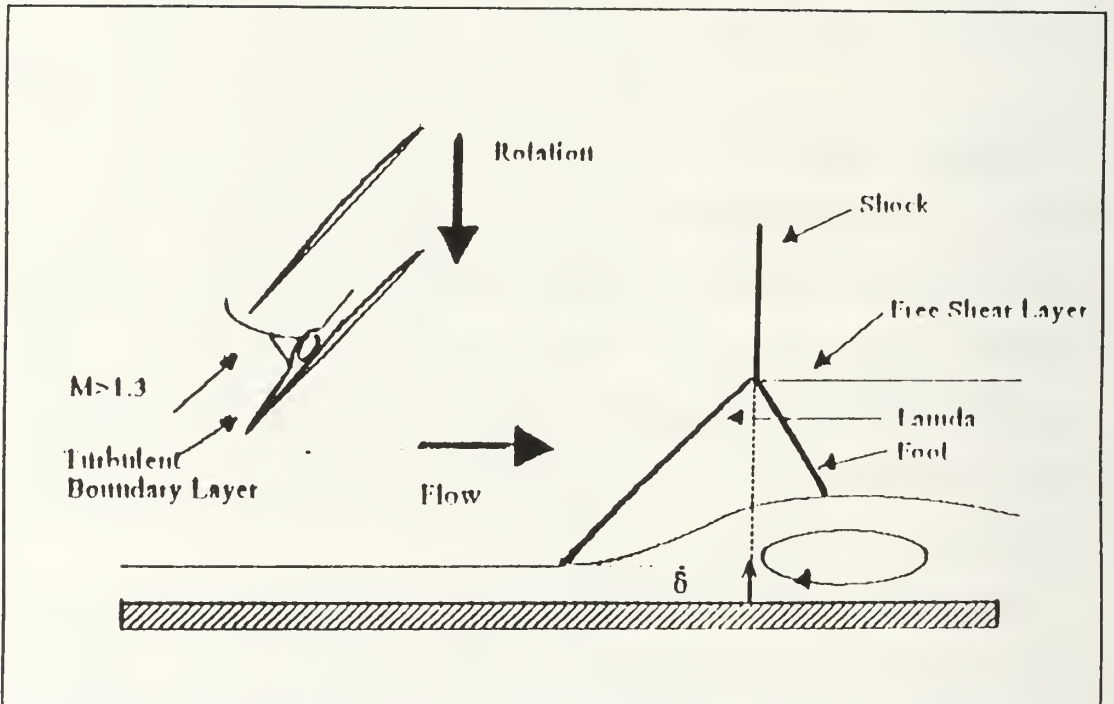
Figure 4. Shock-Boundary Layer Interaction, From Ref. 18

[Ref. 14] In order to understand and better control the losses associated with this type of shock system, detailed velocity measurements must be obtained in a non-intrusive manner. LDV is perfectly suited for this type of measurement.

Another aspect of LDV that has been studied in detail is particle dynamics in the flow field. Since the basis of LDV techniques is the measurement of particle velocity, it is essential that accurate models are developed to predict particle behavior in regions of instability or high velocity gradients. Studies done on particle lag prediction, Chesnakas and Andrew [Ref. 15], and particle dynamics effects on LDV measurements, Bloomberg, Dutton, and Addy [Ref. 16], have attempted to verify the accuracy of theoretical models used to predict particle behavior through planar oblique shocks.

C. PURPOSE

The purpose of the present work was to establish the capability to make LDV measurements in transonic flow. This would allow additional studies to be conducted in the area of shock-boundary layer interaction. The objectives of the present work focused on three areas. First, the existing supersonic tunnel located in the Gas Dynamics Laboratory (GDL) of the Naval Postgraduate School was refurbished, instrumented, and modified to allow introduction of seeding material. Secondly, a traversing LDV system capable of accurate one-dimensional velocity measurements was set up.

Finally, experimental LDV measurements were taken in the free stream, through the test section boundary layer, and across a normal shock.

II. EXPERIMENTAL APPARATUS

A. SUPERSONIC WIND TUNNEL

The wind tunnel used was a blow-down type supersonic tunnel located in the GDL at the Naval Postgraduate School. A photograph and schematic of the tunnel are shown in Figures 5 and 6, respectively. Supply air was produced by a 3 stage centrifugal compressor, dried, and stored at 150 psi in an 8000 cubic foot tank farm. A supply air schematic is shown in Figure 7.

Supply air at 150 psi was controlled to the wind tunnel by means of a pneumatic control valve. Additional supply air was regulated at 12-14 psi and routed to the valve to allow manual control. A pressure probe and absolute pressure gauge were installed at the top center of the plenum to allow precise control of plenum pressure. The plenum consisted of a cylindrical chamber approximately 20 inches in diameter containing a 9 inch diameter circular flat plate mounted perpendicular to the flow as shown in Figure 8. The plenum contained no other screens or flow straightening devices.

The contraction and circular to rectangular transition section had an area ratio of 5.7:1. Sets of interchangeable aluminum blocks could be attached downstream of the contraction to form the convergent-divergent nozzle and test

15
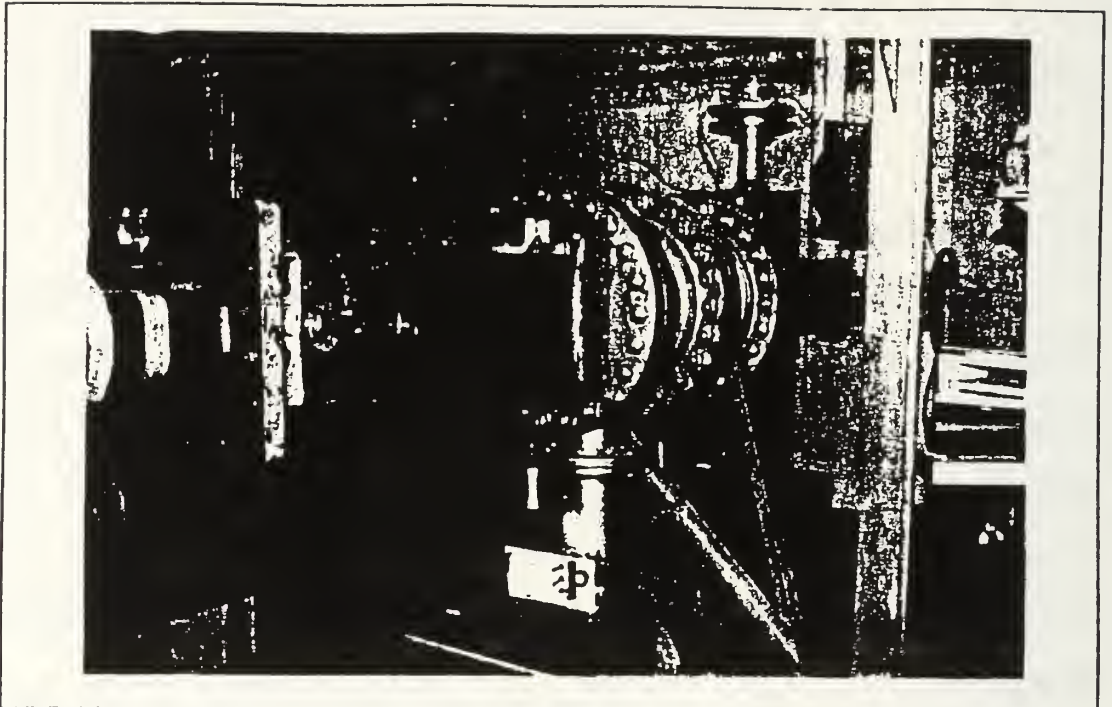
Figure 5. Supersonic Wind Tunnel
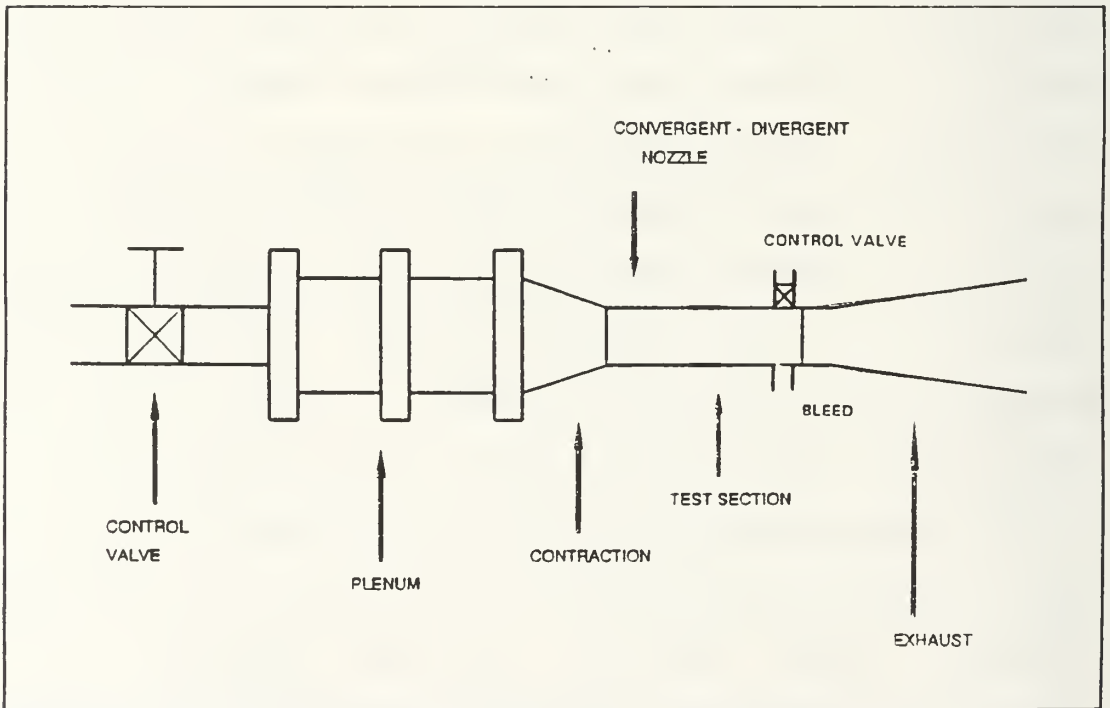
Figure 6. Schematic of Supersonic Wind Tunnel

16
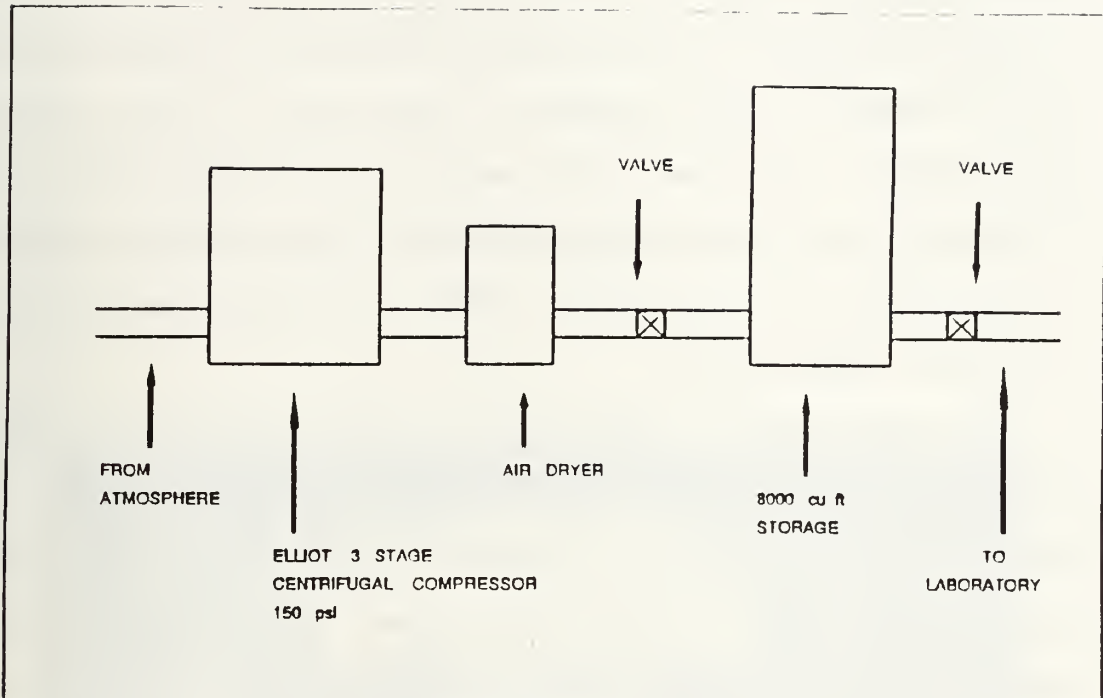
Figure 7. Supply Air Schematic
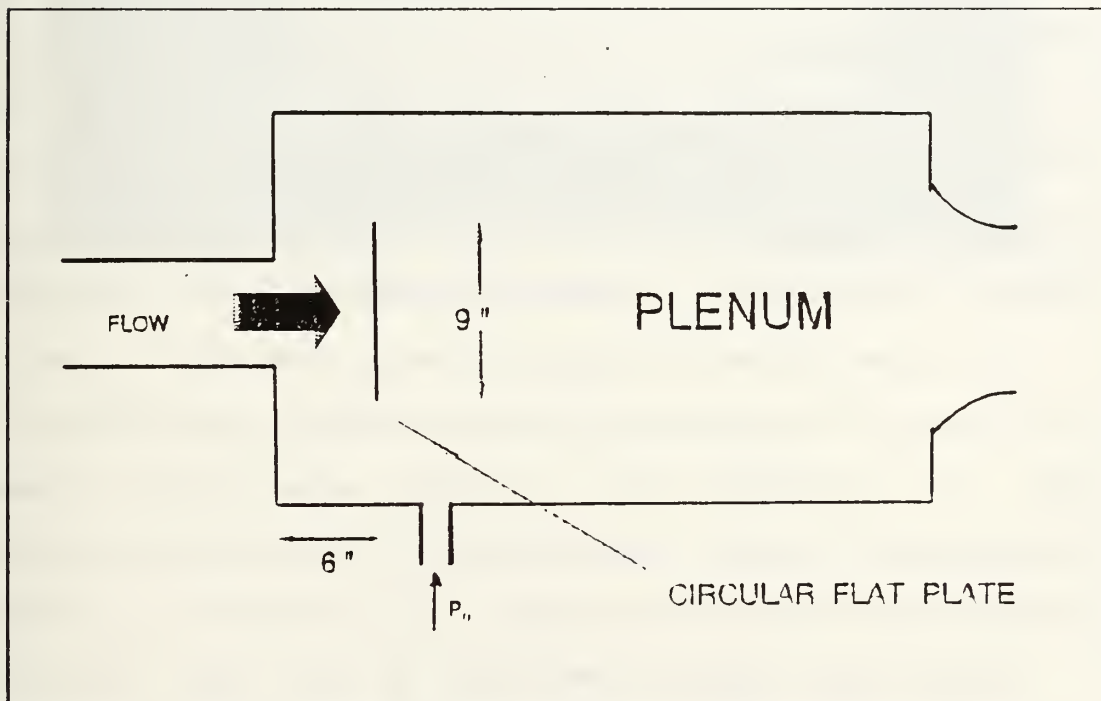
Figure 8. Plenum Configuration

17

section. The blocks, as shown in Figure 9, were comprised of an identical pair which were held in place, top and bottom, by two flat plates which formed the side walls of the nozzle and test section. There were four sets of blocks available in the laboratory, each designed to produce a specific Mach number in the test section. The nominal Mach 1.4 blocks were utilized throughout this study.

The test section measured 4 inches horizontally and 4 inches vertically. Optical access was provided by 6 inch diameter circular glass windows on each side of the test section side walls. Pressure ports were located upstream and downstream of the test section and metal blanks could be installed in the window frames to provide additional pressure ports across the test section. Pressure transducers were installed just upstream of the test section and on the plenum to record the pressure ratio during each run. Instrumentation and software for these transducers is discussed in Appendix A. Air was exhausted downstream of the test section through ducting to atmosphere outside the laboratory.

Run times, based on constant plenum pressure, varied from a minimum of 2 minutes with plenum pressure maintained at 30 psig, to a maximum of 4 minutes with plenum pressure maintained at 15 psig. Approximately 15 minutes were required between each run to allow supply air to build up to 150 psi.

Ports were opened downstream of the test section to relieve back pressure and allow the shock to travel past the
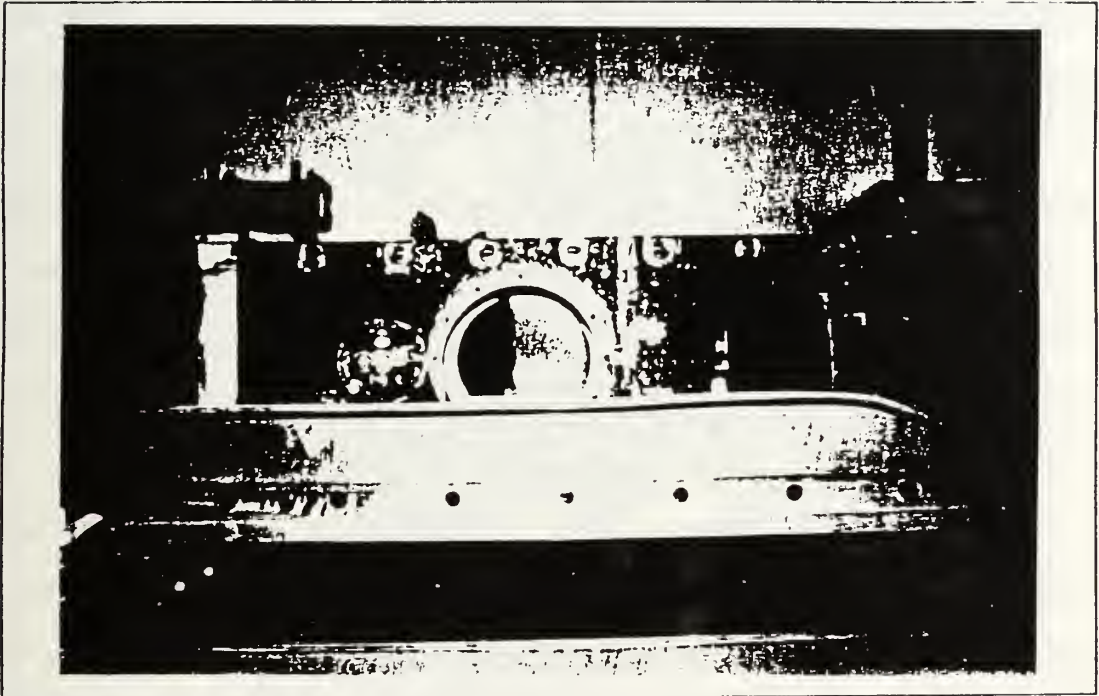
Figure 9. Mach 1.4 Nozzle Block

test section. A valve was installed on one of the ports as a means of controlling the back pressure and positioning the normal shock.

B. LASER DOPPLER VELOCIMETRY SYSTEM

   1.   Laser and Optics

The laser and optics used were the Lexel model 95 four-Watt argon-ion laser and the TSI four-beam, two color LDV system. The system was mounted on a TSI aluminum base which was attached to the bed of a commercial milling machine modified to serve as a traverse mechanism. The milling machine could be manually traversed in the X (streamwise), Y (vertical), and Z (horizontal) directions to allow surveying within the test section. A photograph of the laser, optics, and milling machine is shown in Figure 10.

Output from the laser was initially passed through a beam collimator to ensure that the waist, (minimum diameter of the beam), and the focal point coincided. The beam then entered the color separator which consisted of an attenuator, dispersion prism, and mirror set. The attenuator provided control of the beam intensity and the dispersion prism separated the laser beam into the two strongest color lines, the 514.5 nm (green) and 488 nm (blue). The mirror set then reflected the beams out of the color separator parallel to the base. For the present study, only one-dimensional velocity

20
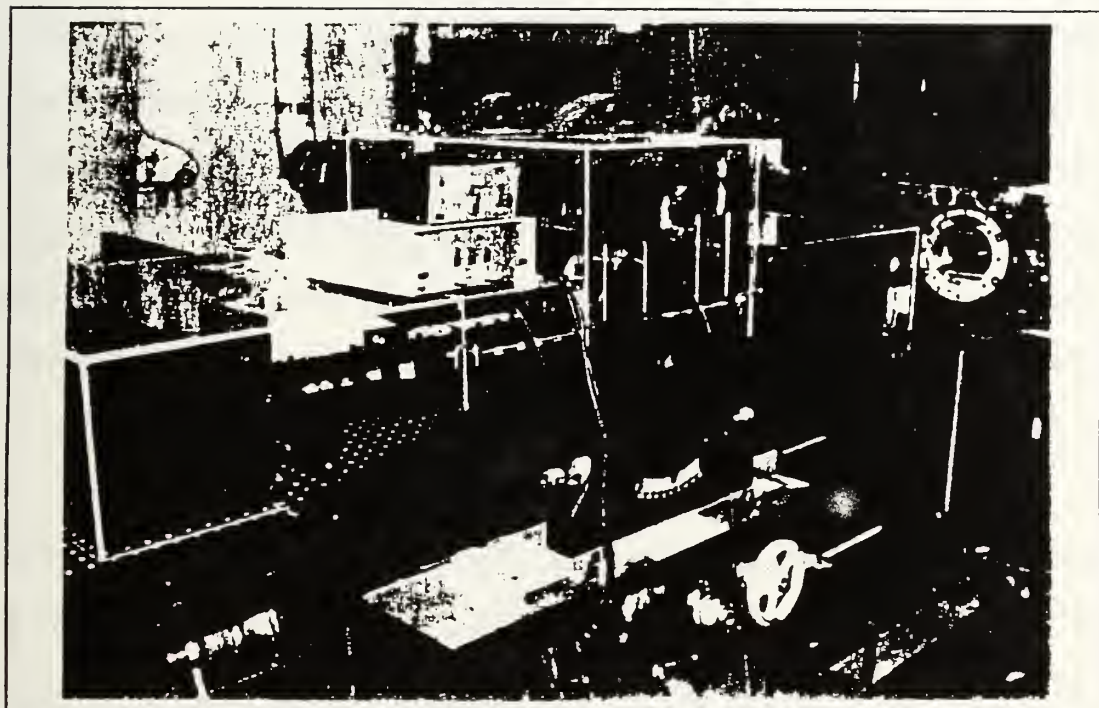
Figure 10. Laser, Optics, and Milling Machine

measurements were made therefore the green beam was blocked at this point allowing only the blue beam to continue.

After leaving the color separator the blue beam passed through a polarization rotator which ensured vertical beam polarity. The beam was then split in the horizontal plane to allow velocity measurements in the flow direction. A single beam was frequency shifted with the use of a Bragg cell causing the fringe pattern to move in the direction of the flow. The frequency was shifted 40 Mhz, but downshifting was not used. All data from histograms and statistics, therefore, had to be corrected for the 40 Mhz shift. Both beams passed through a divergence section (beam expander) which decreased the probe volume and increased the SNR. An end lens produced a focal length of 762 mm. [Ref. 17]

The optic configuration produced a 3.1 degree half angle and a probe volume that was 133 μm in diameter and 2.5 mm in length. Fringe spacing was 4.51 μm with 28 fringes in the probe volume. A TSI model 9160 photomultiplier system was used to collect the backscattered light after it passed back through the end lens and beam expander. [Ref. 17] A schematic of the laser and optics is shown in Figure 11.

2. Data Acquisition

Data acquisition was accomplished with a TSI model 1990C counter-type signal processor unit. The unit included an input conditioner, timer, digital readout, and data interface.

22
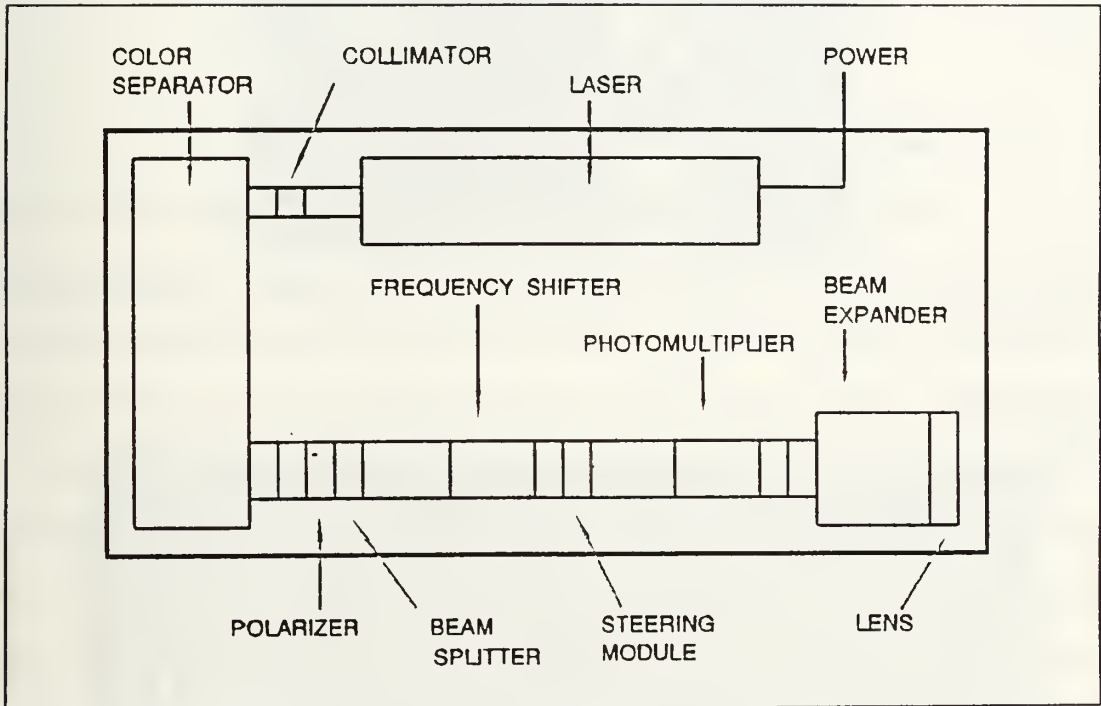
Figure 11. Schematic of Laser and Optics

Signals from the photodetector were sent to the processorwhich transformed the signal into voltages proportional to the Doppler frequency. The signal processor was interfaced with a 386 personal computer which utilized "FIND" software provided by TSI to analyze, present, and store the acquired data. The LDV software is discussed in detail in Appendix B. A photograph of the data acquisition system is shown in Figure 12.

3. Seeding

Seeding was accomplished with a TSI model 9306 six-jet atomizer. Designed specifically for LDV applications, the TSI atomizer consisted of a liquid reservoir, pressure regulator, atomizers, dilution system, and aerosol outlet. Regulated air was used to draw liquid droplets from the reservoir and impinge them on a spherical impactor which caused the formation of an aerosol that exited through the outlet. [Ref. 18]. A photograph and schematic of the atomizer are shown in Figures 13 and 14, respectively.

The TSI atomizer was capable of generating particles from virtually any liquid or suspended particle solution. The majority of work performed in the present study was done with a 2% solution of 1 μm sized polystyrene latex (PSL) particles suspended in alcohol. The particles were introduced into the flow at the contraction section, as shown in Figure 13. The outlet of the atomizer was tapered and fit with a 3/8 inch
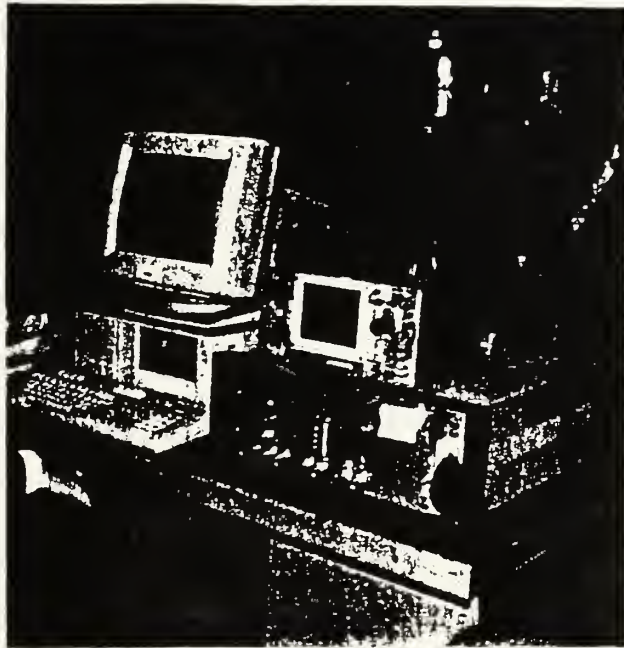
Figure 12. LDV Data Acquisition System
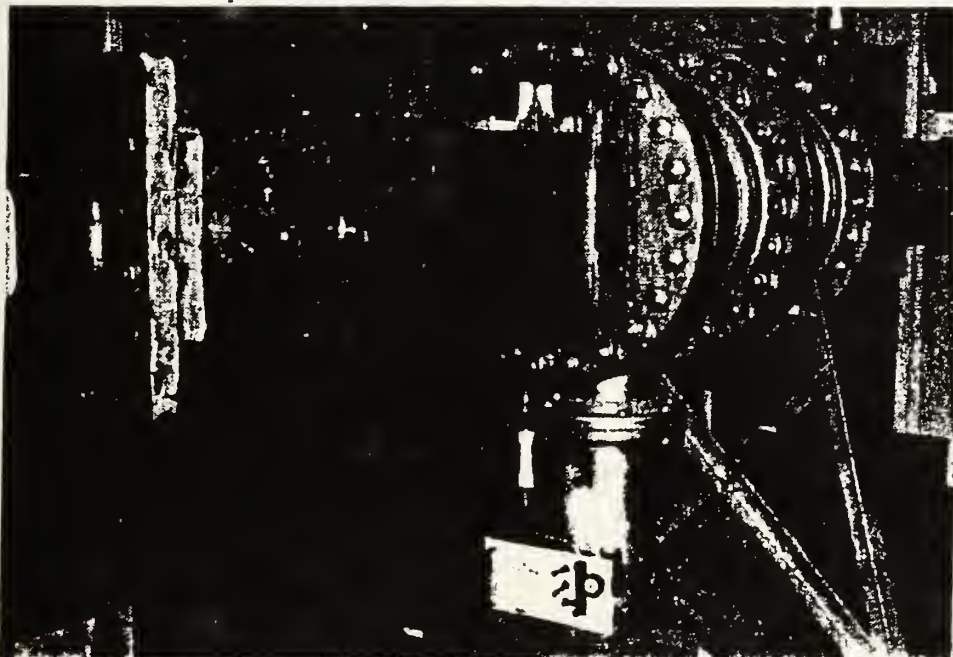
Figure 13. TSI Six-Jet Atomizer
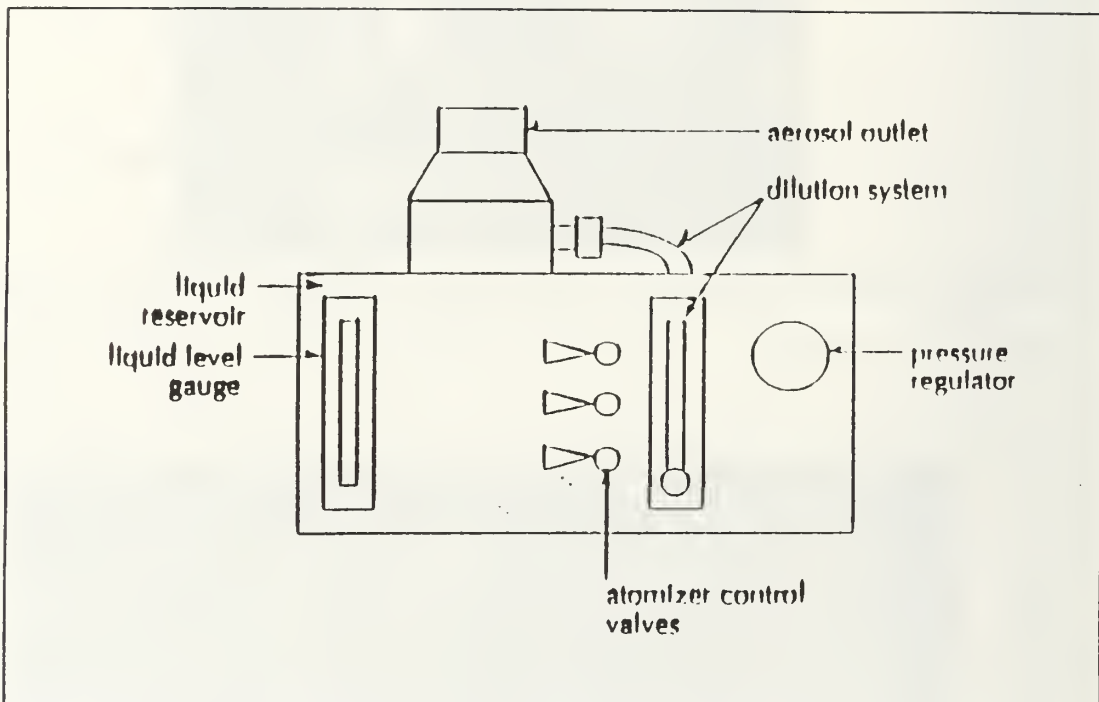
Figure 14. Atomizer Schematic, From Ref. 18

inside diameter aluminum tube, open at the end, and extending into the tunnel. The open end of the tube was positioned at the center of the flow. Typically, the atomizer was operated at a supply pressure of 65 psi with 0% dilution air.

Care had to be taken to ensure that the atomizer was not over pressurized either from the supply or outlet side. Each situation potentially caused spillage of seed material and in the latter case, prevented seed from entering the contraction section. To avoid both situations the supply pressure was regulated at a minimum of 40 psi (to overcome the tunnel back pressure on the atomizer) and a maximum of 65 psi.

C. SCHLIEREN SYSTEM

A schlieren system was utilized to record shock position and structure within the test section. A continuous or spark light source was available from a combination unit. The light source was directed to a parabolic mirror which reflected the beam through the test section. The light was then passed through a collimating lens, filter, and knife edge arrangement before entering the camera. Most photographs were impact shadowgraphs taken using the spark source without utilizing the filter or knife edge. A diagram of the arrangement is shown in Figure 15.
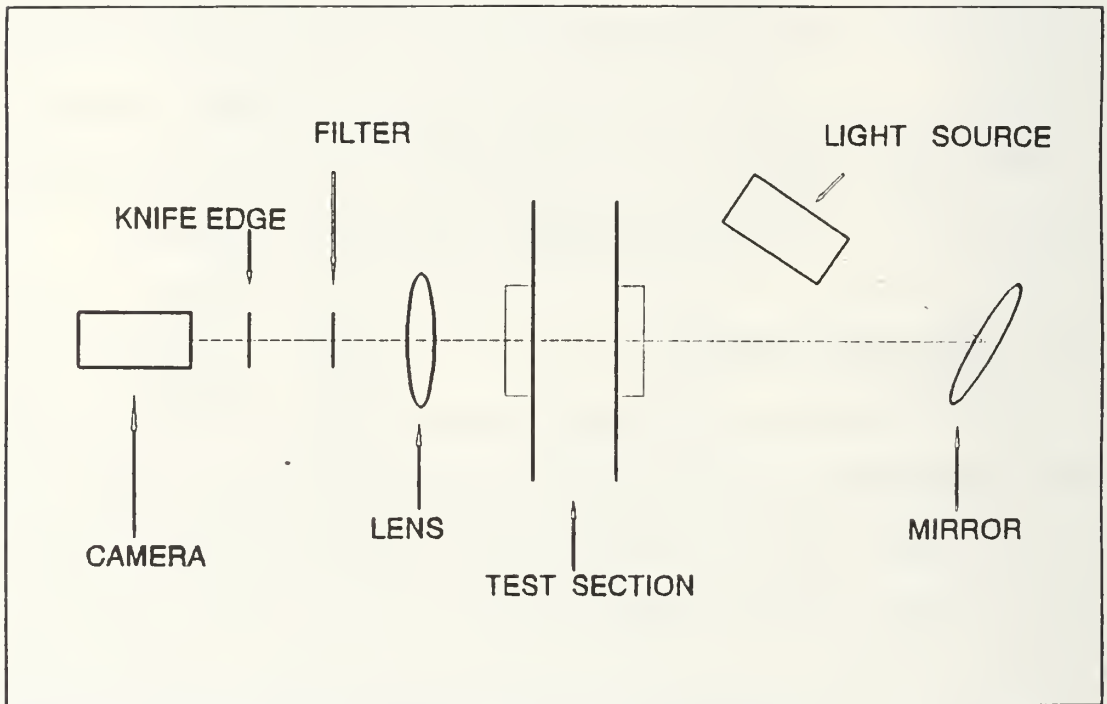
Figure 15. Schematic of Schlieren System

III. EXPERIMENTAL PROCEDURE

A. OVERVIEW

The objective of the present study was to perform LDV measurements, in back scatter mode, in transonic flow. The experimental procedure was divided into the following phases: apparatus set-up, schlieren visualization, and LDV measurements. Due to the limited run time of the supersonic tunnel, set-up procedures were critical in assuring that each run was valid, well documented, and efficient. schlieren visualization was used extensively as a means of determining experimental conditions prior to LDV measurements. Three types of LDV measurements were performed: free stream, boundary layer surveys, and normal shock surveys.

One of the main objectives during the experiment was consistent test section conditions. After the initial set-up, special attention was given to operating the tunnel under identical conditions for each subsequent run. This was accomplished by keeping plenum pressure and back pressure valve position constant for each run after the set-up.

B.   SET-UP PROCEDURES

1.   Wind Tunnel

Two set-up runs were required before LDV measurements could be performed. The tunnel was first run at a plenum pressure of 15 psig with the back pressure ports full open. This produced conditions such that the normal shock would travel downstream of the test section. The passage of the normal shock was observed visually. As the shock passed the test section, the back pressure valve was manually adjusted closed, moving the shock upstream, until the shock was positioned in the test section.

Knowing that the adjustments to the back pressure valve would restrict the flow while starting the tunnel and cause the stabilized shock position to change (locate further upstream) when the tunnel was restarted, the shock was visually positioned slightly downstream of the desired location. The tunnel was then shut down and run again with no adjustments to the back pressure valve to determine the shock position for subsequent runs.

Pressure transducers on the plenum (P_2) and test section (P_1) were calibrated after the set-up runs using the HP Data Acquisition/Control system and "SPEED_5" software as described in Appendix A. P_1 and P_2 were then calibrated just prior to each additional run. Several runs were performed with a temperature transducer installed in the plenum to measure the total temperature which was used to calculate static

30

temperature in the test section. Test section static temperature was used to calculate velocity and Doppler frequency which provided information used to adjust filter settings on the counter.

2. Schlieren

The set up of the schlieren system involved checking the alignment and spark source. Also, a wire and a metal pointer were attached to the exterior of the test section window. Since the position of the wire and pointer and the distance that separated them were known, the position of the normal shock could be exactly determined in all photographs. A small free jet nozzle was used to focus and adjust the schlieren optics prior to tunnel operation.

3. LDV and Data Acquisition

Initial alignments were performed on the LDV optics to ensure proper beam polarization and crossing. Additional periodic alignment checks were performed to maintain initial alignments. Proper beam alignment to the test section was also checked during the set-up phase to ensure that the beams were oriented parallel to the flow and the LDV optics were perpendicular to the test section.

Data acquisition set-up was accomplished utilizing "FIND" software as described in Appendix B and by manually setting processor filters. Cycles per burst, and timer

comparison were fixed throughout the study. The LDV and data acquisition systems were then checked by operating the atomizer "open air" and directing the probe volume into the flow. Data rate and histogram appearance were checked to ensure proper operation of the optics, processor, and software.

As previously mentioned, 40 Mhz shifting was used without downshifting. The 40 Mhz shift corresponded to a velocity shift of 180 m/s with fringe spacing at 4.512 μm. Therefore, all velocity data obtained from the LDV data acquisition system was corrected by adding 180 m/s. Since the values for turbulence intensity were a function of the mean velocity, turbulence intensity data was also corrected.

C. SCHLIEREN VISUALIZATION

After completion of set-up procedures, the tunnel was run for the purpose of recording shock position and movement by schlieren visualization. The LDV optics were removed from the field of view of the schlieren system by traversing the laser and optics base below the test section. The spark light source was powered and tested and high-speed film was preloaded into the camera.

The tunnel was allowed to start and stabilize at a plenum pressure of 15 psig before schlieren photographs were taken. Multiple photographs were shot during the run until plenum pressure dropped below 15 psig. The visual data was then

examined and recorded as a means of verifying shock position and determining the extent of shock unsteadiness (movement).

D. LDV MEASUREMENTS

1. Free Stream

Initial LDV measurements were made upstream and downstream of the normal shock at a midstream location. The tunnel was started and "SPEED_5" was run to monitor the plenum-to-test section pressure ratio. Seeding was introduced as the plenum pressure stabilized at 15 psig. All six atomizer jets were used with dilution air set at zero and supply pressure set at 65 psig.

Several single point measurements were taken upstream to verify supersonic flow at approximately Mach 1.4 and several single point measurements were made downstream to verify subsonic flow at approximately Mach 0.8. Processor filters were set at 100 Mhz (high) and 20 Mhz (low) for upstream locations and 50 Mhz (high) and 10 Mhz (low) for downstream locations. Cycles-per-burst was fixed at 4 and timer comparison was fixed at 5% throughout the entire study. Laser power was also a constant throughout the entire study at 3 Watts.

2. Boundary Layer Survey

After the LDV system was verified as accurate during the free-stream measurements, a boundary layer survey was

33

performed. The tunnel was, again, operated at 15 psig plenum pressure but a change was made to the seeding location. The outlet tube of the atomizer was lowered in the contraction to approximately the height of the test section lower wall in an attempt to introduce more seeding particles in the lower half of the test section.

The probe volume was manually positioned as close as possible to the lower wall of the test section at a point well upstream of the normal shock location. After the tunnel was started, seeding was introduced and the probe volume was traversed manually upwards in 0.02 inch increments through the boundary layer. Processor filters were set at 100 Mhz (high) and 10 Mhz (low) during the entire run. Plenum to test section pressure ratios were monitored throughout the run and the survey was ended when plenum pressure dropped below 15 psig.

3.   Shock Survey

The atomizer outlet was positioned in the middle of the contraction section and a shock survey was performed at a midstream location. Operation of the tunnel was identical to the boundary layer survey. Seeding was introduced after the plenum pressure was stable at 15 psig and processor filters were set at 100 Mhz (high) and 10 Mhz (low). The survey was started at a point upstream of the normal shock and traversed downstream of the shock in increments of 0.05 inches. The run was stopped when plenum pressure dropped below 15 psig.

34

IV. RESULTS AND DISCUSSION

A. OVERVIEW

The results of the present study are divided into four areas: schlieren visualization, free stream LDV measurements, LDV boundary layer surveys, and LDV surveys across the normal shock. Selected data from each area is presented as it applies to the overall results of the study. Tabulated data appears in Appendix D.

Wind tunnel runs were recorded by dating each run and identifying a particular run on a particular day by letter. For example, 030293a indicates the run was performed on March 3rd, 1993 and it was the first run of the day. All data, (schlieren photographs, pressure measurements, LDV files), are identified with a particular tunnel run.

Horizontal position in the test section was defined as inches downstream from the maximum upstream position of the probe volume. The maximum upstream position of the probe volume was restricted to 1.5 inches from the upstream side of the test section due to traverse table limitations. Vertical position in the test section was defined as inches from the bottom of the test section.

B. SCHLIEREN VISUALIZATION

Initially, schlieren visualization, using a continuous light source, was utilized to view the normal shock movement during tunnel operation. This established the fact that the normal shock was positioned on the far upstream side of the test section with plenum pressure set at 30 psig. Ports were opened downstream of the test section to relieve the back pressure. With the ports full open, the shock was observed to move downstream of the test section.

A valve was installed to control the back pressure and video recordings of the schlieren images revealed that the position of the shock could be controlled by means of back pressure. Closing the valve (increasing the back pressure) moved the normal shock upstream. It was eventually concluded from multiple test runs that the shock could be positioned in the test section by means of back pressure adjustment with the plenum pressure set at 15 psig. All subsequent runs were performed at 15 psig plenum pressure which approximately doubled the run times.

Spark source schlieren photography was used to obtain information on the movement and characteristics of the normal shock within the test section. Multiple photographs were taken during single runs to establish a maximum and minimum on the extent of shock movement. Figures 16 and 17 show 10 spark source photographs taken during run 030393b.
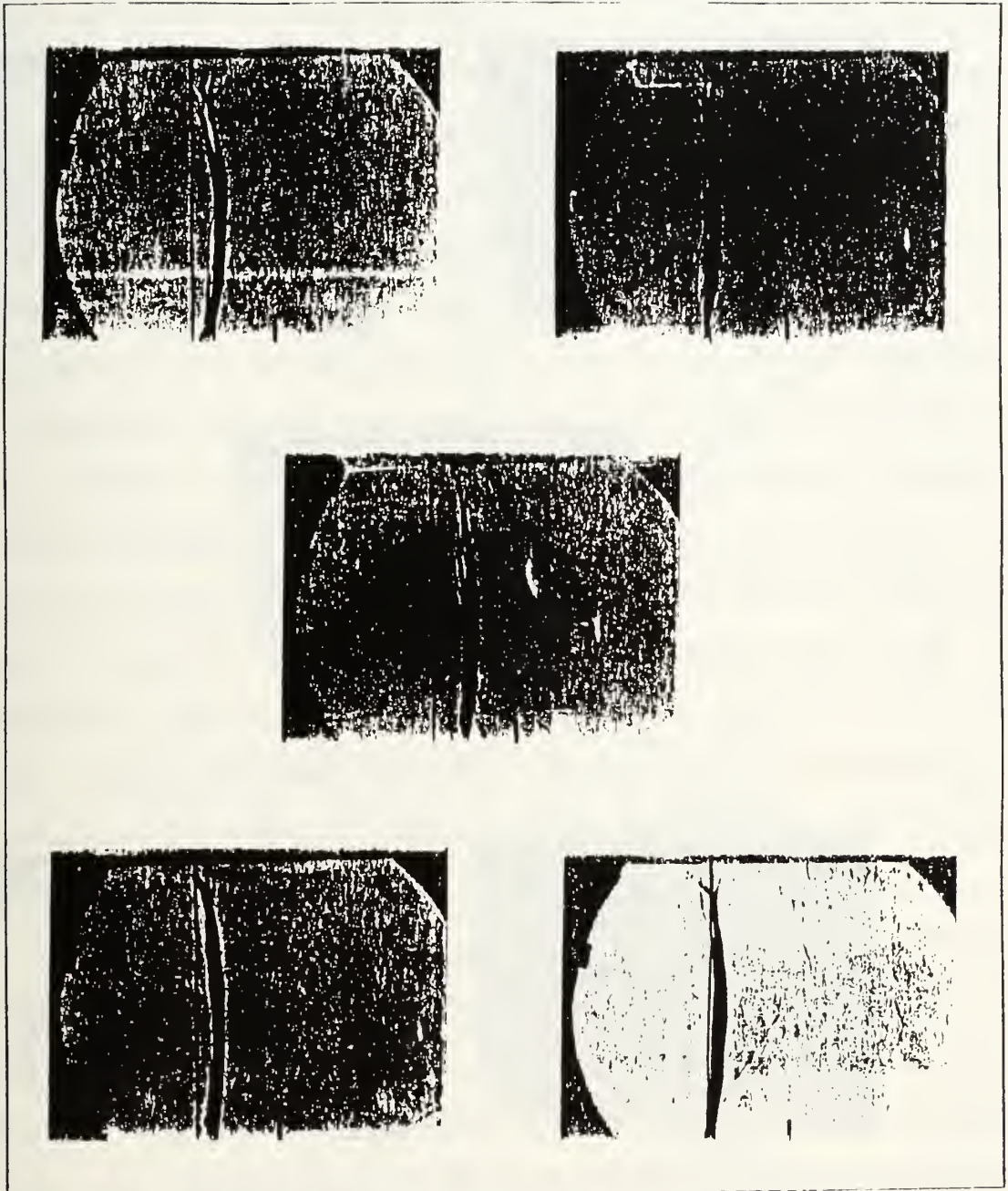
Figure 16. Spark Source Schlieren, Run 030393b
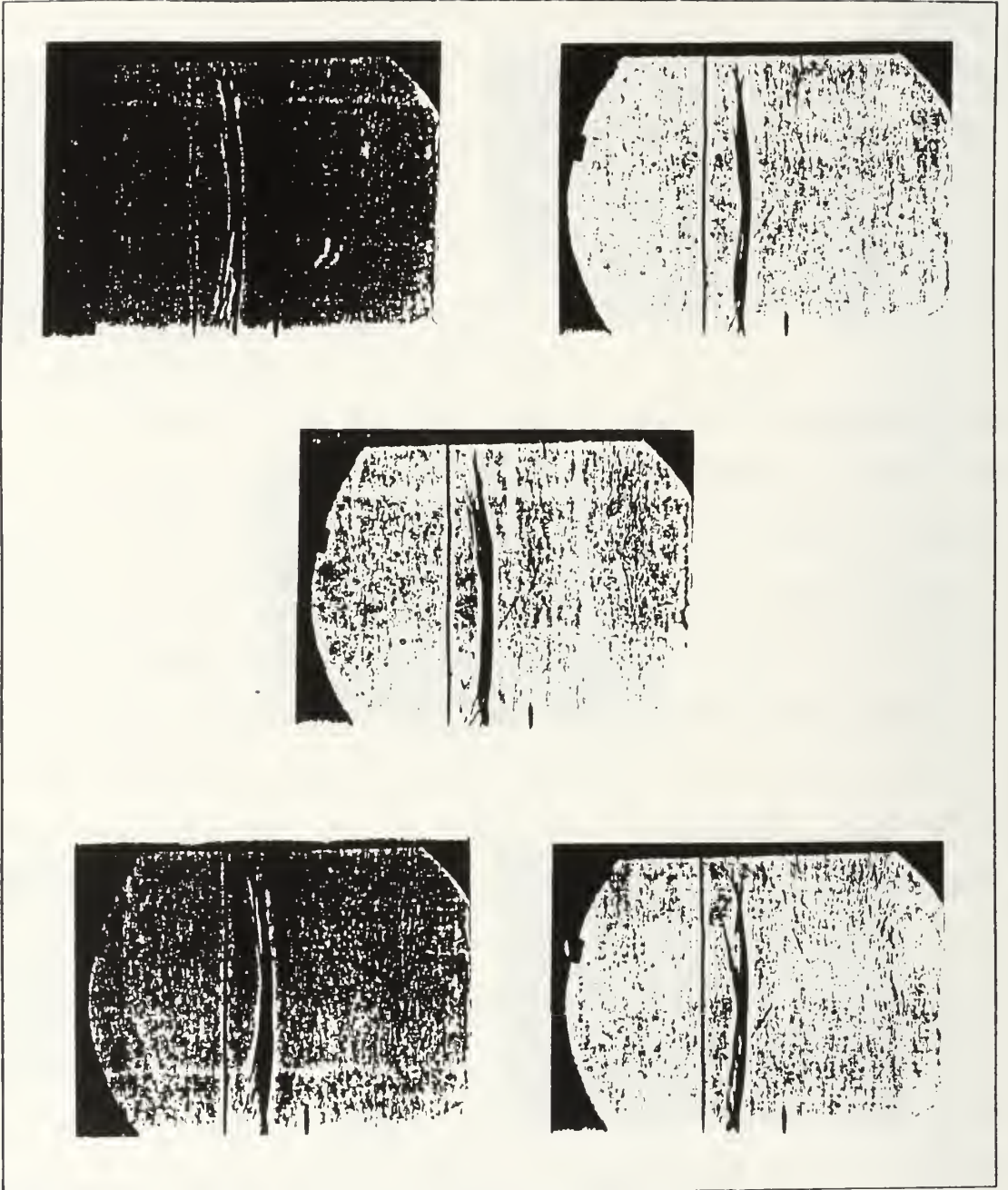
Figure 17.   Spark Source Schlieren, Run 030393b

The photographs clearly identify the normal shock. Position and scale could be obtained from the wire and pointer which were also clearly visible in the prints. The wire was at 0.75 inches and the pointer was located 1 inch downstream from the wire. The extent of the normal shock movement was therefore determined to be 0.5 inches with a maximum upstream position of 0.75 inches and a maximum downstream position of 1.25 inches. Although the position of the shock varied from run to run, the extent of movement was found to be almost constant.

Multiple exposure photography was attempted during several runs. Figure 18 shows a triple exposure taken during 030593a. An upstream position of the shock is clearly identifiable. The downstream shock image appears darker on the actual photograph which indicates that two exposures captured the shock in essentially the same position. It was found, however, that the print became overexposed with more than two exposures, therefore this type of visualization proved to be of limited value.

The resolution in most of the photographs was adequate enough to accurately determine position and structure of the shock. The lambda foot of the normal shock was clearly identified in some photographs. Figure 19 shows a well defined lambda foot at the top of the test section where the normal shock interacted with the boundary layer.

Figure 18. Triple Exposure Spark Source Schlieren Photograph, Run 030593a
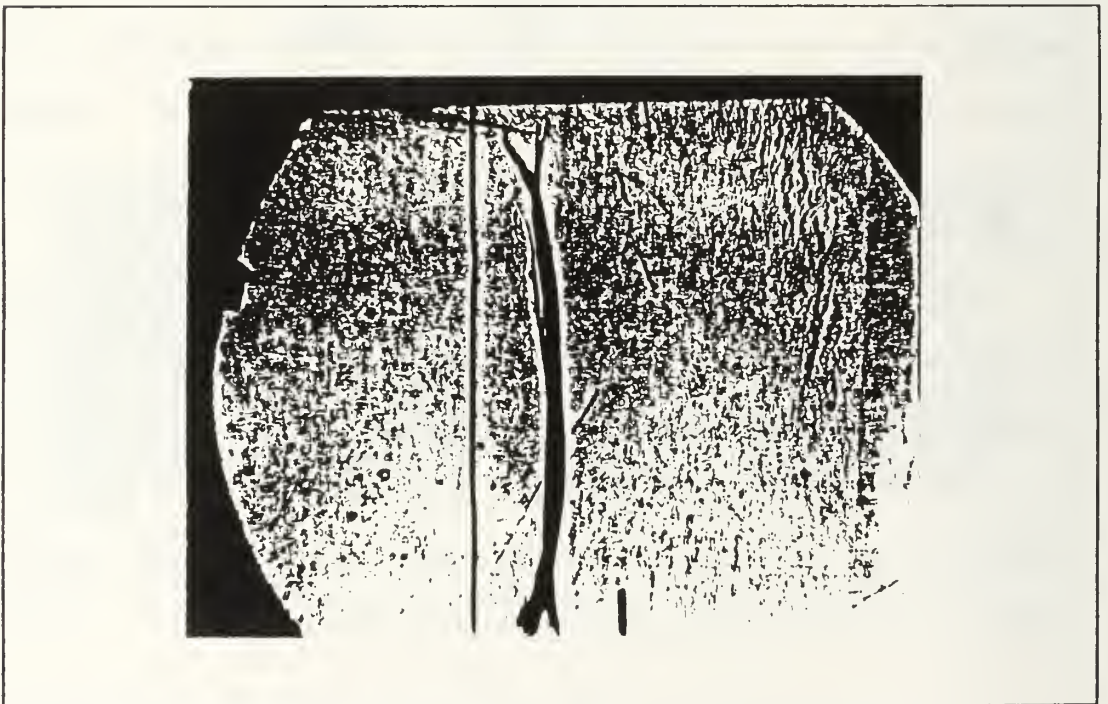
Figure 19. Spark Source Schlieren, Run 030493a

C. FREE STREAM LDV MEASUREMENTS

Several upstream and downstream LDV measurements were taken at a midstream location with the shock positioned in the middle of the test section. These runs were performed to determine the accuracy of the LDV data and as a means of finetuning the LDV and data acquisition systems. Filter settings on the processor were 100 Mhz (high) and 20 Mhz (low) upstream of the shock and 50 Mhz (high) and 10 Mhz (low) downstream of the shock.

The ratio of total plenum pressure to static test section pressure (upstream of the shock) was acquired by the tunnel data acquisition system and processed as described in Appendix A to determine upstream Mach number. A printout of the tunnel data acquisition system results are shown in Figure 20. The data indicates a rise in P_2 (plenum pressure) as the tunnel was started. A P_2 reading of 34 psia corresponded to a plenum pressure of 20 psi (as read from the plenum pressure gauge). When the normal shock passed the upstream side of the test section, as indicated by the abrupt decrease in P_1, the flow in the upstream side of the test section became supersonic, as shown in the Mach column of the printout.

Pressure measurements show the upstream Mach number to be stable at approximately 1.35. Each line of data on the printout was generated in about 5 seconds. By counting the number of lines in the printout at a constant plenum pressure, a rough approximation of run time can be calculated.

P2	P1	Pratio	Mach	Length
14.8964	14.9799	1.00051029300	.03 0105901101	1 015 3006077
14.8748	14.9792	.99970420517	.02005 056 70601	1. 10104570697
14.8868	14.9764	1.09069909307	.011509 7505060	1 0005 1100 532
14.098	14.8744	1.001586610627	.04 7505 77 3501	1 0007 7500503
14.899	14.9849	1.00080681071	.03590 261 716 76	1. 111047 7 1405
14.8908	14.8904	1.00069090591	.01504111 2167	1 0007 7371707
14.9924	14.8776	1.09032263269	.02146 5474 11606	1 707 31570701
14.9044	14.9841	1.0006719443G	.0700 7656 26637	1 351 77171790
14.8964	14.89	1.00110715054	.0 3907771 7406 31	2 1001 66 10076
15.034	14.909	1.01526207053	.1120506 15094	0 7759 7054177
15.3504	14.4344	1.06345951330	.207 70952 7100	10. 7597131901
16.2396	13.2948	1.22241960737	.547409 7694907	71 7 7070541
22.1212	11.7476	1.88303991007	.997 503514152	67. 7119436099
28.7608	9.5324	3.37077492851	1.4406199543	90. 7529 7 10061
35.524	10.9012	3.25972381027	1.41691669500	99. 7526 486269
32.6648	11.2928	2.99509696175	1.7 7209 51 7029	97 9119415031
33.7224	11.206	3.00931643762	1.36009 7 39067	95 57 70049671
34.5652	11.5992	2.97996413546	1.357097070064	95 7 7970106 76
34.5112	11.6372	2.965593098	1.319509 1079	95 01 0576 1950
34.474	11.6084	2.96974604597	1.7505 19409 31	95.0761902955
34.3836	11.662	2.94834505231	1.745709 519174	94. 747 70119501
34.5116	11.6372	2.96562747853	1.319069655756	95.01 30634071
34.4944	11.6424	2.95196669482	1.7196745099 3	91. 9569699919
34.5212	11.6276	2.968901579	1.350 71219111	95. 0677 479096
34.6424	11.6464	2.97151573010	1.7516 7604667 7	95. 1401 589342
34.3852	11.6016	2.96383257482	1. 3490 7975 6169	94 9955774 779
34.3494	11.59	2.96362391363	1. 3490 7701917	94 99 7 7 17 9979
34.4556	11.572	2.97719740754	1.357 599177 79	95 1946 735051
34.2792	11.6096	2.9526599677	1. 7416 75051 770	94 91 76 1 9 9675
34.2452	11.6112	2.94932179986	1.74953744065	94. 7571 161 764
34.2894	11.5772	2.96102684587	1.7 49 705 79175	94. 947 17 95201
34.1736	11.5652	2.95486459378	1.7169900715	94 91 7504564
34.3648	11.5472	2.97602982084	1. 7570 1 756069	95 1771 7531516
34.2412	11.4944	2.97094626949	1.352 7503030 7	95. 2167 79709
34.1844	11.496	2.9735908142	1.3514577419	95 1769026303
34.3056	11.5208	2.97770988176	1. 70 7160916 75	95. 19 70161 7 75
34.2504	11.4688	2.98639787946	1. 354591 70000	95. 730 7501 7 7
34.1292	11.484	2.97199132706	1.751 0 70607 75	95. 10901 33007
34.4712	11.4752	3.00397378695	1. 7507 7 7967 7 17	95.5905 7 97164
34.1244	11.4728	2.97437417195	1. 7516 17 30607	95. 11697 57159
34.064	11.4596	2.97252958218	1. 75119165 707	95. 1 107 759792
34.052	11.6644	2.97023838282	1. 3506 39170 70	95 09 77167959
33.9248	11.4676	2.95931731626	1.347 77 591051	91. 700 7660607
34.17	11.4356	2.9980 3775 703	1.7 7 10 47 7 37606	95. 3551 297097
33.7956	11.4484	2.95199329164	1.316192 7700	91 99 57 76 3516
34.0092	11.3832	2.98766603416	1. 75406 700 797	95. 7196 365006

Figure 20.   "SPEED_5" Output

Free-stream LDV measurements indicated an upstream velocity of 390 m/s. By knowing the value of plenum stagnation temperature (typically 48 F) and substituting the measured LDV velocity over the speed of sound for the Mach number, the test section upstream static temperature and Mach number could be calculated as follows:

$$M = \frac{V}{\sqrt{\gamma R T}} \tag{4}$$

$$\frac{T_o}{T} = 1 + \frac{\gamma - 1}{2} M^2 \tag{5}$$

$$T_0 = T + \frac{V^2}{2C_p} \tag{6}$$

$$T = T_0 - \frac{V^2}{2C_p} \tag{7}$$

$$M = \frac{V}{\sqrt{\gamma R \left(T_0 - \frac{V^2}{2C_p} \right)}} \tag{8}$$

The Mach number calculated from LDV measurements and the methodology described above was 1.36 which was within 1% of the Mach number calculated from pressure measurements.

Free-stream LDV measurements indicated a downstream velocity of 270 m/s. Using the same method as shown above, a Mach number of 0.86 was calculated downstream of the normal shock. The expected downstream value obtained from normal shock tables was Mach 0.76. The difference between the measured and the theoretical values is at least partially due to the boundary layer growth in the test section downstream of the shock. The tunnel was poorly designed in that no allowances were made for boundary layers which form on all walls. The boundary layers create a contraction in the test section which must cause the subsonic flow downstream of the shock to accelerate. Because of this effect, a Mach number higher than that shown in the normal shock tables could be expected.

D. LDV BOUNDARY LAYER SURVEYS

Boundary layer surveys were performed to characterize the flow in the test section. All surveys were done between midstream and the bottom surface of the test section with the normal shock positioned well downstream. The probe volume was positioned as close to the wall as possible and traversed upwards. Overlapping surveys were done starting below midstream and traversing down into the boundary layer.

Several problems were encountered while conducting the boundary layer surveys. First, limited run time prevented taking surveys of more than approximately 12 points. This

limited the amount of survey travel with small increments between each point. Secondly, positioning the probe volume near the wall by visual methods was less than exact. Due to the nature of the beams and the theoretical assumption that the velocity measurement is taken at the center of a probe volume with finite diameter, obtaining a velocity measurement at the wall is impossible.

The probe volume diameter created by using the TSI model 9169-750 lens was 133μm [Ref. 19]. If the probe volume was resting on the wall, the velocity measurement were actually taken at a height of 66.5μm or 0.0026 inches (1/2 the probe volume diameter). Also, since the beams were waisted, the entire probe volume had to be positioned at a finite distance above the center of the wall in order for the beams to clear the wall as they entered the test section. This distance was approximately 0.0004 inches [Ref. 19]. Thus, when the probe volume was placed as low as possible in the test section, the approximate distance from the wall to the center of the probe volume was .003 inches.

Figures 21 and 22 show the results of boundary layer surveys 031693a and 031693b, respectively. In 031693a, the traverse was upwards from the wall and in 031693b the traverse was downward from 0.2 inches, to overlap measurements taken in 031693a. Both surveys were made with the normal shock positioned downstream of the test section.

45

```
Velocity in M/SEC
Data is from the following files:
031693a.1.9

        Y(in)       U-MEAN        U-TURB
                   CORRECTED     CORRECTED
        0.02          299          14.7
        0.04          365          7.3
        0.06          376          7.8
        0.08          385          6
        0.1           387          6.5
        0.12          387          6
        0.14          387          6
        0.16          390          5.5
        0.18          393          4.6
```

Figure 21.   Boundary Layer Survey 031693a

```
Velocity in M/SEC
Data is from the following files:
031693b.1.11

        Y(in)       U-MEAN        U-TURB
                   CORRECTED     CORRECTED
        0.2           391          7.6
        0.18          392          6.7
        0.16          389          7.5
        0.14          388          7.8
        0.12          384          7.5
        0.1           377          8.3
        0.08          366          7.8
        0.06          357          8.3
        0.04          304          10
        0.02          304          11.2
        0            226.2         12.2
```

Figure 22.   Boundary Layer Survey 031693b

The extent of the boundary layer was determined by analyzing not only velocity distribution but also turbulence intensity changes. The boundary layer edge velocity was established in the free stream LDV measurements as approximately 390 m/s. An examination of the velocity distribution in 031693a and 031693b indicated a boundary layer thickness of between 0.18 inches. The turbulence intensity measurements taken in 031693a and 031693b, which should theoretically increase in the boundary layer, supported the velocity data in that they indicated a similar boundary layer thickness. In general, the data obtained from the boundary layer surveys was repeatable and indicated a surprisingly small turbulent boundary layer.

The data obtained in both surveys were normalized and compared with theoretical predictions as shown in Figures 23 through 26. Experimental u/U_e was calculated as the ratio of measured velocity to free-stream velocity. The outer edge of the boundary layer, δ, was defined as the value of y for which u/U_e was 0.99. The theoretical value of u/U_e was calculated from the 1/7 th power velocity distribution law [Ref. 20]:

$$\frac{u}{U_e} = (\frac{y}{\delta})^{\frac{1}{7}} \qquad (9)$$

which is used to model the velocity profile in the boundary layer on a flat plate. The displacement thickness, δ^*, which

y(in) NORMAL	U MEAN CORRECTED	U TEMP CORRECTED	EXPERIMENT u/U	THEORY y·(U/ν)
1	372	1.6	1	1
0.89071038	390	5.5	0.??????????	0.??????????
0.78142076	345	6	0.??????????	0.??????????
0.67213114	309	6	0.??????????	0.??????????
0.54284153	387	6.5	0.??????????	0.??????????
0.45355191	395	6	0.??????????	0.??????????
0.34426229	376	?.8	0.??????????	0.??????????
0.29497267	365	7.?1	0.??????????	0.??????????
0.12568306	299	10.?	0.??????????	0.??????????
0	0		0	0

EXPERIMENT (1-u/U)	DISPLACEMEN THICKNESS	EXP (1-u/U)u/U	MOMENTUM THICKNESS
0	0.00041713	0	0.??????????
0.00763350	0.00097331	0.00757571	0.??????????
0.01017811	0.00111236	0.01007452	0.??????????
0.01017811	0.00139045	0.01007452	0.??????????
0.01526717	0.00194663	0.01503408	0.??????????
0.02035623	0.00347613	0.01994185	0.??????????
0.04325699	0.00625703	0.04138582	0.??????????
0.07124681	0.01696352	0.06617021	0.??????????
0.23918575	0.07787232	0.18192592	0.??????????
1	0	0	0

Dis thick= 0.11040893

Mom thick= 0.03998672

Shape fac= 2.76112127

Figure 23. Normalized Boundary Layer Data and Calculations, 031693a, Near Wall to Free-Stream

48

Figure 24. Boundary Layer Survey, 031693a, Near Wall to Free-Stream

Y(in) NORMAL	U MEAN CORRECTED	U ??? CORRECTED	EXPERIMENT u/U	THEORY u/U
1	392	7.7	1	1
0.82471030	392	7.75	0.?????????	0.?????????
0.73142026	308	7.0	0.?????????	0.9?????708
0.67213114	304	7.?5	0.?????????	0.9???????5
0.56204158	327	8.?	0.?????????	0.?????????
0.45355191	364	7.9	0.?????????	0.?????????
0.34426229	357	8.?	0.?????????	0.?????0?7?
0.234972267	334	1?	0.?????????	0.?1???????
0.12568306	341	11.?	0.?????????	0.?????????
0.01639344	276	12.?	0.?????????	0.?????????
0	0		0	0

EXPERIMENT (1-u/U)	DISPLACEMEN THICKNESS	EXP (1-u/U)u/U	MOMENTUM THICKNESS
0	0.00041820	0	0.0004141??
0.00765306	0.00097580	0.00759449	0.0009264??
0.01020408	0.00167200	0.01000795	0.00166449?
0.02040016	0.00320620	0.01799167	0.00310342?
0.03826530	0.00571540	0.03680107	0.00539499?
0.06632653	0.00850340	0.06192732	0.00702733?
0.08928571	0.01296420	0.08131377	0.01133?29?
0.14795918	0.02077060	0.12606726	0.0166?7?4?
0.23214285	0.02885580	0.178?5?5?	0.0?11??3?6
0.29591836	0.01062228	0.20035068	0.004?2????
1	0	0	0

Dis thick= 0.09370469

Mom thick= 0.07014751

Shape fac= 1.33582??6

Figure 25.   Normalized   Boundary   Layer   Data   and
Calculations, 031693b, Free-stream to Wall

50
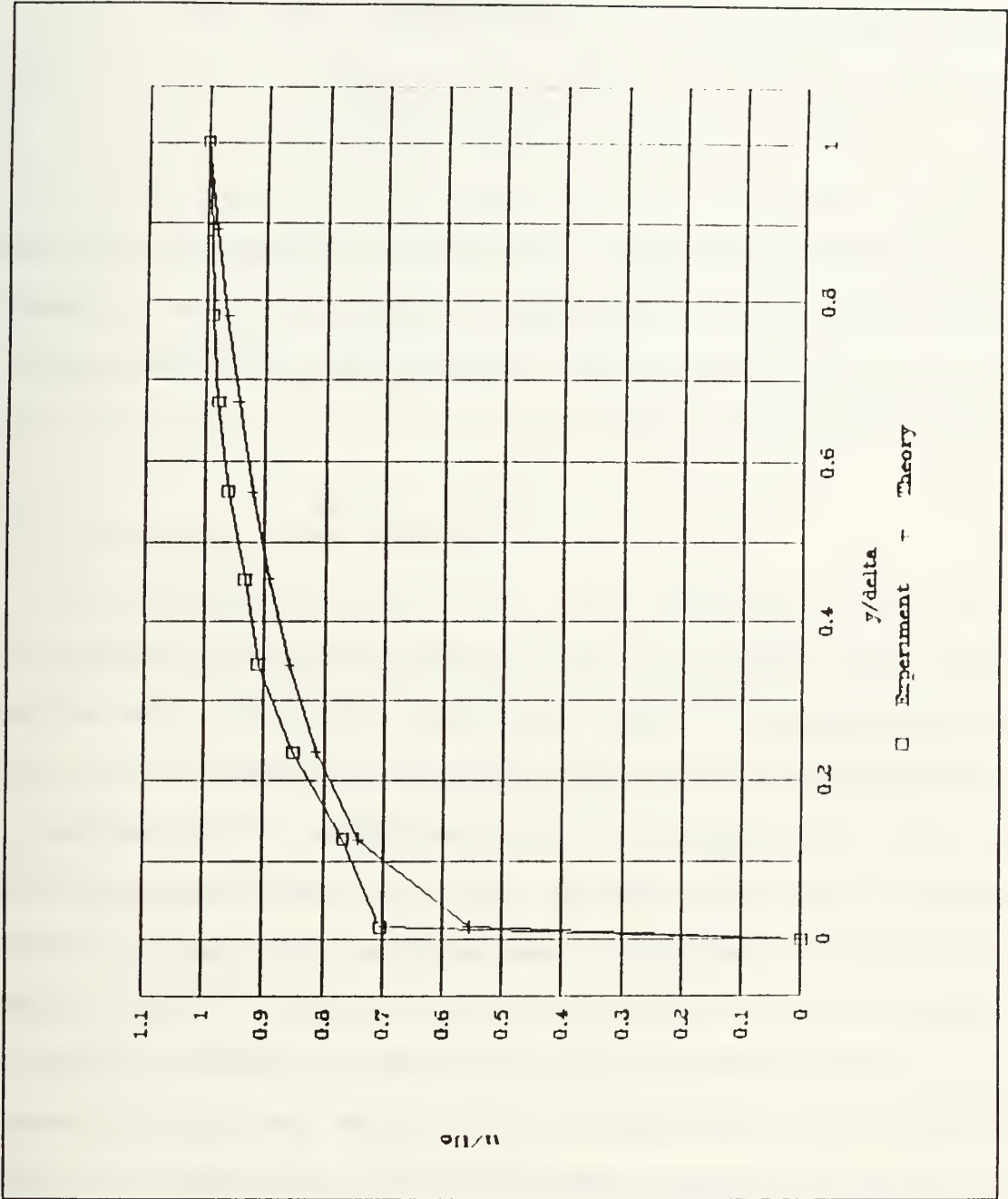
Figure 26. Boundary Layer Survey, 031693b, Free-Stream to Wall

51

represents the extent of the displacement of the external streamlines due to the growth of the boundary layer, was calculated by the following equation [Ref. 21]:

$$\delta^* = \int_o^\delta [1 - \frac{u}{U_e}]\, dy \qquad (10)$$

The momentum thickness, θ, which is an alternate definition of boundary layer thickness defined in relation to the momentum deficit in the boundary layer, was calculated from the following equation [Ref. 21]:

$$\theta = \int_o^\delta \frac{u}{U_e} [1 - \frac{u}{U_e}]\, dy \qquad (11)$$

The form factor, H, which measures the fullness of the velocity profile was determined by taking the ratio of displacement thickness to momentum thickness.

In both surveys, the experimental curves agreed with curves generated from the 1/7th law model. Experimental data from 031693b indicated a displacement thickness of 0.09 and a momentum thickness of 0.07 which yielded a shape factor of 1.34. Experimental data from 031693a, however, indicated a displacement thickness of 0.11 and a momentum thickness of 0.04 which yielded a shape factor of 2.76. Since the flow was turbulent, and a shape factor above 2.4 generally indicates laminar flow, the data from 031693a must be reanalyzed.

The difference between the two surveys was that in 031693a, a velocity measurement close to the wall was not obtained. During all boundary layer surveys, the experimental velocities were biased high. By adding a velocity measurement at the wall, biasing it low (by setting it equal to the theoretical value), and recalculating, the results were in much better agreement with theory. The recalculations and redefined curve are shown in Figures 27 and 28. Displacement thickness was recalculated as .08 and momentum thickness was recalculated as .05 which yielded a shape factor of 1.5.

E. LDV NORMAL SHOCK SURVEYS

Multiple surveys across the normal shock were conducted at a midstream location. The shock was positioned in the test section and various increments were used to traverse upstream and downstream of the shock. The purposes of the surveys were to determine if shock position and movement could be accurately predicted with LDV measurements and to study particle dynamics through the shock. schlieren visualization was also used to determine shock position.

The tabulated results from surveys 030393a and 031093b are shown in Figures 29 and 30. The plotted data for the surveys appear in Figures 31 and 32. In both surveys, velocity and turbulence data clearly indicate that the probe volume was traversed from a point upstream of the shock to a point downstream of the shock. The measured velocity decreased from

53

Y(in) NORMAL	U MEAN CORRECTED	U CORR CORRECTED	...	THICK...
1	193	...	1	1
0.89971038	178	...	...	...
0.78142076	309	...	...	...
0.67213114	302	...	...	...
0.56284153	302	...	...	...
0.45355191	305	...	...	...
0.34426229	276	...	...	...
0.23497267	365	...	...	...
0.12568306	299	...	...	...
0.01639344	220		...	...
0	0		0	0

EXPERIMENT (1-u/U)	DISPLACEMEN THICKNESS	EXP (1-u/U)u/U	MOMENTUM THICKNESS
0	0.00041713	0	0.00041395
0.00763358	0.00097331	0.00757531	0.00092447
0.01017811	0.00111236	0.01007452	0.00110104
0.01017811	0.00139045	0.01007452	0.00137005
0.01526717	0.00194663	0.01503408	0.00191125
0.02035623	0.00247613	0.01994185	0.00135122
0.04325699	0.00625703	0.04139582	0.00593724
0.07124681	0.01676352	0.06617021	0.01415592
0.23918575	0.03718509	0.18197592	0.02350985
0.44020356	0.01180494	0.24642438	0.00201205
1	0	0	0

Dis thick= 0.00146665

Mom thick= 0.05378107

Shape fac= 1.50917069

Figure 27. Recalculated Data for Boundary Layer Survey
031693a, Wall to Free-Stream
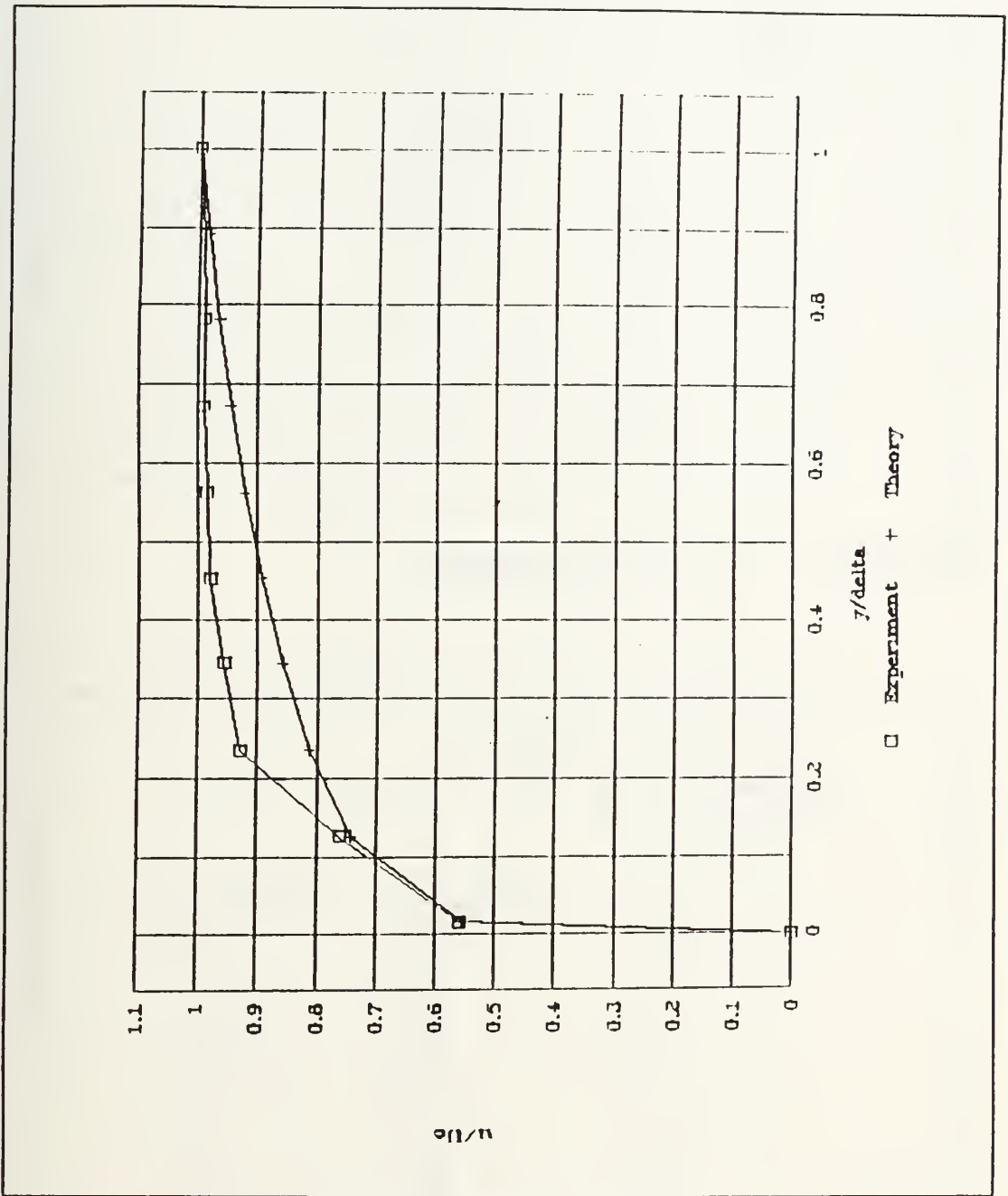
Figure 28. Recalculated Boundary Layer Survey, 031693b, Wall to Free-Stream

```
Velocity in M/SEC
Data is from the followi
030393a,1,10

        X(in)      U-MEAN      U-TURB.
                 CORRECTED)  CORRECTED)
        0.6        291         3.4
        0.7        309         5.1
        0.8        387         .
        0.9        342        12.5
         1         328        13.8
        1.1        347        14.1
        1.2       276.9        8.5
        1.3       274.9        5.8
        1.4        284         5.3
        1.5        282         5.3
```

Figure 29.   Shock Survey 030393a

```
Velocity in M/SEC
Data is from the following files:
031093b,1,11

        X(in)      U-MEAN      U-Turb.
                 CORRECTED   CORRECTED)
        0.9        397         4.9
         1         397         5.2
        1.1        369        13.3
        1.2        309        18.2
        1.3        302        16.1
        1.4        290        11.8
        1.5       276.6        5.9
        1.6        281         6
        1.7        281         5.3
        1.8        289         5.5
        1.9        271         4.7
```

Figure 30.   Shock Survey 031093b
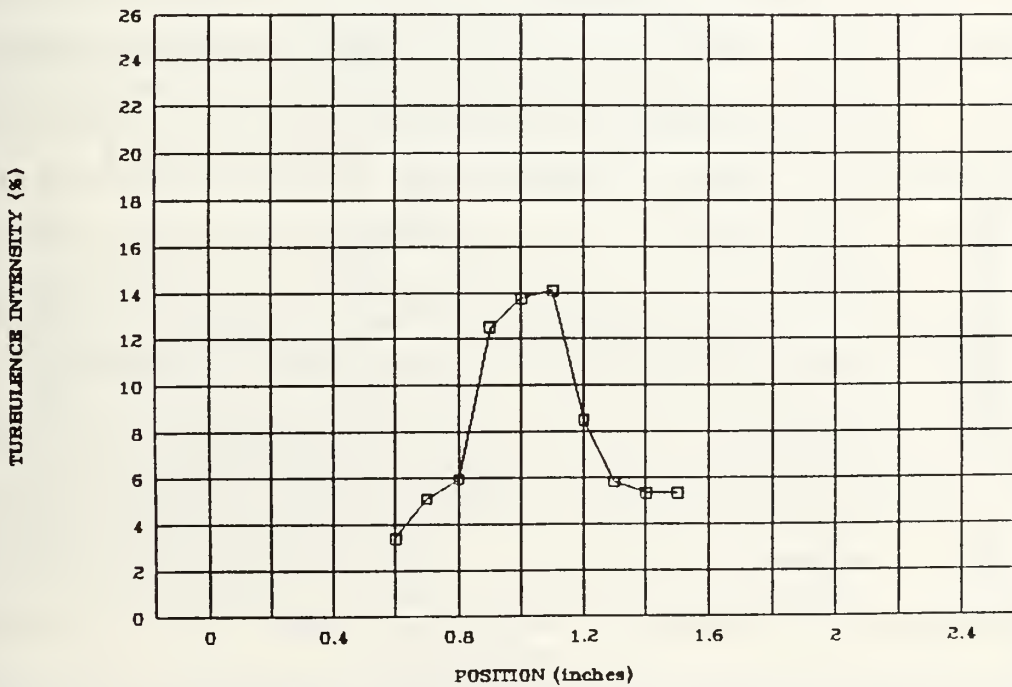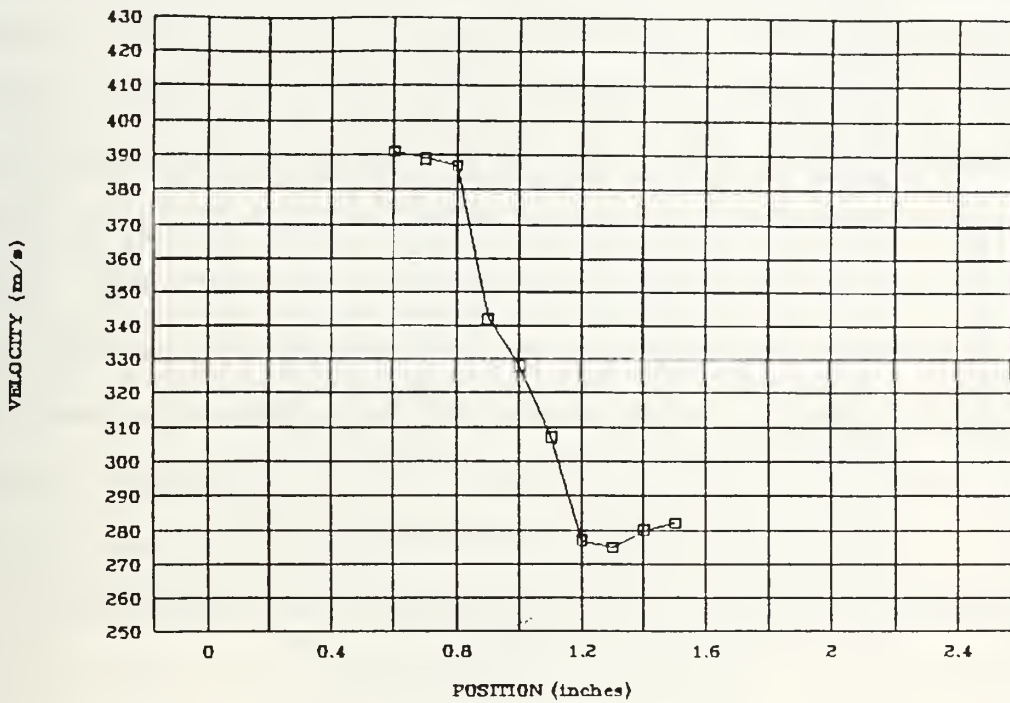
Figure 31. Velocity and Turbulence Intensity Plots, Shock Survey 030393a

57
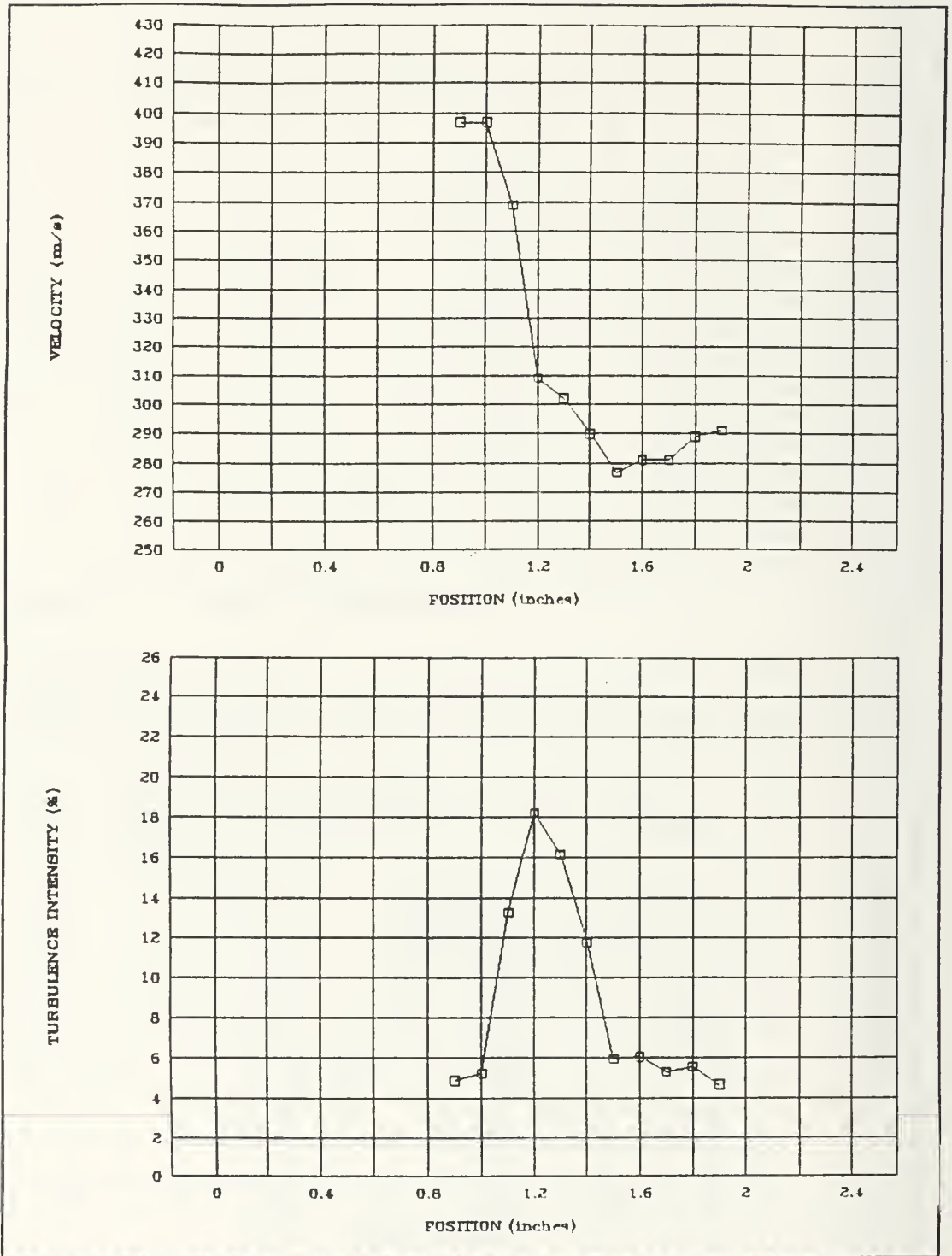
Figure 32. Velocity and Turbulence Intensity Plots, Shock Survey 031093b

a known free-stream supersonic value to a known free-stream subsonic value as the probe volume was traversed across the normal shock position. Also, turbulence intensity increased from free-stream conditions as the probe volume crossed the shock then decreased to free-stream values downstream of the shock. The dramatic increase in turbulence intensity (above 10%) indicated a region of flow unsteadiness. Between 0.8 and 1.2 inches on survey 030393a and between 1.0 and 1.4 inches on survey 031093b there was a region of decreased mean particle velocity and double peaked histograms.

This region was interpreted as the region of unsteadiness of the shock. The schlieren visualization for both runs, as shown in Figures 33 and 34, supported this conclusion. The random photographs taken immediately prior to each LDV survey indicated the shock to be fluctuating between 0.75 and 1.25 inches during 030393a and between 1.0 and 1.4 inches during 031093b. This corresponded very closely to the information taken from the plot of the LDV data.

In the region where the probe volume was traversed through the shock, the LDV data became difficult to interpret due to the presence of double peaked histograms. The points in this region on the plots in Figures 31 and 32 represent the mean velocity taken from the double histogram. The appearance of the double histogram in this area was concluded to be a result of the shock movement or unsteadiness. As the normal shock moved back and forth across the stationary probe volume, the
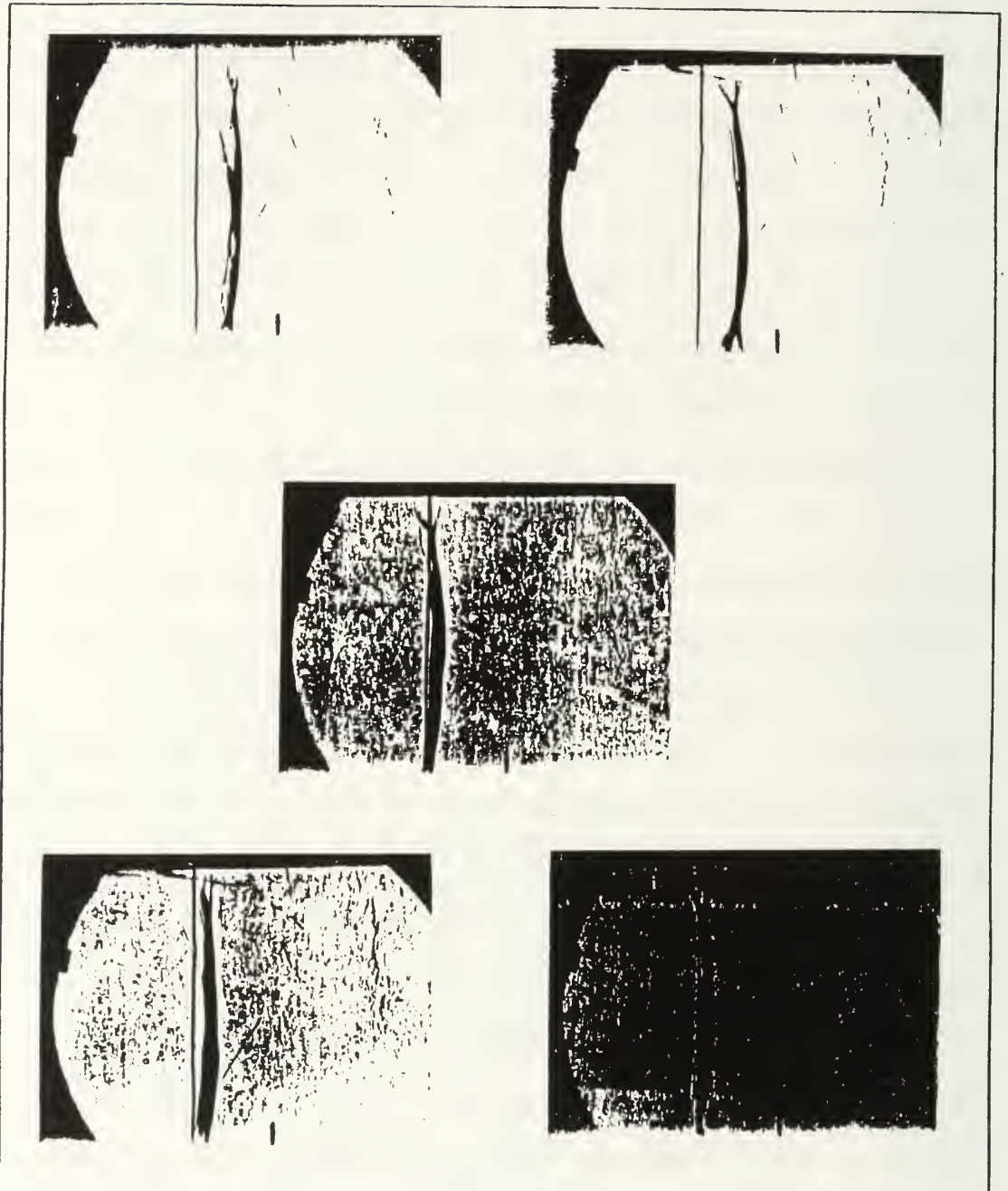
Figure 33. Schlieren Spark Source Photography, 030393a

Figure 34. Schlieren Spark Source Photography, 031093b

LDV system would alternately measure supersonic and subsonic particle velocities. The relative strength of each peak of the histogram would logically be related to the the length of time the probe volume spent in either the subsonic or supersonic region of the flow. This conclusion is supported by experimental data obtained by Strazisar [Ref.22] and Chriss et.al. [Ref 23] in which double histograms were observed during LDV surveys through a normal shock.

Figure 35 shows an additional plot of the LDV data taken in 031093b in which an attempt was made to further characterize the velocity distribution across the region of unsteadiness. In each survey, the points where double histograms appeared were separately analyzed by splitting the double histograms into a low and a high peak. By editing each double histogram, a mean value for each peak was determined. The amount of variance of each high and low mean was calculated, and this was an indication of the turbulence intensity. The separation of the histograms was a measure of the flow unsteadiness. Figure 35 shows the high and low means and the amount of variance associated with each point inside the region of unsteadiness. Ideally, a more rational mathematical method of splitting the histograms by using the statistical information is required in order to obtain a full understanding of the velocity information obtained in the double peaked histograms, as apposed to the manual editing technique used here.
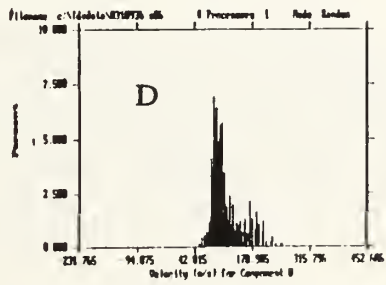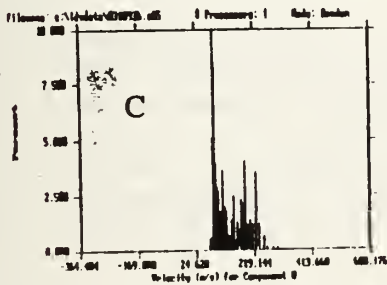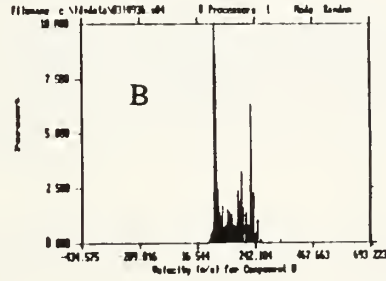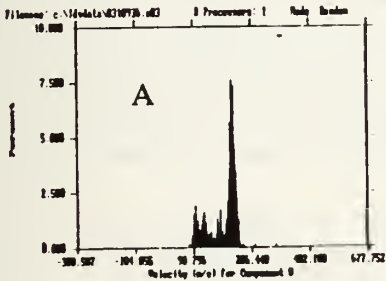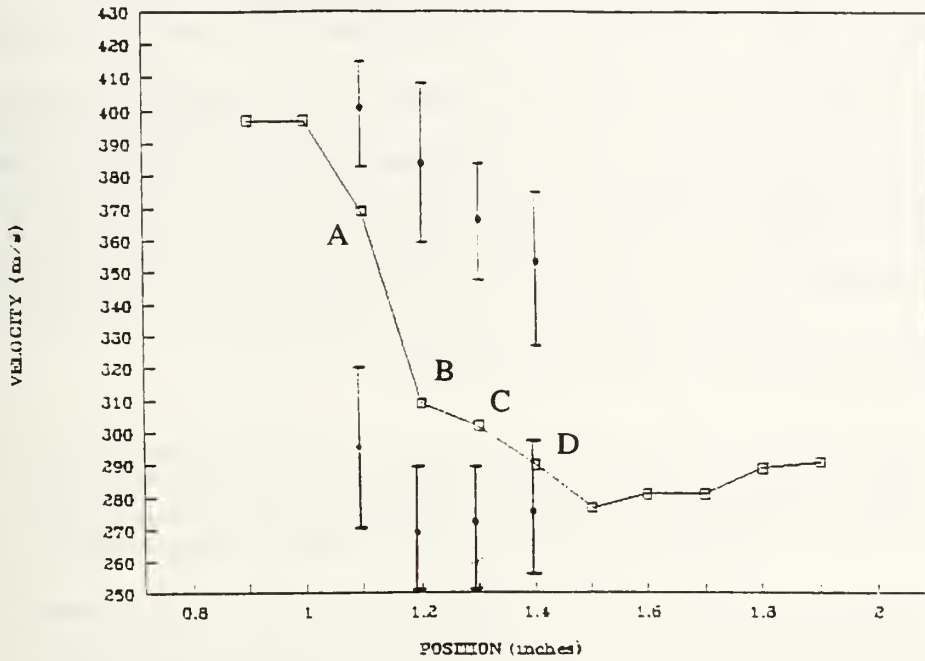
Figure 35. Shock Survey 031093b, Characterization of Unsteadiness and Turbulence Through the Normal Shock

63

One very repeatable phenomenon associated with the normal shock surveys was the region just downstream of the shock movement where the velocity bottomed out before rising to a free-stream value. This can be seen in Figures 31 and 32. This behavoir agrees with That reported by Chriss et.al. [Ref. 23] who hypothesized that it was due to the acceleration of the free stream flow as a result of the significant growth of the boundary layers on all four walls.

V. CONCLUSIONS AND RECOMMENDATIONS

A. CONCLUSIONS

The analysis of the data in this study leads to a number of conclusions about LDV measurements in a transonic flow and about particle dynamics across a normal shock:

* LDV measurements made upstream and downstream of the shock were very successful and provided accurate and repeatable velocity magnitudes in backscatter mode in a transonic flow.

* Seeding at the contraction with 1 μm sized PSL particles proved adequate. Data rates were more than sufficient in all phases of the experiment.

* The design of the supersonic wind tunnel nozzle blocks was flawed in that insufficient expansion was provided to compensate for boundary layer effects. The tunnel must presently be run with back pressure relief in order to allow movement of the starting normal shock downstream of the test section.

* The design of the plenum, specifically the absence of any screens or flow straightening devices, caused turbulence which might have contributed to shock unsteadiness.

* Shock position and movement could be accurately determined with schlieren visualization and LDV measurements. Spark source schlieren photography proved to be successful as a means of recording the extent of shock movement. Data obtained from LDV measurements also proved to be accurate in the determination of shock location.

* There was an apparent region at the downstream edge
  of the normal shock movement where particle velocity
  reached a minimum before accelerating to free stream
  velocity. This phenomenon was highly repeatable and
  may be a function of the downstream boundary layer
  growth.

* Instability of the normal shock caused an area of
  double peaked histograms which can possibly be
  statistically analyzed to obtain particle dynamic
  information through the normal shock.

B. RECOMMENDATIONS

LDV is a powerful tool with the ability to provide
accurate velocity measurements under specific conditions. The
accuracy of the data does, however, depend a great deal on the
ability to fully understand and correctly model particle
dynamics. More experimentation and improvements in the current
test facilities and apparatus are required to continue LDV
work in the supersonic tunnel. The following recommendations
are made:

* The supply air pressure must be increased at the
  facility to provide longer run times. Certifying
  additional storage tank would also increase run
  time by increasing the storage volume. Longer run
  times are the key to obtaining more detailed surveys.

* The control and monitoring of the supersonic tunnel
  (supply valve, plenum pressure gauge) should be
  incorporated into a master control panel which would
  allow better management of the tunnel operation.

* Reduction of turbulence can be accomplished by placing
  screens or other flow straightening devices in the
  plenum.

*   The HP data acquisition system can be utilized further
    by incorporating thermal compensation cards and the
    ability to measure real-time values of plenum and test
    section temperature.

*   The current traverse table for the LDV optics is
    unable to fully traverse the test section and must
    be operated manually. An automatic traverse system
    with position indication would allow more accurate
    surveys.

APPENDIX A.   WIND TUNNEL DATA ACQUISITION SYSTEM

A.   DESCRIPTION OF SYSTEM

The data acquisition system for the supersonic wind tunnel consists of the following items: 2 pressure transducers, HP 9000 series 300 computer data acquisition/reduction system, HP 3455A digital voltmeter, HP 3497A data acquisition/control unit, Lockheed MT-1758 test panel, and "SPEED_5" software. The purpose of the data acquisition is to measure total plenum pressure (P_2) and static test section pressure (P_1). This information is then used to calculate test section Mach number upstream of the normal shock based on the following isentropic flow equation:

$$\frac{P_2}{P_1} \; = \; [1 \, + \, \frac{\gamma \, - \, 1}{2} M^2]^{\frac{\gamma}{\gamma \, - \, 1}}$$

Test section stagnation temperature (measured in the plenum and input by the user) and Mach number are then used to calculate velocity upstream of the shock. Finally, by dividing velocity by the known fringe spacing, a Doppler frequency is calculated.

Once the system is calibrated and started, all measurements and calculations are automatically and continuously performed throughout the entire wind tunnel run.

A continuous display of P_2, P_1, P_2/P_1, Mach number, and frequency are presented on the computer CRT and sent to the printer. The presented data can be utilized during the run to monitor tunnel conditions and properly set frequency filters on the processor. The data is also useful as a means of recording a time history of tunnel conditions for each run.

The "SPEED_5" program was developed from the "READ_ZOC" utility program given in Reference 24. A small portion of the original program was adapted for use with the supersonic wind tunnel acquisition system.

B.   OPERATING THE DATA ACQUISITION SYSTEM

1. Start-up

    *   Turn on the HP9000, HP3455A, and HP3497A.

    *   Verify supply air is connected to MT-1758 and calibration pressure is set, using the high pressure regulator knob, to 50.9 inches Hg (25 psi).

    *   Type SHIFT-RESET to enter HP BASIC.

    *   LOAD "SPEED_5"

    *   RUN "SPEED_5"

2. Calibration

    *   Type 0 to continue program after the introduction.

    *   ENTER the atmospheric pressure in psi.

    *   ENTER the test section static temperature (calculated from previous runs where plenum stagnation temperature was directly measured).

    *   ENTER 0 to calibrate P_1. Open P_1 to atmosphere and zero reading on HP3455A then apply calibration

69

pressure and adjust to 12.5 on HP3455A.

* ENTER 4 and repeat above process to calibrate P_2.

* Type an out of range value (any number other than 0 through 9) to run the program.

* The program will run continuously until SHIFT-RESET is typed.

A listing of the "SPEED_5" program can be seen in Figure A1.

```
10    !  PROGRAM: SPEED_5
20    !  By:      Dave Perretti
30    !
40    !  DESCRIPTION:  Modified version of SCAN_700_06 by Richard Pedlard
50    !               and Dave Hyre. Used to control the HP 3455A digital
60    !               voltmeter, and the HP 710 A aquisition control unit
70    !               to obtain pressure and temperature data in the
80    !               supersonic tunnel.
90    !
100   !
110   !................INTRODUCTION..........   ...........
120   PRINTER IS 1
130   PRINT
140   PRINT
150   PRINT
160   PRINT
170   PRINT                    Welcome to SPEED_5
180   PRINT
190   PRINT
200   PRINT
210   PRINT  "This Program is designed as an aid to running the supersonic"
220   PRINT  "wind tunnel. The user will be asked to input atmospheric"
230   PRINT  "pressure, and test section temperature.
240   PRINT  "You will then be asked to calibrate the transducers.
250   PRINT  "The Program will display and record P1(test section pressure),
260   PRINT  "P2(plenum pressure), pressure ratio(P2/P1), test section Mach
270   PRINT  "number, and frequency.  The frequency information can be used to"
280   PRINT  "set high and low filters on the signal processor."
290   PRINT
310 A:!
320   INPUT  "TYPE 0 TO CONTINUE",X
330   IF X=0 THEN B
340   GOTO A
350 B:!
360   CLEAR SCREEN
370   PRINT
380   PRINT
390   !
400   !.....................INPUTS....................  ...
410   !
420   INPUT  "Input the atmospheric pressure in Psi",P_atm
430   INPUT  "Input the test section temperature in Kelvin",T_test
440   !
450   !....................INITIALIZATION AND CALIBRATION.............   ...
460   !
470   Dacu=709
480   Dvm=720
490   ASSIGN @Listeners TO Dvm,Dacu
500   CLEAR @Listeners
510   OUTPUT Dvm;"F1R7N3A0H0T1"
520   CLEAR SCREEN
530   PRINT
540   PRINT
550   PRINT
560   PRINT "INSTRUCTIONS:"
570   PRINT
580   PRINT "TYPE IN TRANSDUCER ID OF TRANSDUCER TO BE CALIBRATED (0-3)"
590   PRINT "THEN CALIBRATE THAT TRANSDUCER."
600   PRINT "0  CORRESPONDS TO P1"
610   PRINT "1  CORRESPONDS TO P2"
620   PRINT "TYPE AN OUT OF RANGE VALUE TO CONTINUE THE PROGRAM"
630 C:INPUT "INPUT DESIRED TRANSDUCER TO BE CALIBRATED (0-9)",Id
640   IF Id<0 OR Id>3 THEN Continue
650   GOSUB Switch
```

Figure A1.   "SPEED_5" Listing

71

```
         FOR  ont  n:1
650          Id$=VAL$(Id)
660          Ac$="AC"
700          OUTPUT Dacu;Ac$&Id$
710 RETURN
720 Continue:!
730          CLEAR Dacu
740          CLEAR Dvm
750          CLEAR SCREEN
760 PRINT "  F2  ","  P1  ","   Fratio ","     Mach ","         Freq(Hz)
770 PRINT
780 PRINT
790 PRINTER IS 702
800 PRINT "  F2  ","  P1  ","   Fratio","     Mach ","        Freq(MHz)
810 PRINT
820 PRINT
830   !
840   !.................PRESSURE RATIO AND MACH NUMBER.................!
850   !
860   ASSIGN @Dacu TO Dacu
870   ASSIGN @Dvm TO Dvm
880   ASSIGN @Instruments TO Dvm,Dacu
890   CLEAR @Instruments
900   OUTPUT @Dvm;"F1R7M3R0H0T3"
910 Ratio_loop: !
920          FOR Id=0 TO 4 STEP 4
930          GOSUB Read_stdy
940          SELECT Id
950             CASE 0
960                P1=P_stdy*1000+P_atm
970             CASE 4
980                F2=P_stdy*1000+P_atm
990          END SELECT
1000         NEXT Id
1010         Pratio=P2/P1
1020         Mach=SQRT(ABS(((Pratio)^(1/3.5)-1)*.2))
1030         Sos=SQRT((1.4)*(287)*(T_test))
1040         U=(Mach)*(Sos)
1050         F=(U)/4.5
1060         PRINTER IS 1
1070         PRINT F2,P1,Pratio,Mach,F
1080         PRINTER IS 702
1090         PRINT F2,P1,Fratio,Mach,F
1100   GOTO Ratio_loop
1110 Read_stdy:  !
1120         CLEAR @Dacu
1130         Ac$="AC"
1140         Id$=VAL$(Id)
1150         OUTPUT @Dacu;Ac$&Id$
1160         Total=0
1170         FOR I=1 TO 5
1180            TRIGGER @Dvm
1190            ENTER @Dvm;P_stdy
1200            Total=Total+P_stdy
1210         NEXT I
1220         CLEAR @Dacu
1230         P_stdy=Total/5
1240         P_stdy=2*P_stdy
1250         RETURN
1260   CLEAR @Instuments
1270   ASSIGN @Dacu TO *
1280   ASSIGN @Dvm TO *
1290   ASSIGN @Instuments TO *
1500   END
```

Figure A1 (cont.).   "SPEED_5" Listing

72

APPENDIX B.   TSI "FIND" SOFTWARE

TSI Flow Information Display (FIND) software was used as the data acquisition interface for the LDV system. The software is designed to acquire, analyze, and reduce LDV raw data. FIND also allows the user to establish and set up hardware parameters. Three subprograms (data acquisition, statistical data analysis, and flow field plot) were extensively used during the course of this study. Figures B1 through B8 show a typical sequence of displays within the FIND software used to set up and run an LDV survey.

The main menu is shown in Figure B1. From the main menu, "A" is selected to access the data acquisition program which is shown in Figure B2. From Figure B2, "I", "P", and "O" are selected to set the I/O port and processor selections, processor set up, and optics configurations. Typical selections and settings are shown in Figures B3, B4, and B5. To complete the set up, "F" is selected from the main menu to enter the data files management screen as shown in Figure B6. After acquiring the raw data from an LDV survey, the Statistical Analysis and Flow Field Plot programs are selected as shown in Figures B7 and B8 to analyze and reduce the data.

```
    Flow Information Display (FIND) Software : Main Menu
                    March 16, 1993


                <A> Data Acquisition Program
                <S> Statistical Analysis Program
                <F> Flow Field Profiles Program
                <H> Time History Program
                <T> Traverse Table Control Program

            <F4> Acquire and Analyze New Data

            <Q> Quit the Program
```

Figure B1. "FIND" Main Menu

```
                    3D FIND : Data Acquisition
                         March 16, 1993
    Color Link : Off
        Traverse: None            Processors: 1      Mode: Random
    Data File: c:\ldvdata\031593a.R09    Data Sample Size: 1   K Data Points


            <I>  I/O port and Processor type selection
            <P>  Processor Settings
            <O>  Optics Configuration
            <E>  Experiment Documentation and Units
            <H>  Hardware Diagnostics
            <F>  Data File Management
            <T>  Automatic Traverse Parameters
            <R>  Realtime Histogram
            <M>  Return to Main Menu

            <F2> Acquire Data for 15 Raw Data Files.
            <F3> Store program documentation
```

Figure B2. "FIND" Data Acquisition Menu

74

```
                    3D FIND : Data Acquisition
                            , March 16, 1993
     Color Link : Off
          Traverse: None              Processors: 1      Mode: Random
    Data File: c:\ldvdata\031593a.R09    Data Sample Size: 1   K Data Points

                  <I>  I/O port and Processor type selection

            I/O Port Selection              LDV Processor Type

        Traverse Controller  = COM1         First Processor   = 1990
        Sony Position Enc:   = COM1         Second Processor  = 1990
        Printer Port         = LPT1         Third Processor   = 1990
        Processor I/O Port   = COM2
        ColorLink            = OFF          Master Interface  = MI990

                        Program Installation Settings

     Computer Bus Type --==> PCBUS      Graphics Type   ==> EGA
     Monitor Type         ==> Color     Toggle Selection ==> High Light
     DMA Chan: 1; Port Addr: 300H;   Com1 - Com4 Addr: 3F8H;2F8H;3E8H;2E8H
```

Figure B3. "FIND" I/O Port and Processor Type Selection Screen

```
                    MI990 Processor SetUp Screen

                      Interface / DMA Selections
          Number of Processors: 1
          Number of K-Data Points: 1
          Data Sampling Method: TBD_On
     Coincidence Window width (µs): 2.0E5
          DMA Timeout (Sec): 30
          Acquisition Mode: Random
          Sample Time (µs): 1.0e1
          Number of C-words: 0
                         Processor Selections
                     Processor 1      Processor 2      Processor 3
          Number of Cycles: 4
          Processor Type : 1990
          Processor Mode: CONT
     Filter Range - Hi Limit: 50
               Lo Limit: 20
          Timer Comparison: 5
                    Gain: 1
```

Figure B4.   "FIND" Processor Set Up Screen

75

Figure B5. "FIND" Optics Configuration Screen

Figure B6. "FIND" Data Files Management Screen

```
                FIND : Statistical Analysis Program
                       March 16, 1993

                   Filename: c:\ldvdata\031693a.r01

                <F> Data Files Management Menu
                <I> I/O Selection - Printer Port: LPT1
                <V> Velocity Bias Correction -  Off
                <R> Refinement Bounds Off
                <F2> Analyze 12 raw data files.

                <F3> Store Program Documentation
                <F4> Acquire and Analyze New Data

                <S> Statistics Tabulation Display
                <H> PDF Histogram Display
                <M> Return to Main Menu
```
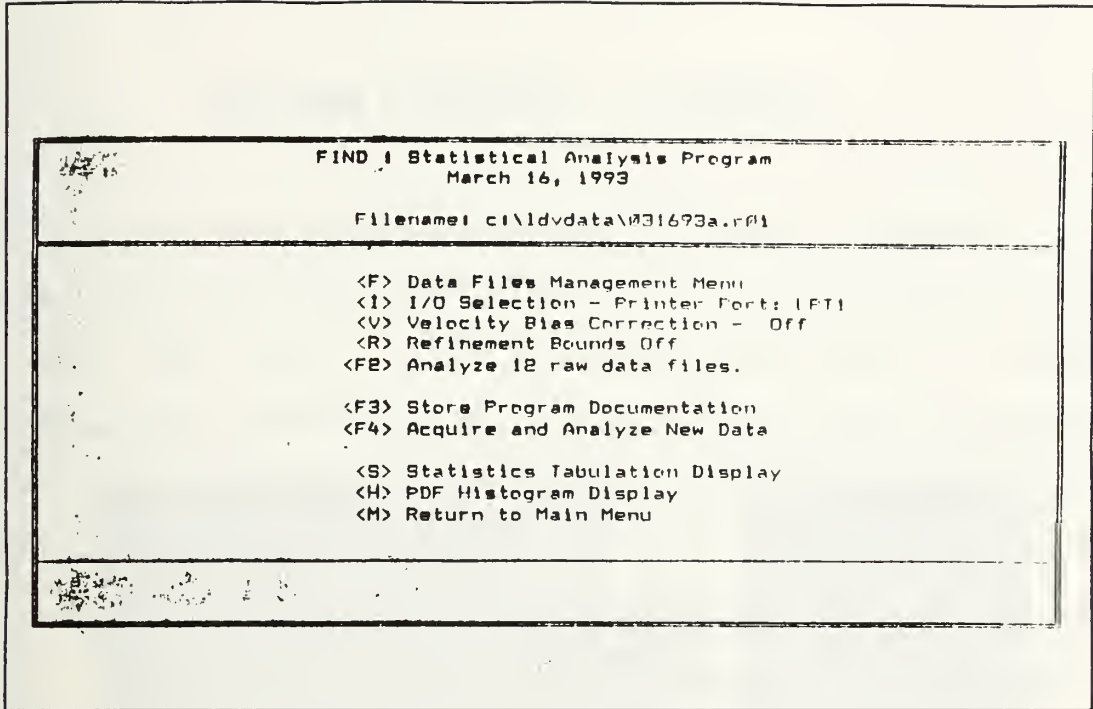
Figure B7. "FIND" Statistical Analysis Program Menu

```
                FIND : Flow Field Plot Program
                       March 16, 1993
                Plot File: c:\ldvdata\CLOSED

                <F> Plot File Management.
                <E> Edit Plot File.
                <I> I/O Port Configuration.
                <G> Graphics Display Menu.
                <M> Return to Main Menu.

                <F2> Graph Plot File.
                <F3> Store Plot File Data in ASCII Format.
```
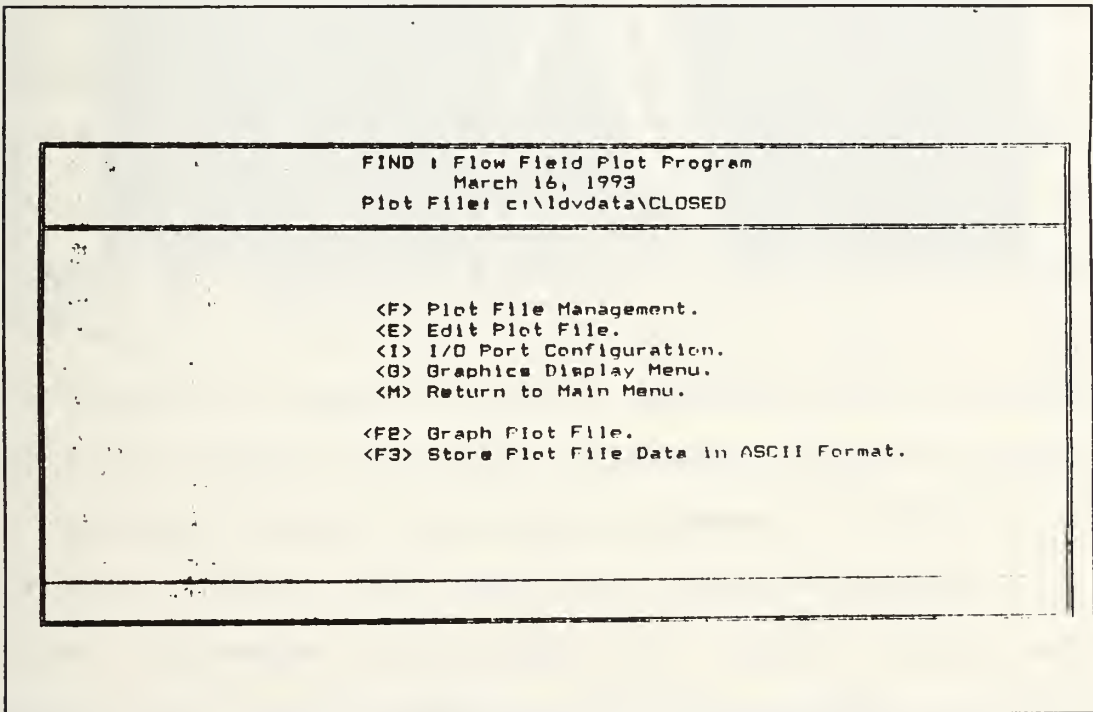
Figure B8. "FIND" Flow Field Plot Program Menu

77

APPENDIX C.   SUPERSONIC FREE-JET

A supersonic free jet was designed and constructed during the course of this study. The intent was to have available a means of producing supersonic flow in the event that the supersonic blow down tunnel proved inoperable due to design errors or unusable due to limited run times. The free jet, as shown in Figure C1, is capable of essentially continuous operation with supply pressure at 150 psi and has the advantage of direct optical access.

Supply air is routed directly to a regulator which serves as the control valve for the free jet. The regulator connects directly with an 4 inch diameter straight pipe that serves as the plenum. The regulator is also supplied with back pressure from the plenum which it uses to maintain the pressure within the plenum. A solid aluminum nozzle is attached to the end of the plenum. Air exits the nozzle and is captured a few feet away by conical ducting which routes the discharge to the exterior of the building. A pressure gauge is attached to the plenum to monitor operating conditions and additional ports are available to measure temperature and allow seeding.

The aluminum nozzle is an ASME low β series, long-radius flow nozzle [Ref 25]. The coefficient β represents the ratio of nozzle exit diameter to inlet diameter where low β indicates
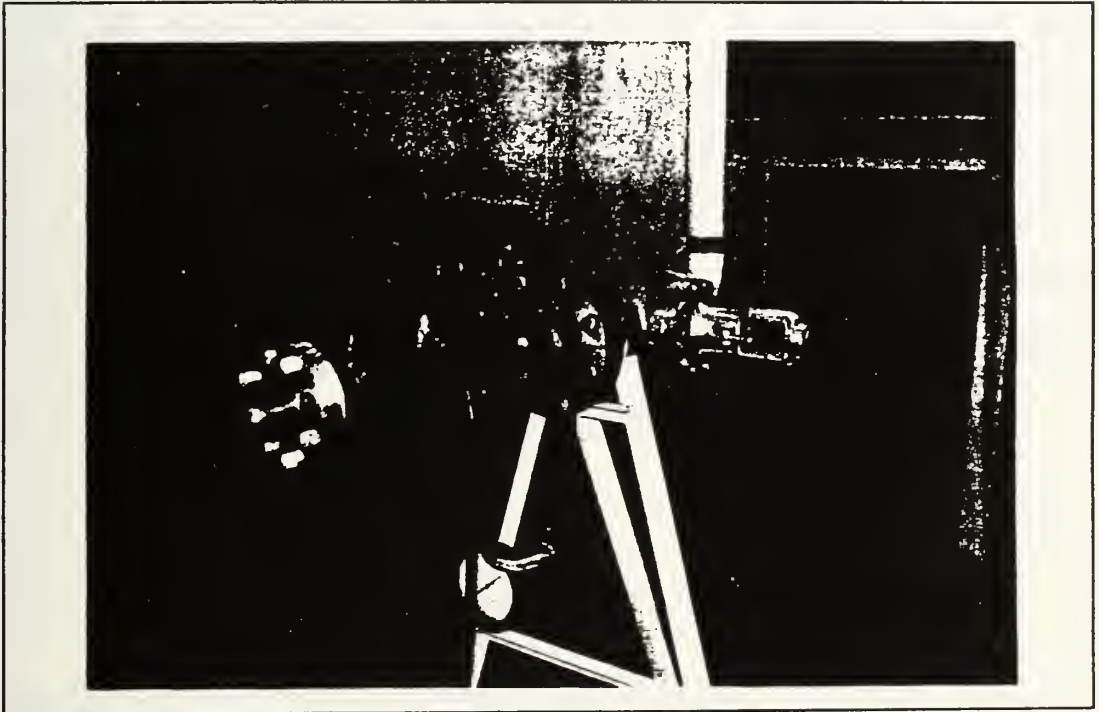
Figure C1. Supersonic Free-Jet

a ratio below 0.5. The free-jet nozzle exit was chosen as 1.25" giving it a diameter ratio of about 0.31. The remaining dimensions of the nozzle, including the elliptical approach to the throat, are determined by the choice of exit diameter. Throat length is defined as 0.6 times the exit diameter. The minor axis of the elliptical approach is defined as 0.66 times the exit diameter and the major axis is defined as equal to the exit diameter. The design of the nozzle is further illustrated in Figure C2. Although the free jet was not utilized during this study, it is a useful addition to the laboratory in that it will allow further LDV studies to be performed under continuous, predictable, and highly controllable conditions.

Figure C2. Supersonic Free-Jet Nozzle Design, From Ref. 24
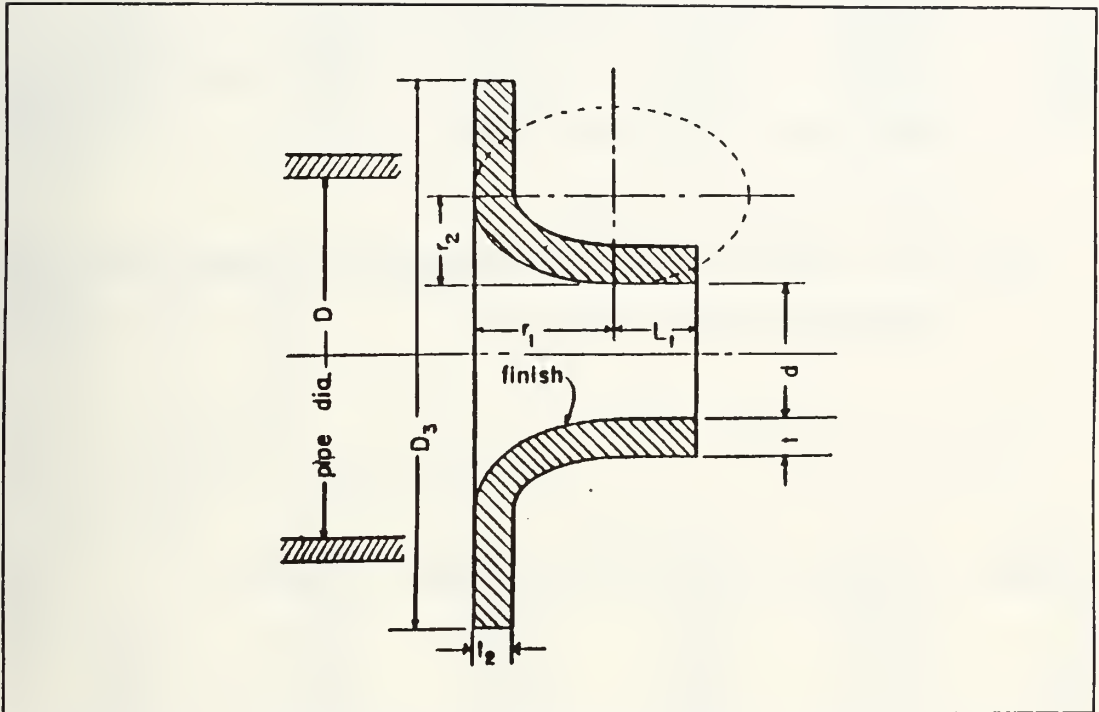
APPENDIX D.   TABULATED RESULTS

The following is a compilation of the results from the present study. The data are presented in the following format:

* BOUNDARY LAYER SURVEY RAW DATA

* BOUNDARY LAYER SURVEY PLOTS OF MEAN VELOCITY AND TURBULENCE VERSUS POSITION

* SHOCK SURVEY RAW DATA

* SHOCK SURVEY PLOTS OF MEAN VELOCITY AND TURBULENCE INTENSITY VERSUS POSITION

A	B	C	D	E	F

Velocity in M/SEC
Data is from the following files:
031093f,1,9

Y(in)	U-Mean Velocity	U-MEAN CORRECTED	U-Standard Deviation	U-Turb. Intensity	U-TURB CORRECTED
0	107	287	30.4	28.3	10.6
0.01	172	352	37.8	21.9	10.7
0.02	185	365	43.4	23.5	11.9
0.03	184	364	46.3	25.2	12.7
0.04	185	365	47	25.4	12.9
0.05	184	364	47.7	27.1	13.7
0.06	191	371	45.2	23.7	12.2
0.07	195	375	39.9	20.4	10.6
0.08	179	359	48.4	27	13.5

-Mar-93 11:16 AM   UNDO   NUM

Y(in)

A	B	C	D	E	F

Velocity in M/SEC
Data is from the following files:
031193a,1,12

Y(in)	U-Mean Velocity	U-MEAN CORRECTED	U-Standard Deviation	U-Turb. Intensity	U-TURB CORRECTED
0	100	280	31	30.9	11
0.01	95.1	275.1	33.2	34.9	12
0.02	146	326	47.8	32.7	14.6
0.03	145	325	53.8	37.1	16.6
0.04	129	309	52.4	40.6	16.9
0.05	140	320	54.7	39.1	17.1
0.06	135	315	54.8	40.1	17.8
0.07	148	328	57.1	38.6	17.4
0.08	151	331	57.3	38	17.3
0.09	136	316	55.9	41.1	17.7
0.1	165	345	56.3	34	16.3
0.11	160	340	58.1	36.2	17

-Mar-93 11:17 AM   UNDO   NUM

83

A B C D E F

Velocity in M/SEC
Data is from the following files:
031193b,1,12

Y(in)	U-Mean Velocity	U-MEAN CORRECTED	U-Standard Deviation	U-Turb. Intensity	U-TURB CORRECTE
0	159	339	33.4	20.9	9.8
0.01	147	327	46.4	31.6	14.8
0.02	162	342	44.3	27.3	12.9
0.03	166	346	41.5	25	12
0.04	179	359	32.8	18.3	9.1
0.05	179	359	35.2	19.6	9.8
0.06	181	361	36.5	20.1	10.1
0.07	180	360	38	21	10.5
0.08	185	365	35.5	19.1	9.7
0.09	188	368	36.6	17.5	10
0.1	186	366	36.1	19.4	9.9
0.11	192	372	34.4	17.9	9.8

-Mar-93   11:18 AM   UNDO   NUM

: '   Y(in)

A B C D E F

Velocity in M/SEC
Data is from the following files:
031193d,1,8

Y(in)	U-Mean Velocity	U-MEAN CORRECTED	U-Standard Deviation	U-Turb. Intensity	U-TURB CORRECTE
0	141	321	32.4	23	10.1
0.01	153	333	42.6	27.8	12.8
0.02	154	334	43.1	27.9	12.9
0.03	164	344	40.2	24.5	11.7
0.04	163	343	42.9	26.3	12.5
0.05	167	347	42	25.1	12.1
0.06	164	344	45.6	27.7	13.2
0.07	84.9	264.9	28.8	33.9	10.9

-Mar-93   11:20 AM   UNDO   NUM

	A	B	C	D	E	F

Velocity in M/SEC
Data is from the following files:
031593a,1,10

Y(in)	U-Mean Velocity	U-MEAN CORRECTED	U-Standard Deviation	U-Turb. Intensity	U-TURB CORRECTED
0	119	299	41.1	34.4	13.7
0.1	117	297	38.8	33.2	13.1
0.2	126	306	51.8	41.1	16.9
0.3	204	384	36.8	18.1	9.6
0.4	208	388	28.5	13.7	7.3
0.5	173	353	57.4	33.1	16.2
0.6	164	344	59.2	36.2	17.3
0.7	161	341	59.9	37.2	17.6
0.8	201	381	29.5	14.7	7.8
0.9	198	378	33.9	17.1	9

-Mar-93 11:21 AM   UNDO   NUM

Y(in)

	A	B	C	D	E	F

Velocity in M/SEC
Data is from the following files:
031593b,1,6

Y(in)	U-Mean Velocity	U-MEAN CORRECTED	U-Standard Deviation	U-Turb. Intensity	U-TURB CORRECTED
1.5	213	393	21.8	10.2	5.5
1.4	200	380	40.5	20.2	10.6
1.3	203	383	33	16.3	8.6
1.2	206	386	25.3	12.3	6.6
1.1	203	383	27.7	13.6	7.2
1	202	382	26.5	13.1	6.9

-Mar-93 11:21 AM   UNDO   NUM

	A	B	C	D	E	F

Velocity in M/SEC
Data is from the following files:
031593c,1,9

Y(in)	U-Mean Velocity	U-MEAN CORRECTED	U-Standard Deviation	U-Turb. Intensity	U-TURB CORRECTED
1	211	371	23.8	11.3	6.1
0.9	210	390	20.2	9.63	5.2
0.8	209	389	21.3	10.2	5.5
0.7	208	388	23	11	5.9
0.6	210	390	21.9	10.4	5.6
0.5	211	371	22.6	10.7	5.8
0.4	209	389	23	11	5.9
0.3	210	390	19.7	9.39	5.1
0.2	207	387	19.4	9.35	5

Mar-93   11:22 AM   UNDO   NUM

Y(in)
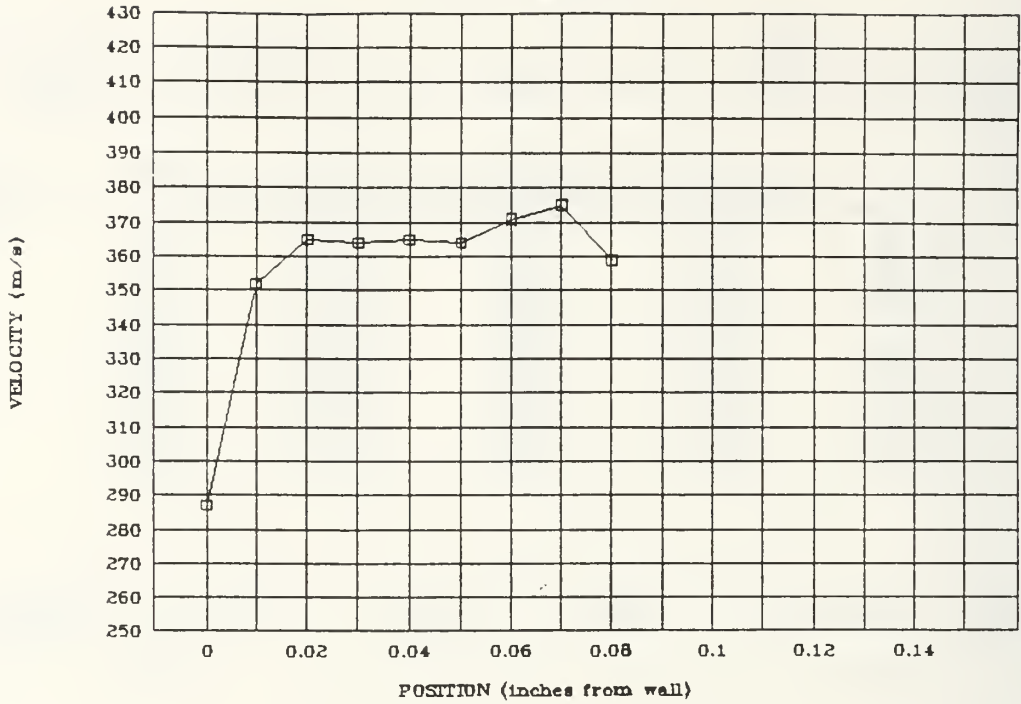
	A	B	C	D	E	F

Velocity in M/SEC
Data is from the following files:
031593d,1,8

Y(in)	U-Mean Velocity	U-MEAN CORRECTED	U-Standard Deviation	U-Turb. Intensity	U-TURB CORRECTED
0.5	208	388	31.1	14.9	8
0.45	209	389	28	13.4	7.2
0.4	209	389	27.9	13.4	7.2
0.35	209	389	29	13.9	7.5
0.3	210	390	26.1	12.5	6.7
0.25	210	390	25.8	12.3	6.6
0.2	208	388	23.3	11.2	6
0.15	179	359	36.6	20.4	10.2

Mar-93   11:23 AM   UNDO   NUM

86

Velocity in M/SEC
Data is from the following files:
031693a,1,9

	Y(in)	U-Mean Velocity	U-MEAN CORRECTED	U-Standard Deviation	U-Turb. Intensity	U-TURB CORRECTED
A		B	C	D	E	F
	0.02	119	299	32	26.9	10.7
	0.04	185	365	26.9	14.5	7.3
	0.06	196	376	29.4	15	7.8
	0.08	205	385	22.9	11.2	6
	0.1	207	387	25.2	12.2	6.5
	0.12	209	389	23.4	11.2	6
	0.14	209	389	23.3	11.2	6
	0.16	210	390	21.3	10.2	5.5
	0.18	213	393	18.1	8.5	4.6

-Mar-93   11:24 AM   UNDO   NUM

 '   Y(in)

Velocity in M/SEC
Data is from the following files:
031693b,1,11

	Y(in)	U-Mean Velocity	U-MEAN CORRECTED	U-Standard Deviation	U-Turb. Intensity	U-TURB CORRECTED
A		B	C	D	E	F
	0.2	211	391	29.5	14	7.6
	0.18	212	392	25.7	12.2	6.7
	0.16	209	389	29	13.9	7.5
	0.14	208	388	30.2	14.5	7.8
	0.12	204	384	28.6	14.1	7.5
	0.1	197	377	31.1	15.8	8.3
	0.08	186	366	28.6	15.3	7.8
	0.06	177	357	29.7	16.8	8.3
	0.04	154	334	33.3	21.7	10
	0.02	121	301	33.9	28	11.2
	0	96.2	276.2	24.2	25.2	12.2

D.01

-Mar-93   11:25 AM   UNDO   NUM
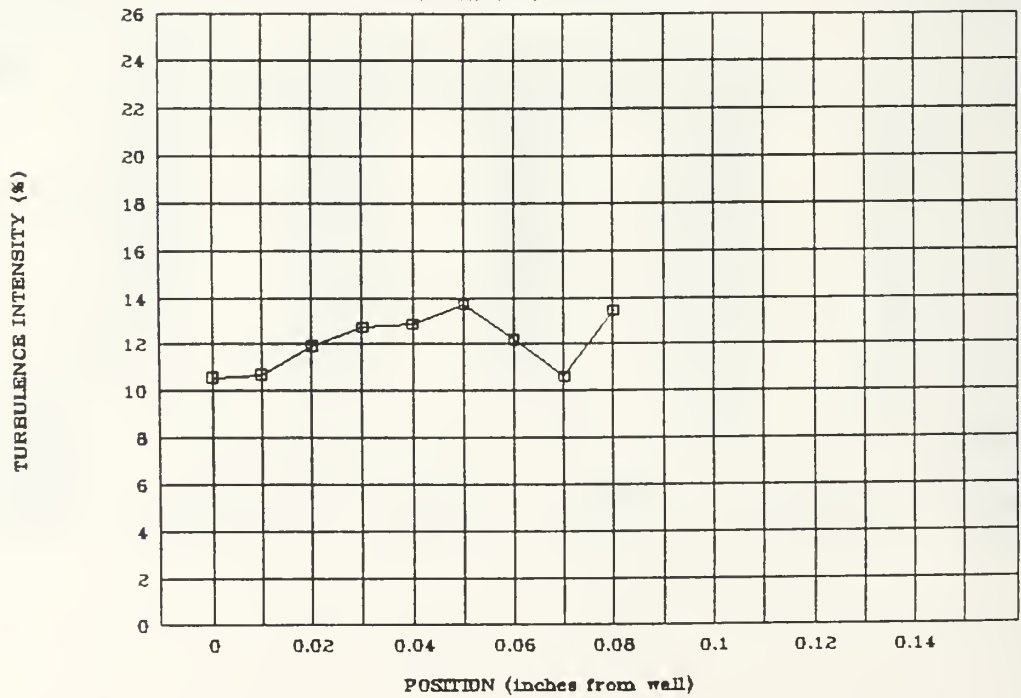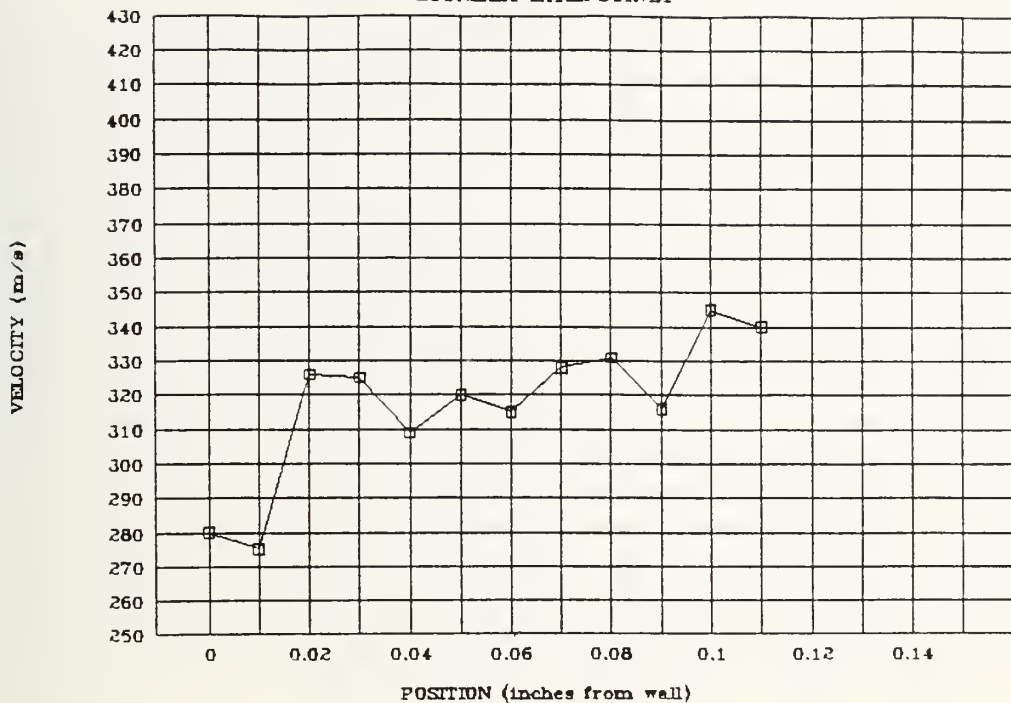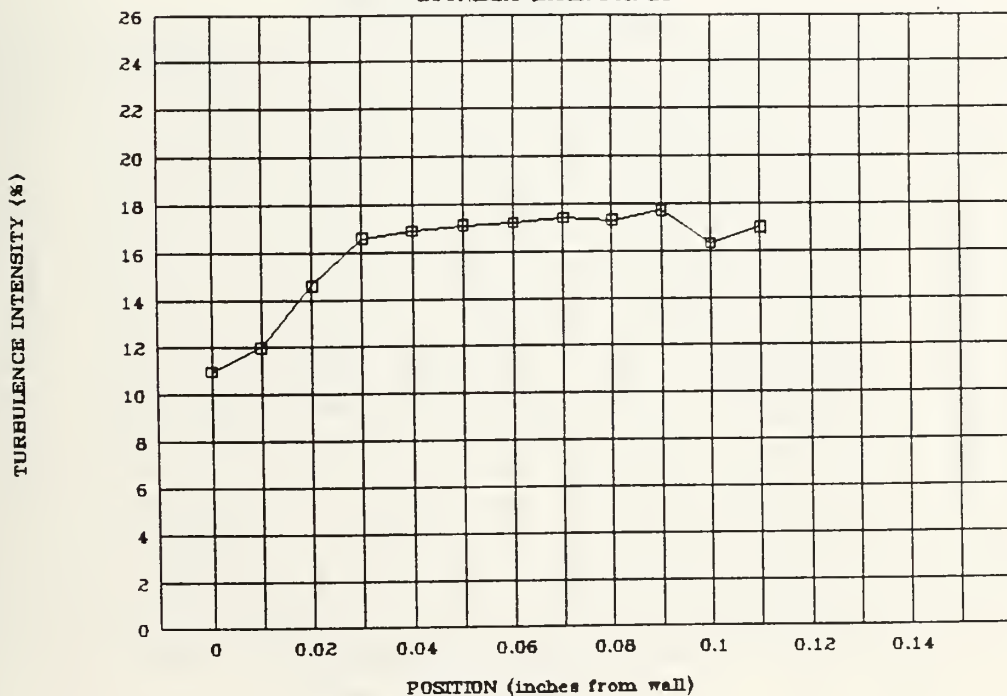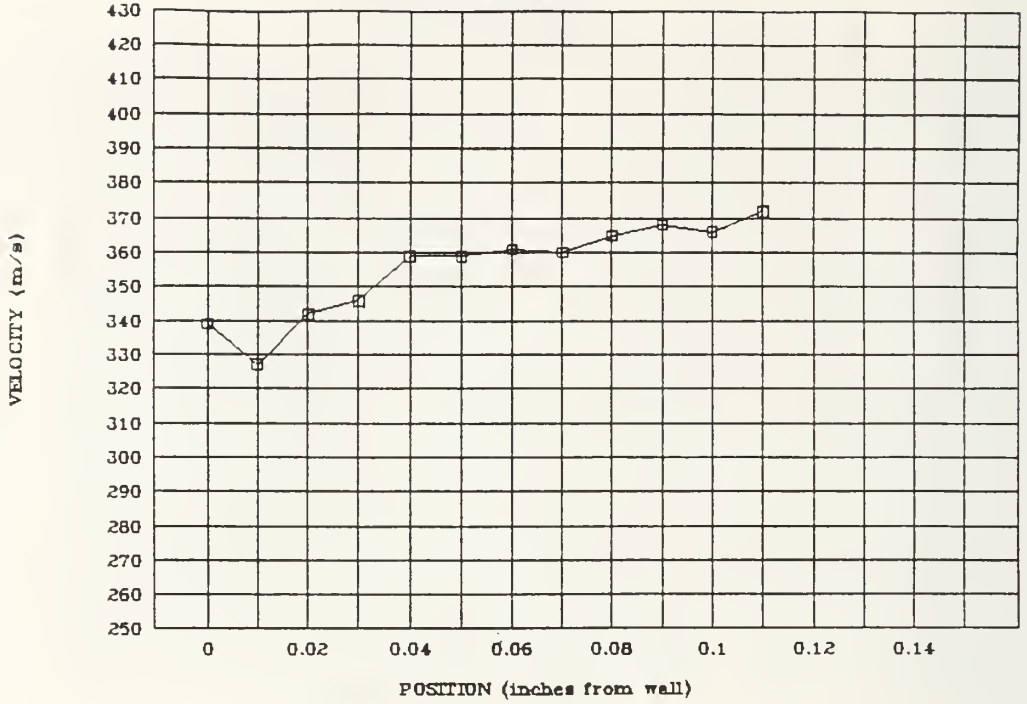
87

031093f

BOUNDARY LAYER SURVEY

031093f

BOUNDARY LAYER SURVEY

88

031193a

BOUNDARY LAYER SURVEY

VELOCITY (m/s) vs POSITION (inches from wall)

031193a

BOUNDARY LAYER SURVEY

TURBULENCE INTENSITY (%) vs POSITION (inches from wall)

031193b

BOUNDARY LAYER SURVEY

031193b

BOUNDARY LAYER SURVEY

90

031193d

BOUNDARY LAYER SURVEY

POSITION (inches from wall)

031193d

BOUNDARY LAYER SURVEY

POSITION (inches from wall)

91

X(in)	U Mean Velocity	U MEAN CORRECTED	U Standard Deviation	U Turb. Intensity	U TURB CORRECTED
0	211	391	12.5	5.?3	3.?
0.3	210	390	13.2	6.3	3.4
0.6	211	391	13.5	6.44	3.5
0.9	97.6	277.6	38.6	39.4	13.9
1.2	101	281	38.7	38.1	13.8
1.5	99.9	279.9	18.4	18.4	6.4
1.8	104	284	12.5	12	4.4
2.1	110	290	11.2	10.6	7
2.4	109	289	11.6	10.7	4

: '

A	B	C	D	E	F

Velocity in M/SEC
Data is from the following files:
030303a.1.10

X(in)	U-Mean Velocity	U-MEAN CORRECTED	U-Standard Deviation	U Turb. Intensity	U TURB CORRECTED
0.6	211	391	13.2	6.25	3.4
0.7	209	389	19.7	9.44	5.1
0.8	207	387	22.9	11.1	6
0.9	162	342	42.9	24.4	12.5
1	148	328	45.1	30.5	13.8
1.1	127	307	43.3	34	14.1
1.2	96.9	276.9	23.6	24.3	8.5
1.3	94.9	274.9	15.9	16.8	5.8
1.4	100	280	14.7	14.9	5.3
1.5	102	282	15	14.7	5.3

6: 6.1

	A	B	C	D	E	F

Velocity in M/SEC
Data is from the following files:
030393b.1,10

X(in)	U-Mean Velocity	U-MEAN CORRECTED	U-Standard Deviation	U Turb. Intensity	U TURB CORRECTED
0.9	126	306	50.2	42.9	17.4
0.95	134	314	43.5	5	15.8
1	130	310	48	36.9	15.4
1.05	118	298	45.7	38.5	16
1.1	116	296	47.2	41.2	16.1
1.15	118	298	47.0	40	15.8
1.2	115	295	44.3	38.5	15
1.25	106	286	37.2	35	13
1.3	102	282	22.8	22.3	9.3
1.35	97.2	277.2	17.6	18.1	6.3

-Mar-93 03:03 PM   UNDO   NUM

8: 6.1

	A	B	C	D	E	F

Velocity in M/SEC
Data is from the following files:
030493a.1,12

X(in)	U-Mean Velocity	U-MEAN CORRECTED	U-Standard Deviation	U Turb. Intensity	U TURB CORRECTED
0.7	207	387	18.4	8.85	4.7
0.75	207	387	18.7	9.03	4.8
0.8	206	386	17.3	9.37	5
0.85	207	387	21	10.2	5.5
0.9	197	377	33.2	16.9	8.8
0.95	168	348	36.2	21.6	10.4
1	166	346	26.5	16	7.7
1.05	171	351	19.5	10.9	5.3
1.1	168	348	19.8	11.8	5.7
1.15	172	352	16.2	9.15	4.6
1.2	168	348	22.1	13.1	6.3
1.25	167	349	21.2	12.5	6.1

Mar-93 03:05 PM   UNDO   NUM

++ 14.2

Velocity in M/SEC
Data is from the following files:
030473b,1,8

X(in)	U-Mean Velocity	U-MEAN CORRECTED	U Standard Deviation	U Turb. Intensity	U TURB CORRECTED
0.7	204	384	25.9	12.7	6.7
0.95	202	382	28.4	14.1	7.5
1	202	382	28.7	14.3	7.6
1.05	140	320	57.8	41.2	18
1.1	119	299	48.1	40.0	16
1.15	115	295	47	41	16
1.2	105	285	39.8	37.9	13.7
1.25	106	286	40.7	38.3	14.2

---Mar-93 03:07 PM   UNDO   NUM

2: 10.3

A   B   C   D   E   F

Velocity in M/SEC
Data is from the following files:
030593a,1,6

X(in)	U-Mean Velocity	U-MEAN CORRECTED	U-Standard Deviation	U-Turb. Intensity	U-TURB CORRECTED
1	97.6	277.6	36.5	32.4	13.1
1.05	93.3	273.3	30.4	32.6	11.1
1.1	92.5	272.5	28.5	30.8	10.5
1.15	90.5	270.5	25.7	28.4	9.5
1.2	92.3	272.3	28.3	30.7	10.4
1.25	91.9	271.9	27.9	30.4	10.3

-Mar-93 03:10 PM   UNDO   NUM

A   B   C   D   E   F

Velocity in M/SEC
Data is from the following files:
030593b.1.9

Y(in)	U-Mean Velocity	U-MEAN CORRECTED	U-Standard Deviation	U-Turb. Intensity	U-TURB CORRECTED
1	10?	287	21	18.5	5.2
1.05	105	285	17.2	18.2	6.7
1.1	107	287	18.1	16.9	6.3
1.15	106	296	16.6	15.?	5.8
1.2	108	288	15.3	14.1	5.3
1.25	109	289	14.6	13.6	5.1
1.3	109	289	15.8	14.6	5.4
1.35	102	282	19.1	18.9	6.8

-Mar-93 03:11 PM   UNDO   NUM

5: 6.9

A   B   C   D   E   F

Velocity in M/SEC
Data is from the following files:
030593c.1.9

X(in)	U-Mean Velocity	U-MEAN CORRECTED	U-Standard Deviation	U-Turb. Intensity	U-TURB CORRECTED
1	93	273	22.9	24.6	8.4
1.05	92.1	272.1	21.3	23.1	7.8
1.1	94.1	274.1	25.8	27.5	9.4
1.15	95.8	275.8	27.5	28.7	10
1.2	95.3	275.3	25.5	26.7	9.2
1.25	103	283	23.5	22.7	8.3
1.3	102	282	17.3	17	6.1
1.35	106	286	17.5	16.5	6.1
1.4	94.6	274.6	18.9	20	6.9

-Mar-93 03:13 PM   UNDO   NUM

	A	B	C	D	E	F

Velocity in M/SEC
Data is from the following files:
031093a,1,11

X(in)	U-Mean Velocity	U-MEAN CORRECTED	U-Standard Deviation	U Turb. Intensity	U TURB CORRECTED
0.8	181	241	58.3		16.1
0.9	153	333	64.4		12.1
1	170	370	55		14.9
1.1	189	369	55.5	27.4	15
1.2	116	236	44.5	38.5	15
1.3	110	290	44.3	40.2	17.2
1.4	105	285	29.9	27.5	10.2
1.5	100	280	27.2	27.1	9.7
1.6	97.4	277.4	15.5	15.9	5.6
1.7	101	281	16.2	16.1	5.8
1.8	105	285	15	14.3	5.3

-Mar-93   03:15 PM   UNDO   NUM

7: 4.7

	A	B	C	D	E	F

Velocity in M/SEC
Data is from the following files:
031093b,1,11

X(in)	U-Mean Velocity	U-MEAN CORRECTED	U Standard Deviation	U Turb. Intensity	U-MEAN CORRECTED
0.9	217	397	17.3	8.9	4.7
1	217	397	20.8	9.5%	5.2
1.1	189	369	49.9	25.9	13.3
1.2	129	309	56.4	43.6	18.2
1.3	122	302	48.6	39.9	16.1
1.4	110	290	34.2	31	11.8
1.5	96.6	276.6	16.4	17	5.9
1.6	101	281	16.7	16.9	6
1.7	101	281	14.8	14.7	5.3
1.8	109	289	15	14.7	5.5
1.9	111	291	13.5	12.2	4.7

-Mar-93   03:17 PM   UNDO   NUM

	A	B	C	D	E	F

Velocity in M/SEC
Data is from the following files:
031093c.1.12

X(in)	U-Mean Velocity	U-MEAN CORRECTED	U-Standard Deviation	U-Turb. Intensity	U-TURB CORRECTED
0.9	172	252	63.8	35.2	19.2
0.75	167	347	60.8	26.2	17.6
1	171	351	55.8	24.5	17
1.05	134	314	54.8	41	17.5
1.1	127	307	52.3	41.1	17
1.15	122	302	45.8	37.5	15.1
1.2	114	294	37.4	32.2	12.8
1.25	98.2	279.2	20.3	20.7	7.3
1.3	97.6	277.6	16.8	17.2	6.1
1.35	103	290	16	16	5.7
1.4	103	283	16.2	15.7	5.7
1.45	105	285	15	14.3	5.3

3: 5.3

	A	B	C	D	E	F

Velocity in M/SEC
Data is from the following files:
031093d.1.12

X(in)	U-Mean Velocity	U-MEAN CORRECTED	U-Standard Deviation	U-Turb. Intensity	U-TURB CORRECTED
0.9	176	356	62.2	35.4	17.5
0.95	181	361	61.6	34	17
1	189	369	56	29.6	15.1
1.05	199	379	47.9	24.1	12.7
1.1	153	333	59.4	38.9	17.9
1.15	124	304	46.8	37.7	15.4
1.2	119	299	44	36.5	14.7
1.25	115	295	38.1	33.2	12.9
1.3	103	283	24.4	23.7	8.6
1.35	103	283	25.8	25.1	9.1
1.4	97.9	277.9	15.8	16.1	5.7
1.45	98.6	278.6	14.9	15.1	5.3

5: 13.5

97
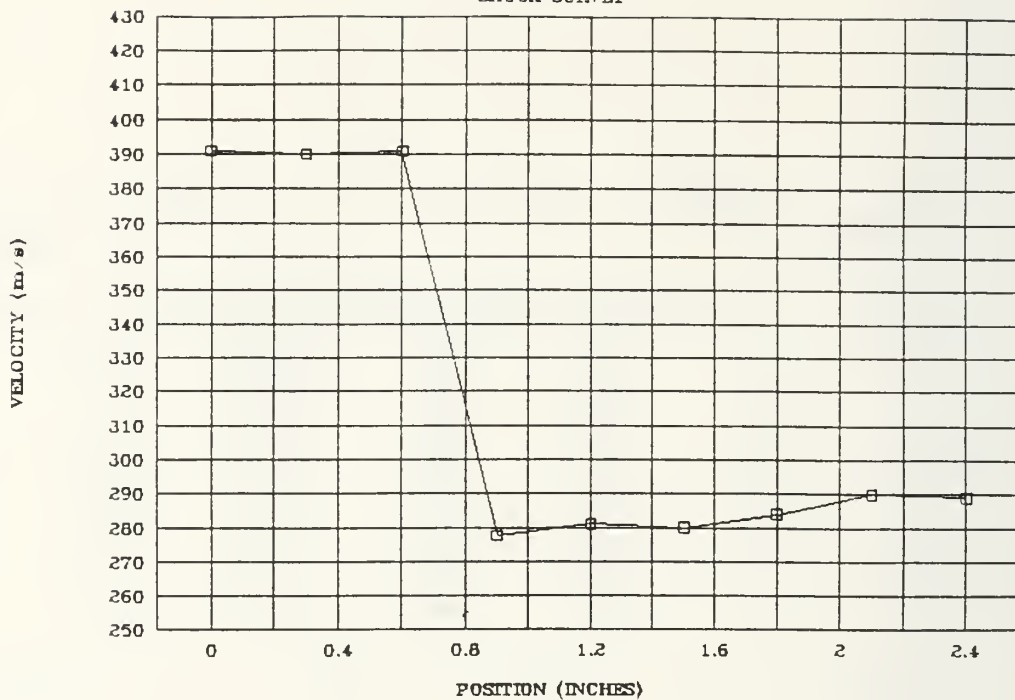
030293b

SHOCK SURVEY

030293b

SHOCK SURVEY

98
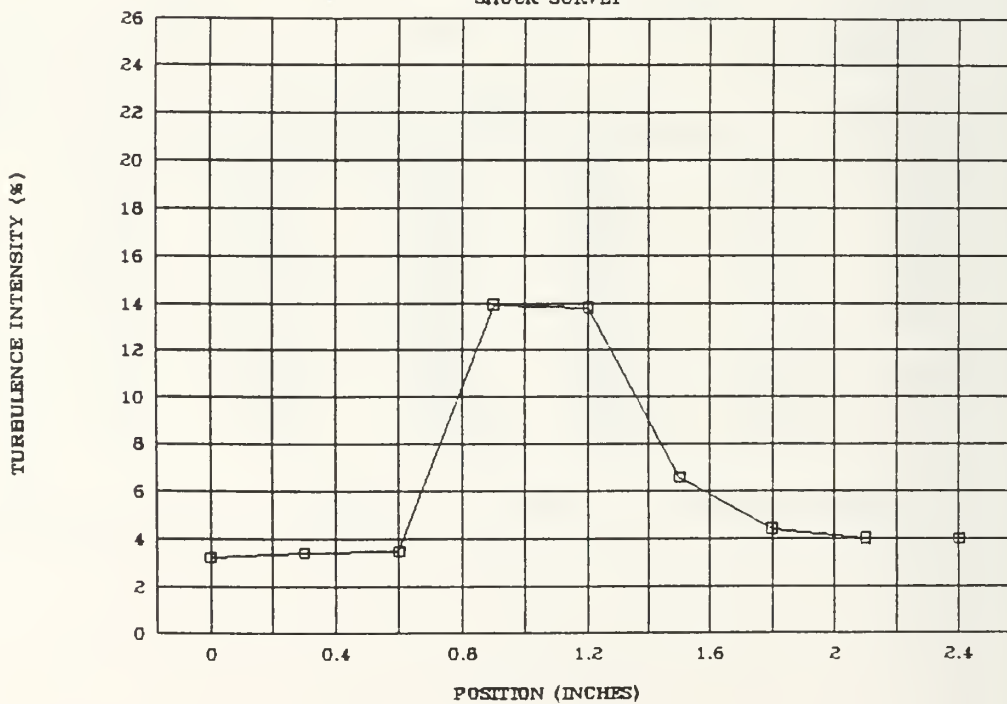
030393b
SHOCK SURVEY

030393b
SHOCK SURVEY

99
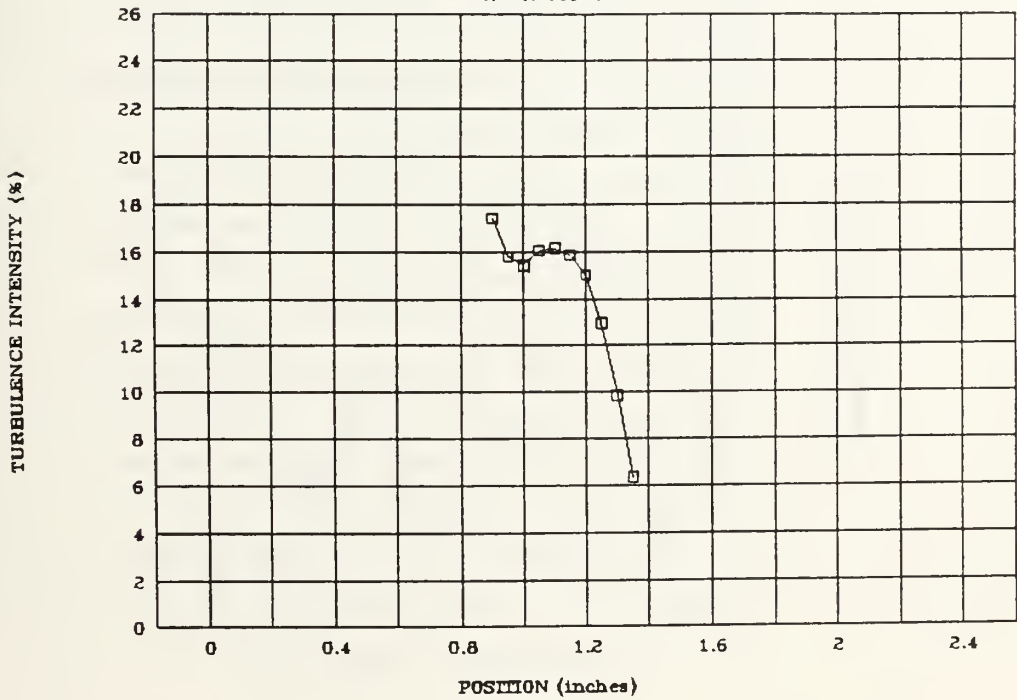
030493a

SHOCK SURVEY

030493a

SHOCK SURVEY

100
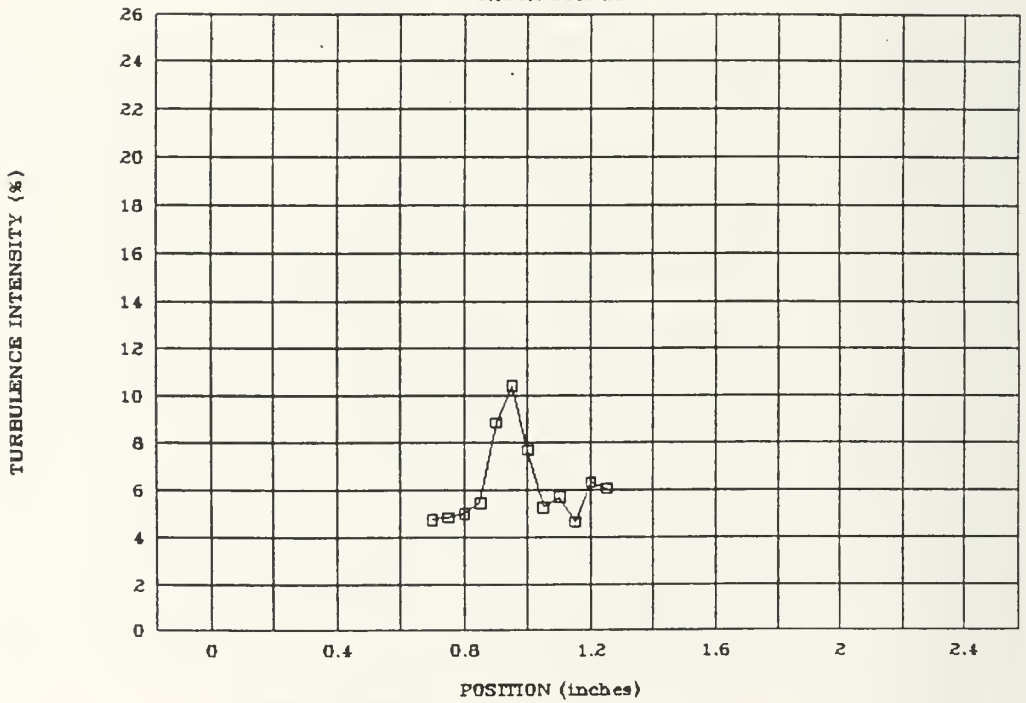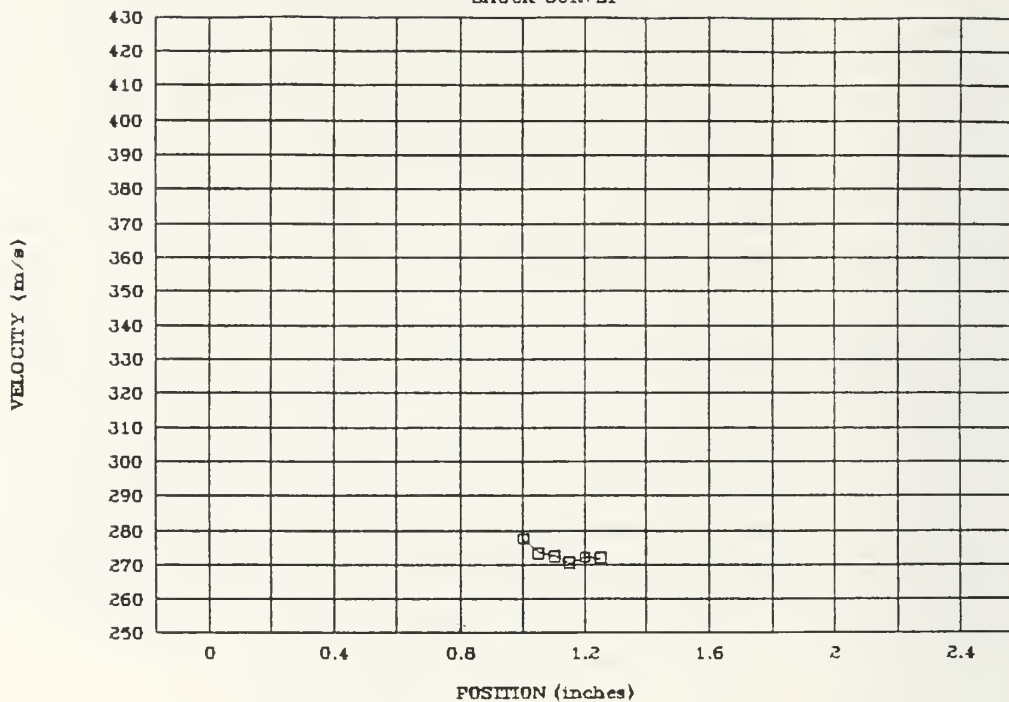
030493b
SHOCK SURVEY

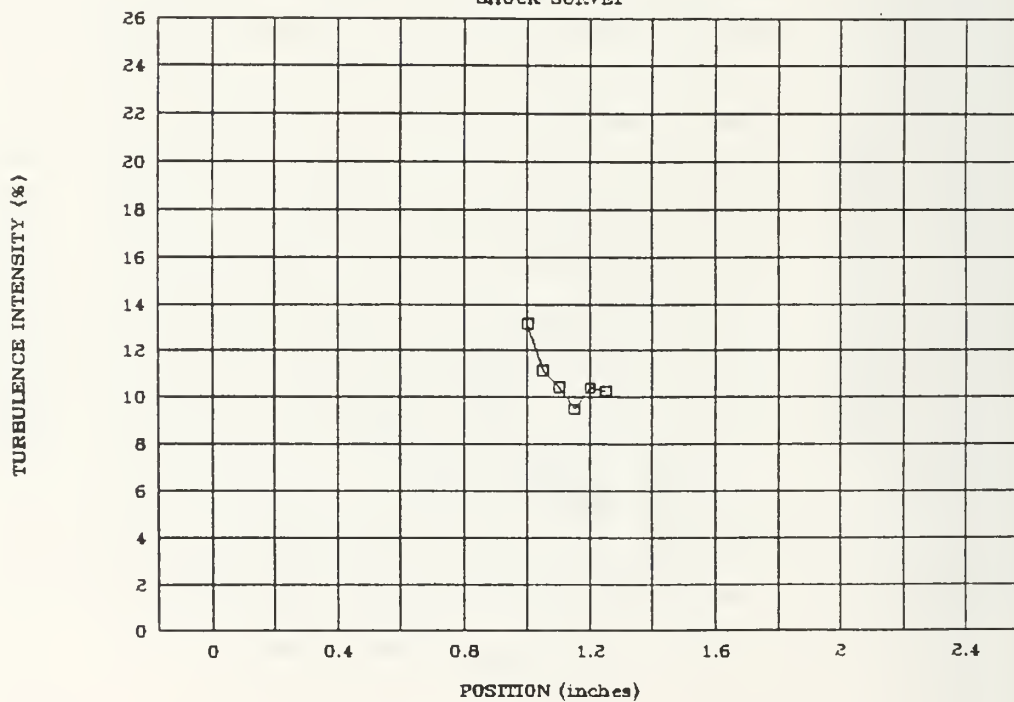
030493b
SHOCK SURVEY

101
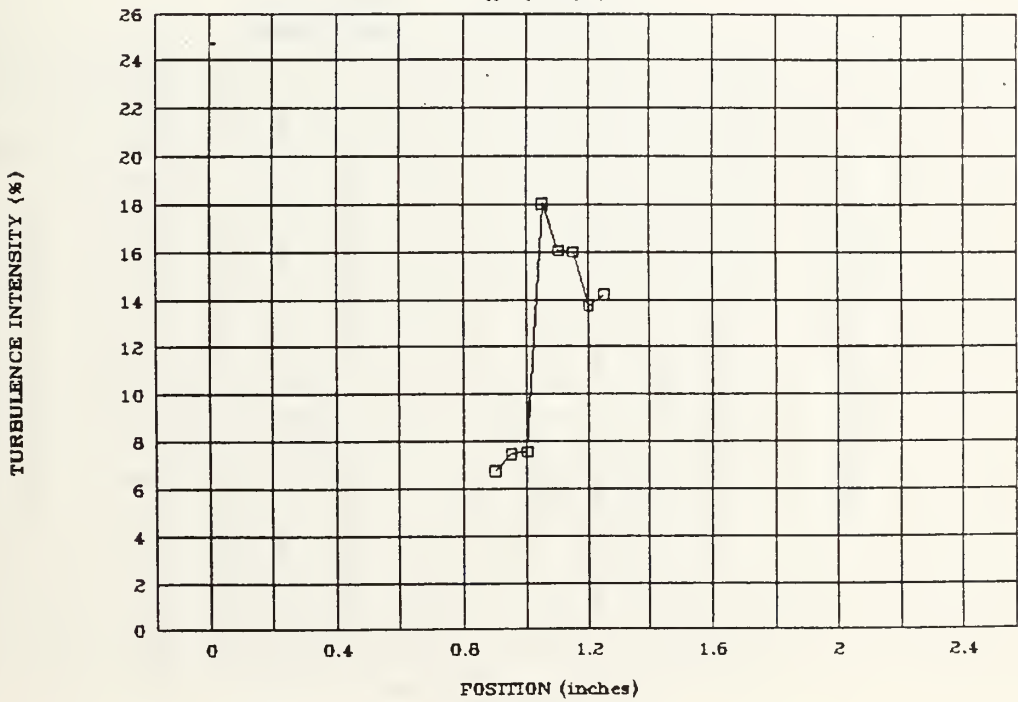
030593a

SHOCK SURVEY

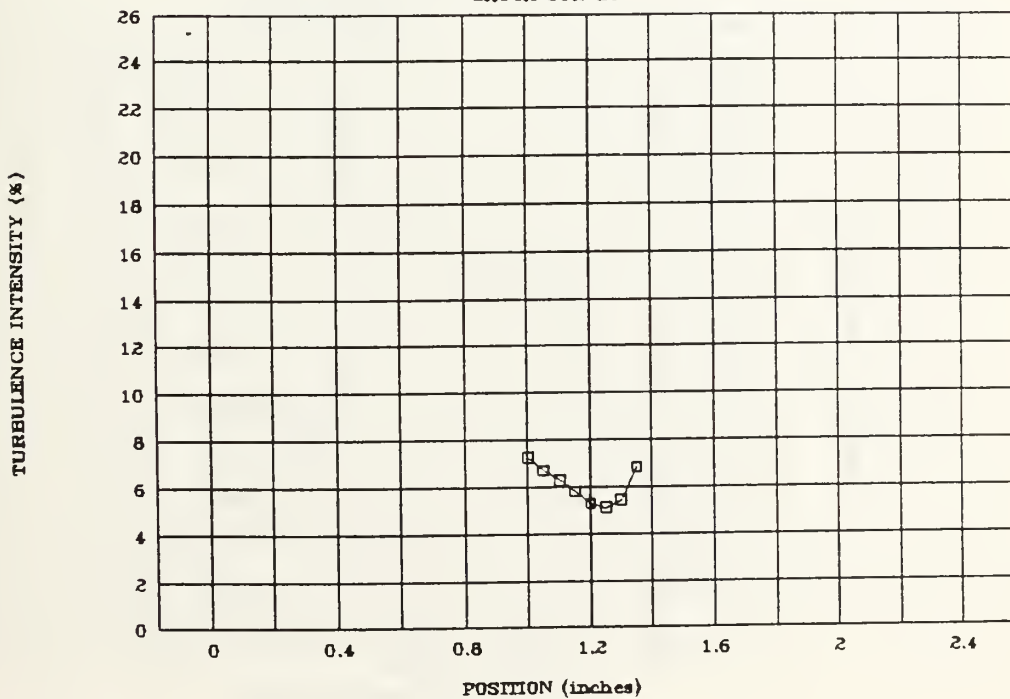

030593a
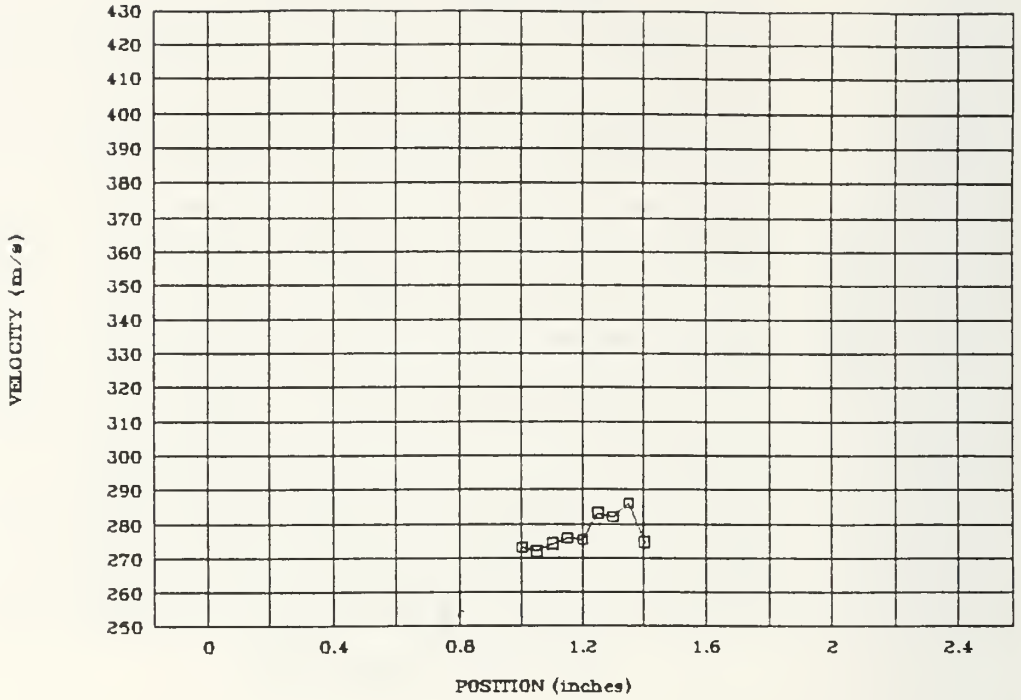
SHOCK SURVEY

102

030593b
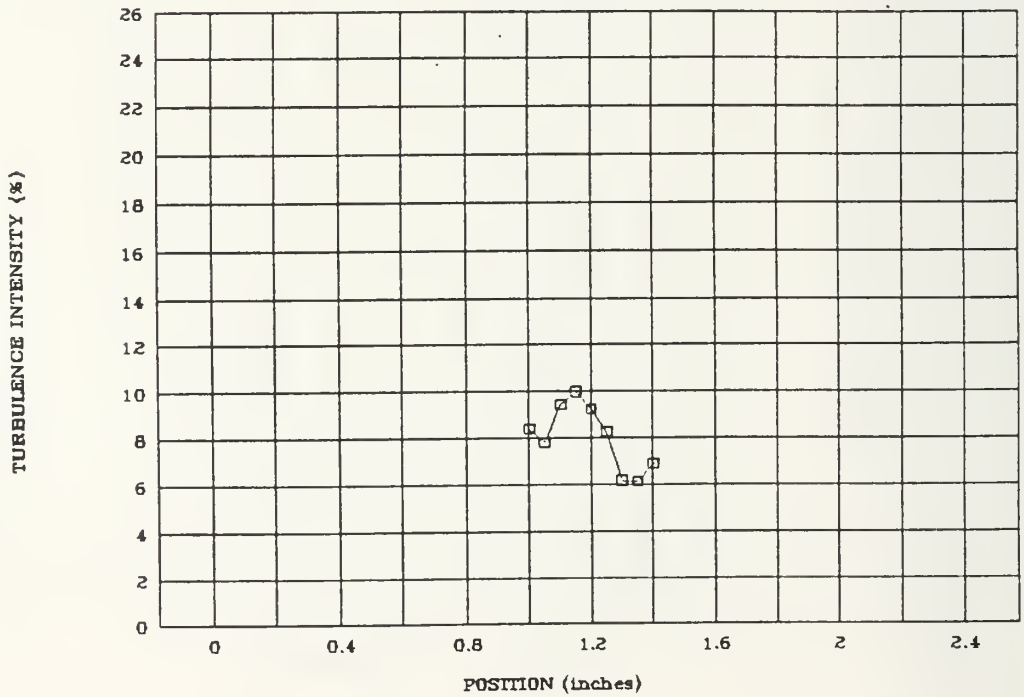
SHOCK SURVEY

030593b

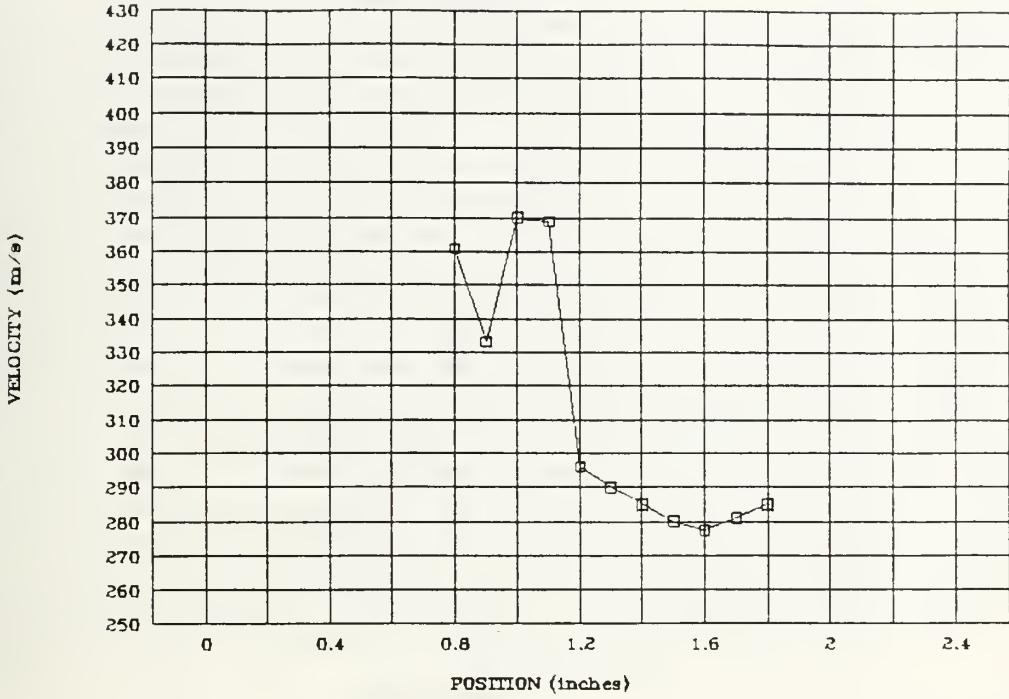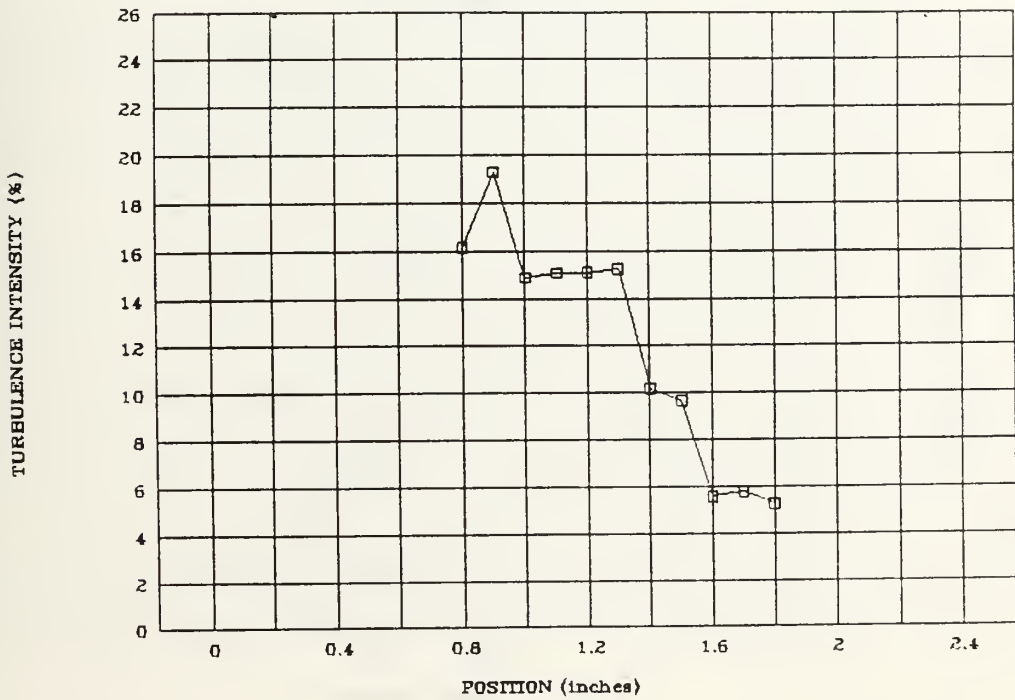## SHOCK SURVEY
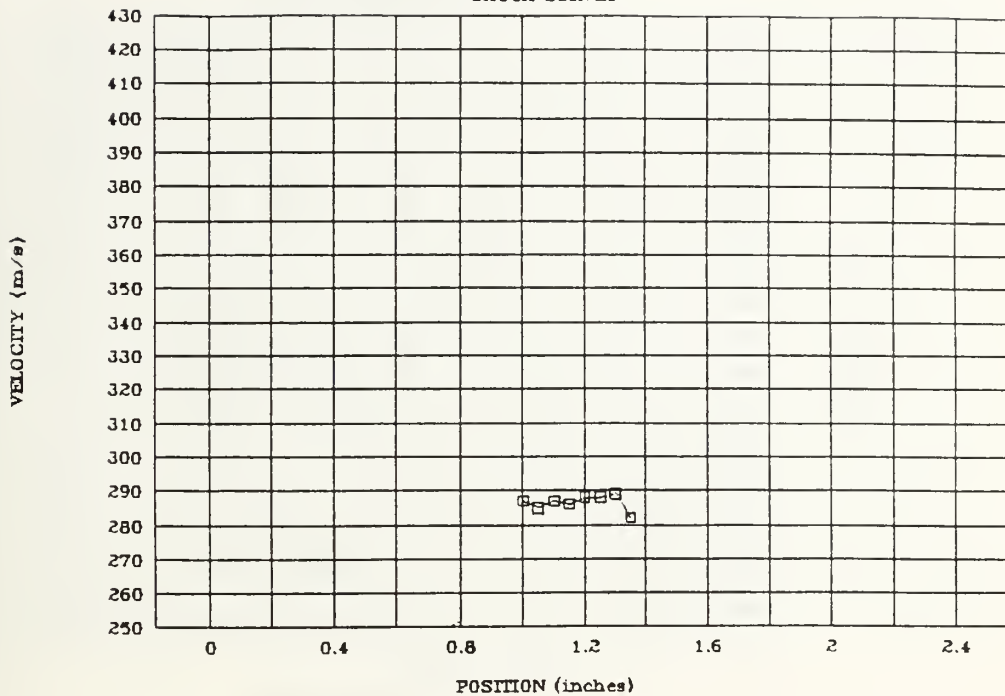
030593c
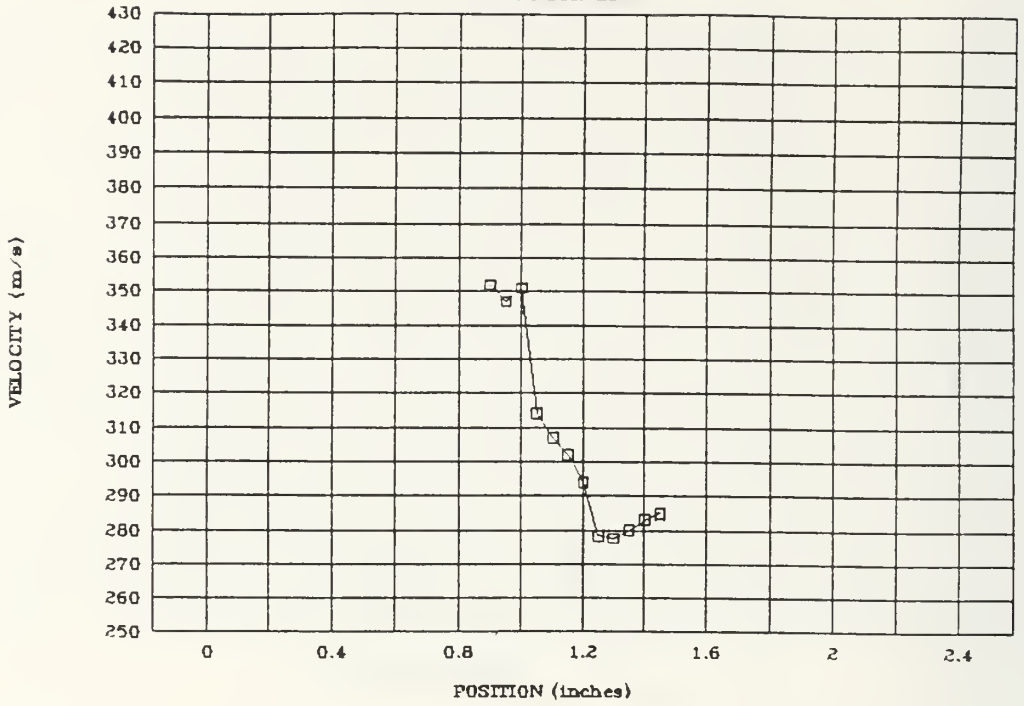SHOCK SURVEY

030593c
SHOCK SURVEY

104

031093a

SHOCK SURVEY

031093a

SHOCK SURVEY

031093c
SHOCK SURVEY

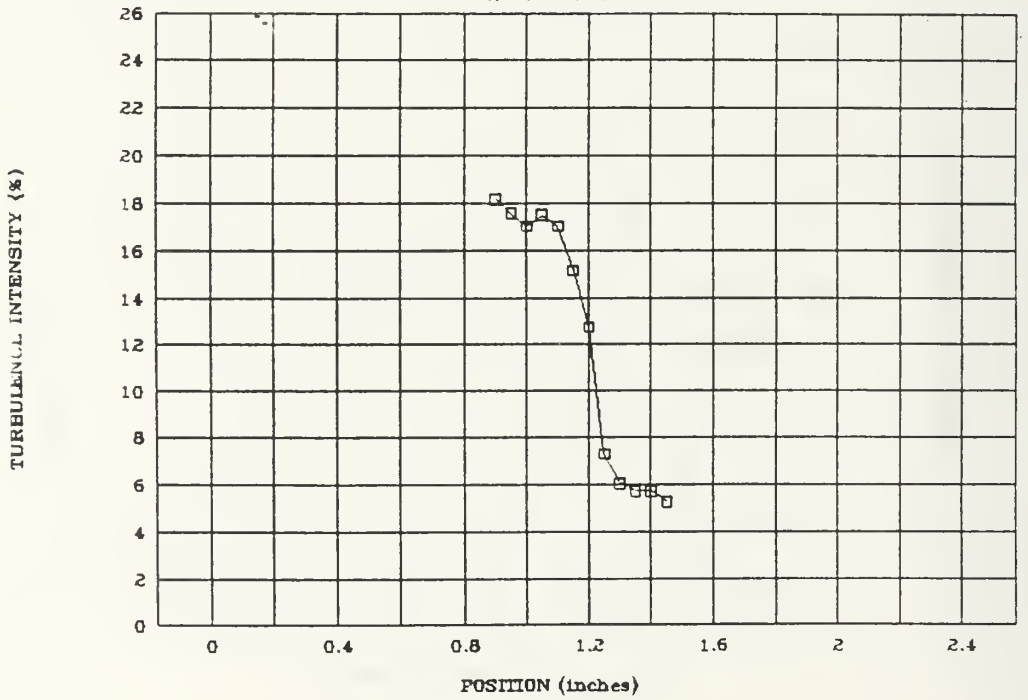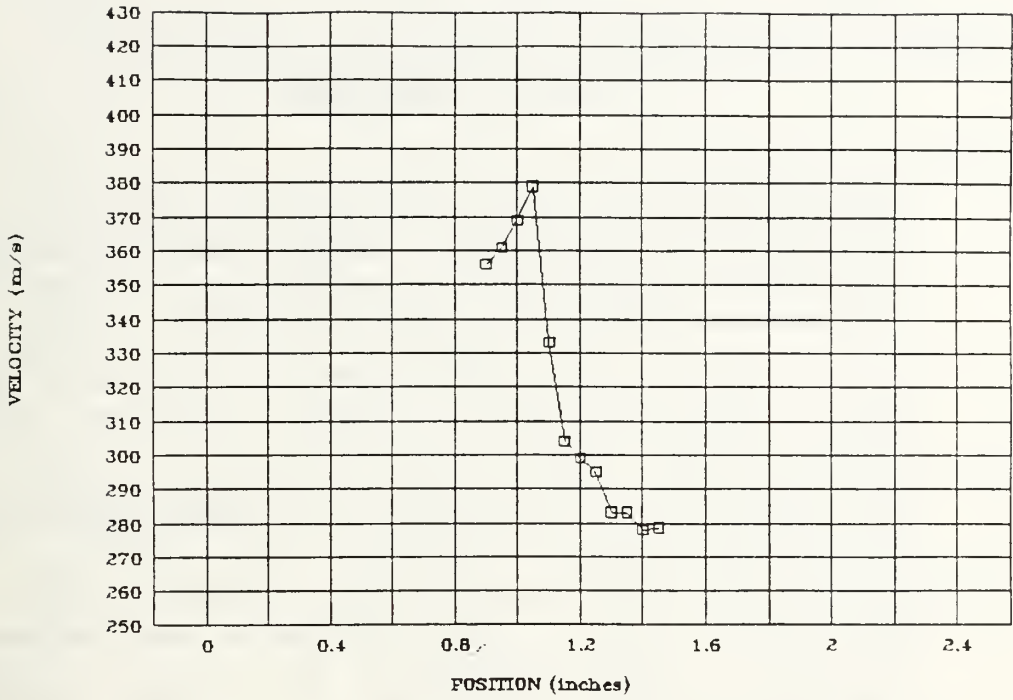# 031093c
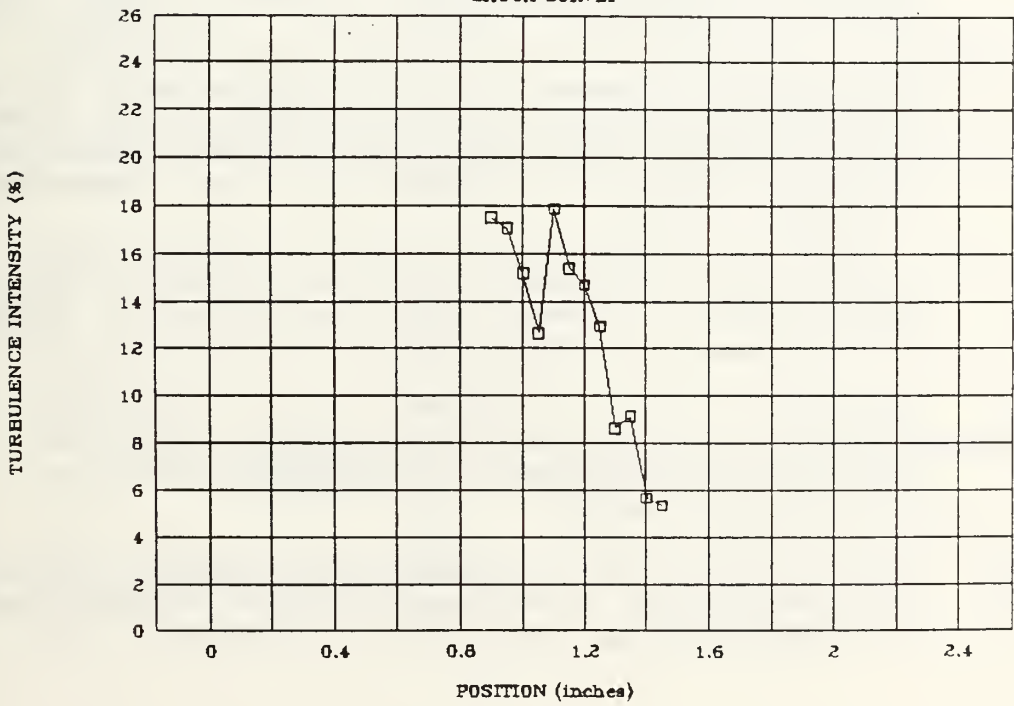## SHOCK SURVEY

106

031093d

SHOCK SURVEY

031093d

SHOCK SURVEY

LIST OF REFERENCES

1.   Yanta, William J., "The Use of Laser Doppler
      Velocimetry In Aerodynamic Facilities", pp 344-345,
      Proceedings of 11th AIAA Aerodynamics Testing
      Conference, AIAA Press, New York, 1980.

2.   Hebbar, S. K., Notes For AE3802 (Aerodynamics Lab),
      pp 1-9, Naval Postgraduate School, Monterey, CA., 1992
      (Unpublished).

3.   Watrasiewicz, B. M., Rudd, M. J., Laser Doppler
      Measurements, p 3, Butterworths Inc., London, 1976.

4.   Stevenson, W. H., "A Historical Review of Laser
      Velocimetry", pp 1-8, Proceedings of 3rd International
      Workshop on Laser Velocimetry and Particle Sizing,
      Thompson, H. Doyle, Stevenson, W. H., ed., Hemisphere
      Publishing Corp., 1978.

5.   Durst, F., Melling, A., Witelaw, J. H., Principles and
      Practice of Laser Anemometry, Academic Press, New York,
      1978.

6.   Durst, F., Stevenson, W. H., "Properties of Focused
      Laser Beams and the Influence On Optical Anemometer
      Signals", p 371, Proceedings of The Minnisota Symposium
      on Laser Anemometry, Eckert, E. R., ed., University of
      Minnisota, 1975.

7.   Pike, E. R., "The Application of Photon Correlation
      Spectroscopy to Laser Doppler Measurements" Journal
      of Physics D, 5, L23, 1972.

8.   McLaughlin, D. K., Tiederman, W. G., "Biasing
      Correction For Individual Realization of Laser
      Anemometer Measurements In Turbulent Flows",
      Physics of Fluids, 16, 2082, 1973.

9.   George, W. K., Jr., "Limitations To Measuring Accuracy
      Inherent In the Laser doppler Signal", Proceedings of
      the LDA Symposium, University of Denmark, 1975.

10. Goebel, S. G., Dutton, J. C., Krier, H., Renie, J. P.,
    "Mean and Turbulent Velocity Measurements of Supersonic
    Mixing Layers", Experiments In Fluids, Vol 8, No. 5,
    pp 263-272, 1990.

11. Baroth, E. C., "Investigation of Supersonic Separated
    Flow in a Compression Corner by Laser Doppler
    Anemometry", Experiments In Fluids, Vol. 1, No. 4,
    pp 195-203, 1983.

12. Ceman, David L., "A Study of Turbomachine Flow
    Velocities", AIAA 89-0839, 27th Aerospace Sciences
    Meeting, Reno, NV., 1989.

13. Absil, L. H., Passchier, D. M., "LDA Measurements in the
    Highly Asymmetric Trailing Edge Flow of an NLR 7702
    Airfoil", LR-646, ETN-92-90416, 1990.

14. Myre, David D., "Model Fan Passage Flow Simulation",
    Masters Thesis, Naval Postgraduate School, Monterey,
    CA., 1992.

15. Chesnakes, C. J., Andrew, P. L., "An LDV Evaluation
    of Particle Lag Prediction Techniques In Supersonic
    Flows", Yokohama International Gas Turbine Congress,
    Yokohama, 1991.

16. Bloomberg, J. E., Dutton J. C., Addy, A. L., "An
    Investigation of Particle Dynamics Effects Related
    to LDV Measurements In Compressible Flows", 1989.

17. System 9100-7 Laser Doppler Velocimeter Instruction
    Manual, TSI Inc., 1984.

18. Model 9306 6-Jet Atomizer Instruction Manual, TSI
    Inc., 1992.

20. Schlichting, H., Boundary Layer Theory, pp 155-157,
    McGraw Hill, New York, 1979.

21. Grimson J., Advanced Fluid Dynamics and Heat Transfer,
    pp 636-637, McGraw Hill, New York, 1971.

22. Strazisar, A. J., "Laser Fringe Anomometry for Aero
    Engine Components", Agard CP-399, Advanced
    Instrumentation for Aero Engine Components, Nov., 1986.

23. Chriss, R. M., Keith T. G., Hingst, W. R., Strazisar A. J., Porro, A. R., "An LDA Investigation of Three-Dimensional Normal Shock-Boundary Layer Interactions in a Corner", AIAA 19th Fluid Dynamics, Plasma Dynamics and Lasers Conference, Honolulu, 1987.

24. <u>Supplement to ASME Power Test Codes</u>, Flow and Measurements, p 13, Part 5-Measurement of Quantity of Materials, ASME,1959.

INITIAL DISTRIBUTION LIST

No. Copies

1. Library, Code 0142   2
    Naval Postgraduate School
    Monterey, California 93943-5002

2. Defense Technical Information Center   2
    Cameron Station
    Alexandria, Virginia 22304-6145

3. Department Chairman, AA   1
    Department of Aeronautics
    Naval Postgraduate School
    Monterey, California 93943

4. Garth V. Hobson, Turbopropulsion Laboratory   7
     Code AA/Hg
    Department of Aeronautics
    Naval Postgraduate School
    Monterey, California 93943

5. Naval Air Systems Command   1
    AIR-536T(Attn: Mr. Paul F. Piscopo)
    Washington, District of Columbia 20361-5360

6. Naval Air Warfare Center   1
    Aircraft Division (Trenton)
    PE-31(Attn: S. Clouser)
    250 Phillips Blvd
    Princeton Crossroads
    Trenton, New Jersey 08628-0176

7. David A. Perretta   1
    1321 Chapelview Dr.
    Odenton, Maryland 21113

111